CONTROLS ON BIOTURBATION AND SEDIMENT DISTRIBUTION WITHIN CARBONATE SHOREFACE DEPOSITS: INSIGHTS FROM HETEROGENEITY IN PLEISTOCENE AND RECENT STRATA

By

Alexa R. Goers

B.Sc., Trinity University, 2012

Submitted to the graduate degree program in Geology and the Graduate Faculty of the University of Kansas in partial fulfillment of the requirements for the degree of Master of Science.

_____

Co-Chair: Dr. Eugene C. Rankey

_____

Co-Chair: Dr. Stephen T. Hasiotis

_____

Dr. Jennifer A. Roberts

Date Defended: December 16, 2021

The Thesis Committee for Alexa R. Goers

certifies that this is the approved version of the following thesis:

CONTROLS ON BIOTURBATION AND SEDIMENT DISTRIBUTION WITHIN CARBONATE SHOREFACE DEPOSITS: INSIGHTS FROM HETEROGENEITY IN PLEISTOCENE AND RECENT STRATA

_____

Co-Chairs: Dr. Eugene C. Rankey

_____

Co-Chairs: Dr. Stephen T. Hasiotis

Date approved: December 16, 2021

ABSTRACT

Burrowing organisms alter sedimentary textures, influence cement distribution, and affect petrophysical characteristics of carbonate strata. Although many descriptions of carbonate successions reference bioturbation, quantitative data on spatial variability of trace fossils are rare, and fewer studies address trace-fossil influence on postdepositional modification of sedimentary deposits, which affects petrophysical properties. To address these unknowns and determine the controls on ichnology in carbonate shoreface successions, this study evaluates the distribution of sediment and bioturbation in recent, Holocene, and Pleistocene shoreface deposits on the leeward margin of Crooked-Acklins Platform (CAP), southern Bahamas. Results illustrate north–to-south along-strike variability on this margin. The extant north margin shelf is characterized by poorly to moderately sorted, very fine–fine, skeletal-peloid-ooid sand with an average of 16% mud (< 62.5 μm), and is moderately to intensely bioturbated (ii3–6). Trace assemblages are diverse, and include horizontal tracks and trails, abundant horizontal deposit-feeding and locomotion traces, as well as dwelling and resting burrows (e.g., *Arenicolites*, *Conichnus*, *Thalassinoides*) attributable to the proximal Cruziana Ichnofacies. South margin shelf deposits are well-sorted, medium ooid-peloid sand with < 1% mud, and display a range of bioturbation, from nonbioturbated to moderately intense bioturbation (ii1–4). Trace-fossil assemblages exhibit low ichnodiversity, and are dominated by vertical dwelling burrows with reinforced wall linings (e.g., *Ophiomorpha*, *Skolithos*), attributable to the Skolithos Ichnofacies. Earlier Holocene and Pleistocene strata show similar proximal-to-distal and along-strike variations in sediment attributes, ichnodiversity, and bioturbation intensity. These trends are interpreted to reflect a progressive, north–to-south increase in energy reflecting the change in margin orientation relative to the direction of dominant wave energy, analogous to the modern system. Results show

relations among biologic processes (i.e., feeding, dwelling, resting, locomotion) of benthic organisms that produce a range of ichnofabrics, thereby altering depositional texture (i.e., primary porosity) as well as lateral and vertical facies patterns. This study provides an integrated conceptual model for sedimentologic-ichnologic processes and patterns of sediment accumulation on carbonate shorefaces that may be distinct from siliciclastic analogs, insights applicable to interpreting and modeling ancient reservoir analogs.

ACKNOWLEDGEMENTS

I would like to thank Dr. Eugene Rankey and Dr. Stephen Hasiotis for serving as both mentors and advisors throughout my time at the University of Kansas. Thanks for never giving up on me, after all these years! I couldn't have done it without your guidance and support. I would also like to thank Dr. Jennifer Roberts for serving on my committee. Thank you to the Kansas Interdisciplinary Carbonate Consortium (KICC) and their sponsors for funding this research, as well as the University of Kansas Geology Department.

Thank you to the Rankey Research Group students for their support, thoughtful revisions, and most importantly, their friendship: Michelle Mary, Adrienne Duarte, Thomas Neal, Hannah Hubert, Maritha Konetchy, and Steven Herbst. Your "cooperate to graduate" mentality kept me going through many late nights in the Lindley basement! Also, thank you to Adrienne, Steven, and Maritha for their help during fieldwork.

Thank you to the IchnoBioGeoSciences research group members for their advice and encouragement: Adam Jackson, James Golab, Sean Hammersburg, and Sean Fischer. Thank you to Tabatha Gabay for being my study partner and friend.

Thank you to my family and friends for their support and encouragement. Most of all I would like to thank my partner, Trevor Osorno, and my dog Otto. I could not have done it without you guys!

TABLE OF CONTENTS

LIST OF FIGURES AND TABLES

Figures

Tables

INTRODUCTION

Carbonate platforms and shelves are common throughout the geologic record and exhibit complex sedimentologic and stratigraphic patterns (e.g., Wilson 1975; James 1983; Read 1985). Numerous studies have documented sedimentary facies and developed conceptual models of carbonate platform and shelf depositional systems (summarized in Wilson 1975; James 1983; Read 1985; Schlager 2005). Although sedimentologic aspects of shorefaces of both modern and ancient carbonate settings are well documented (e.g., Lloyd et al. 1987; Burchette and Wright 1992; Harris et al. 1993; Aurell et al. 1995, Rankey et al. 2009; Rankey 2014), few studies systematically describe and characterize the paired nature and distribution of sediment, traces, and ichnofabrics within these systems (e.g., Shinn 1968; Farrow 1971; Ekdale et al. 1984; Curran and White 1987, 1991; Monaco and Giannetti 2002; Knaust 2007). Such integrated characterization is important because syndepositional biological and diagenetic processes can markedly alter carbonate sedimentary fabrics (e.g., Tedesco and Wanless 1991; O'Leary et al. 2009; Knaust 2009, 2010), and modify the distribution of porosity and permeability, which in turn influence reservoir quality (e.g., Gingras et al. 2004; 2007; Pemberton and Gingras 2005; Tonkin et al. 2010; La Croix et al. 2013; Eltom and Hasiotis 2019; Eltom et al. 2019). For example, numerous oil fields produce from carbonate reservoirs with biogenically mediated permeability zones (e.g., Ordovician Bighorn Dolomite—Zenger 1992, 1996; Ordovician Yeoman Formation—Gingras et al. 2004; Pemberton and Gingras 2005; Mississippian Midale Beds—Keswani and Pemberton 2007; Jurassic Arab Formation, Ghawar Field—Pemberton and Gingras 2005). Each of these fields displays bioturbation-enhanced or decreased porosity and permeability, influencing overall reservoir quality and production.

In this context, the purpose of this study is to compare and contrast carbonate facies and traces in Pleistocene, Holocene, and modern carbonate shoreface deposits on Crooked-Acklins

Platform (CAP), southeastern Bahamas (Fig. 1). Results characterize sedimentologic and ichnologic variability through comparative analysis and interpretation of modern and ancient deposits. Incorporating the ichnology within the context of geomorphic position, depositional setting, and hydrodynamic processes of carbonate shoreface environments reveals the controls on vertical and lateral changes in the character and intensity of bioturbation. Results of this study provide a predictive conceptual model of the multiple scales of sedimentologic and ichnologic heterogeneity within carbonate grainstone shoreface deposits, with implications for their influence on porosity and permeability in reservoir analogs.

STUDY AREA

Crooked-Acklins Platform (CAP) is an isolated carbonate platform covering an area of ~2,600 km^2, with a central platform interior bordered by islands to the east, north, and west (Fig. 1A, B). The western, leeward flank of the platform, the focus of this study, includes a modern depositional shelf with variable width and orientation. The arcuate margin transitions along strike from SW-facing (north margin), to W-facing (central margin), to NW-facing (south margin) orientation (Fig. 1C). On this margin, islands of CAP are composed of Pleistocene and Holocene reef, shoreface, and berm deposits.

The shoreface system of the western, leeward margin of CAP is shielded from the easterly trade winds by the position and configuration of the platform and islands (e.g., Rankey and Reeder 2010). Furthermore, the physical and chemical oceanographic conditions (e.g., water chemistry, nutrient levels, temperature, and salinity) are typical of open marine conditions in the Bahamas (e.g., Rankey 2014). Though influential, tidal processes are not considered to be a major control on hydrodynamic energy or depositional processes on much of the margin,

although the central margin is influenced by the elevated tidal-current velocity in the restricted tidal inlet between Crooked Island and Long Cay (e.g., Rankey 2014; see French Wells tidal inlet, Figs. 1C and 2A).

Tidal range is *ca* 1 m in this area (Rankey and Reeder 2010). Wave-gauge and current-meter data measured mean significant wave height (H_s) of 10 cm and mean peak period (T_p) of < 8 s (from Rankey 2014; measured during April and May 2009 at white star in Fig. 1C). The waves and tides combine to form weak (< 15 cm/s) currents that facilitate net southward longshore transport. As this western, leeward margin is protected from the trade winds, the greatest energy is provided by distal, long-period swell (measured T_p up to 10–15 s; greater periods are likely). The strongest winds and swell come from the W–NW, and are associated with the passage of winter (December–March) cold fronts in the open Atlantic and some of which directly impact this area (Rankey and Reeder 2011). This open-Atlantic swell propagates to the SSE and can have markedly larger H_s than local wind-generated waves. In contrast, the quiescent summer months experience episodic tropical storms during hurricane season (June–November), with winds and waves from various directions.

This leeward shelf extends from the shoreline to the dropoff across distances of less than 5 km, and although it includes patch reefs, it is unrimmed. It thus is referred to as a shoreface system, and is subdivided and described accordingly. We use the term *foreshore* to reflect the relatively steep gradient, seaward-dipping beach exposed between low and high tide. The shoreface we subdivide based on the relative rates of physical and biological reworking; the *upper shoreface* also dips seaward, and is characterized by sandy bottoms with wave ripples, current ripples, nearshore bars, or a mix, and can vary with seasonal changes in waves. We also define a *bioturbated upper shoreface* which was largely bioturbated during 'energetic' winter

field seasons, but which we suspect might still be mobilized during extreme wave events. The bioturbated upper shoreface is comparable to the lower shoreface of Kamola and Van Wagoner (1995).

METHODS

This study examined the geomorphologic, sedimentologic, and ichnologic character of the modern leeward shelf, and of Holocene and Pleistocene strata along the same margin (Fig. 1C). Insights from the modern are applied to the ancient to enhance understanding of the controls on the distribution of sedimentary facies and trace fossils.

Field Characterization of Shoreface Settings

Modern.—Sedimentologic, biologic, and physical oceanographic data collected along six transects capture changes from the backshore to the shelf-slope break to assess sediment accumulation patterns and bottom types on the modern seafloor (Fig. 1C). Previous work by Rankey (2014), combined with QuickBird remote-sensing data, provided the basis for identifying transect and sample locations that represent the range of physical oceanographic (i.e., hydrodynamic) conditions, bottom types, and geomorphic elements on the margin. To understand the hydrodynamics of the modern leeward shelf, field observations were combined with wind, wave, and tide data from weather reports. Quantitative data and qualitative observations of physical oceanographic conditions and hydrodynamic processes were recorded over the course of two field seasons (January 12–24, 2014; December 6–12, 2014), and included wind, waves, tides, and local storm conditions. Quickbird remote-sensing data were examined in ArcGIS to determine the size and spatial distribution of geomorphic features. Onshore–offshore

transects vary from 0.4–2.2-km long, dependent on shelf width, water depth, and conditions during fieldwork. Subaqueous data collection used snorkel and scuba-diving equipment and techniques (e.g., Heine 2000).

On the intertidal through terrestrial portions of the transects, sedimentologic, and geomorphologic features—beach width and gradient, presence of beachrock or beach sediment, berm type and height—of the foreshore and backshore were described systematically for comparison with features in Holocene and Pleistocene strata. At each transect location, photographs and systematic descriptions of hydrodynamic conditions, bottom types, physical sedimentary structures, benthic organisms, and neoichnologic data were recorded.

Hydrodynamic descriptions include qualitative field observations of wind speed and direction, and visual estimates of wave height and period. Water depth was measured with a handheld digital depth sounder and, where possible, confirmed with scuba-diving equipment. Physical processes at each location were inferred based on the type and geometry of bedforms. Seafloor photos include a 0.25 m^2 quadrat for scale and to quantify bioturbation intensity, establish trace assemblages, and compare ichnodiversity along transects and among transects. Tabulated organisms were limited to pelagic, epibenthic, and endobenthic organisms (i.e., trace- and sediment-making organisms). Modern traces were described and assigned to corresponding ichnotaxa based on architectural and surficial morphology and type and pattern of fill (e.g., Hasiotis and Mitchell 1993; Bromley 1996). Neoichnologic descriptions include bioturbation intensity and ichnodiversity, as well as the abundance, spatial distribution, and density of individual traces. Bioturbation intensity was categorized into one of six ichnofabric indices (ichnofabric index, ii; Droser and Bottjer 1986) allowing for comparison with bioturbation intensity of Pleistocene and Holocene strata. Ichnodiversity is defined based on the number of

morphologically distinct traces within a 0.25 m^2 quadrat, normalized and reported per 1 m^2 or per 5 m^2 (for large traces). Burrow density is the number of individual burrows per 1 m^2 or per 5 m^2 for such large traces as stingray-feeding pits and callianassid shrimp mounds. Relative trace abundance includes abundant (> 5 individuals), common (5 individuals), few (3–4 individuals), and rare (1–2 individuals), based on observations of density patterns of traces expressed on the seafloor for each transect.

A total of 107 sediment samples collected for lab analyses included variable field-sample spacing dependent on bottom type, transect length, and dive restrictions. Sediment samples collected in 20-dram plastic vials were capped immediately upon collection to prevent the loss of any fine sediment. Water-depth data (uncorrected for tides) along transects provided a means to estimate the gradient of the shelf along each transect.

Outcrop.—Relative ages of Pleistocene and Holocene beach ridges and beach-ridge progradation patterns were determined by crosscutting relationships interpreted from QuickBird remote-sensing data of Crooked Island and Long Cay. Thirty-six stratigraphic successions were systematically described using standard sedimentological and ichnological techniques. Locations of measured sections were chosen to capture the range of physiographic and geomorphic variability. Measured sections include descriptions of stratigraphic (e.g., stratigraphic succession, thickness, contacts, bedding character), sedimentologic (e.g., lithology, sedimentary structures, and diagenetic and pedogenic features), and ichnologic features.

Ichnologic features recorded from outcrop and hand-sample analysis include bioturbation intensity (ii), ichnodiversity, and burrow density, as well as the morphology, relative size, abundance, and distribution of trace fossils. Classification of ichnogenera abundance into four categories (abundant, common, few, rare) and ichnodiversity into three categories (high,

moderate, low; per lithofacies) were used for qualitative comparison with data reported in the literature (e.g., Mieras et al. 1993). Descriptions of trace-fossil assemblages include uniformity of burrowing, crosscutting, and tiering relationships, and the range of ethological categories (e.g., Bromley 1996; MacEachern and Bann 2008; Jackson et al. 2016).

Laboratory

Sediment analyses.—Sediment samples (N = 107 collected here and by Rankey 2014) were dried and halved for granulometric and thin-section analyses to quantify grain-size trends and determine the relative abundance of constituent grains using standard comparators (e.g., Flugel 2004). Grain-size distributions, determined using an ATM Sonic Sifter, were imported into GRADISTAT v8 software (Blott and Pye 2001) to calculate particle statistics, including mean grain size and sorting, following the classification of Folk and Ward (1957). Sediment was classified by depositional texture (Dunham 1962) based on the abundance of mud (grain size < 62 μm) in the sample. Field observations and laboratory results were integrated in ArcGIS to evaluate the spatial distribution of sedimentary facies and traces.

Rock analyses.—Pleistocene and Holocene rock samples (N = 273) were cut into slabs and/or petrographic thin sections for detailed sedimentologic and ichnologic analysis. Petrographic analysis of 76 blue-epoxy thin sections focused on grain character, bioturbation intensity, pore networks, and cementation characteristics. Image analysis of photomicrographs using the software JMicroVision (Roduit 2008) quantified preserved porosity, grain composition, and cement. Digital scans of thin sections were converted into binary images to evaluate pore networks (e.g., pore types, distribution, and abundance) and cementation patterns within ichnofabrics. Burrows in slab and thin section were differentiated from the matrix based on

morphologic variations in grain type, size, sorting, and packing and were assigned to an ichnotaxon based on architectural and surficial morphologies and other ichnologic features (e.g., fill pattern, presence of meniscae or spreite, wall lining; cf. Hasiotis and Mitchell 1993; Bromley 1996).

High-resolution, x-ray computed tomography (micro-CT and CT; voxel sizes 45–50 μm and 500 μm, respectively) scans were acquired on six grainstone samples at Core Laboratories in Houston, Texas, using a GE Phoenix Nanotom m (micro-CT) and a Picker PQ2000 X-ray tomograph (CT). Scans were used to visualize the nature and spatial distribution of trace fossils in both two- and three-dimensions (2D and 3D). Two-dimensional scan images and data were processed into 3D volumes, imported into Petrel E&P software (2014), and manipulated using progressive filtering to reveal density heterogeneities corresponding to burrow morphology, distribution, and connectivity in 3D, providing perspectives on ichnofabric-related pore networks. The influence of ichnofabric on fluid-flow properties of carbonate grainstone were quantified through integration of image-analysis and CT scans.

Image analysis was conducted on digital scans of polished and unpolished slabbed samples, blue-epoxy-impregnated billet samples, and petrographic thin sections. Petrographic observations and image-analysis data were integrated with macro- and micro-CT images and processed 3D volumes to allow for evaluation of petrophysical heterogeneity within and among facies associations, lithofacies, and ichnofabrics.

Hand samples, polished and unpolished slabs, blue-epoxy-impregnated billets, and petrographic thin sections were digitally scanned and evaluated via image analysis. Integration of such data shows that trace fossils and ichnofabrics modify primary sedimentary fabrics, altering the distribution of grains, pores, and cement. Macro- and micro-CT data, including 2D cross-

sectional scans and processed 3D volumes, shows the distribution of trace fossils. Cross-sectional 2D images help distinguish between trace fossils and matrix, and processed 3D volumes show burrow morphology, orientation, and branching, as well as burrow connectivity (via tiering, cross-cutting, and branching) within samples. Furthermore, CT data show the distribution of porosity, which can be correlated to digital sample scans to reveal the influence of bioturbation on petrophysical characteristics of carbonate grainstone strata.

Synthesis.—Primary data from this study were integrated with information from field observations, weather reports, and published studies (e.g., Rankey 2014) to evaluate controls on spatial variability within and among depositional environments and sedimentary facies. Data were incorporated into ESRI ArcGIS for geospatial visualization, to facilitate the identification of ichnological and sedimentological trends and allow for comparison within and among deposits of all three ages.

RESULTS

Modern Leeward Margin: Geomorphology, Hydrodynamics, Sedimentology, and Ichnology

The leeward margin of CAP includes an unrimmed shelf 0.5–2.7 km wide, and mostly < 25-m deep, bordered to the east by islands (Crooked Island and Long Cay; Fig. 1B, C), and to the west by the dropoff to the deep-water Crooked Island Passage. The modern shelf includes three geomorphic elements: backshore, foreshore, and upper shoreface, each with distinct wave, current, and tidal conditions. In this study, a bioturbated upper shoreface is distinguished, and recognized as areas in which (at least seasonally) the rate of biological reworking exceeds the rate of physical reworking of the seafloor sediment, demonstrated by the pervasive to intense bioturbation (ii4–6) and paucity of physical sedimentary structures. Additionally, an ebb tidal

delta occurs in the central area near French Wells (Rankey 2014), but was not examined in detail. Characteristics of geomorphic elements (Fig. 2; Table 1) as well as shelf width, bathymetry, bottom type (Figs. 3, 4), ichnology (Fig. 5), and sedimentology (Fig. 6) vary along the arcuate leeward margin from north to south (Table 1).

Hydrodynamics.—Largely shielded from the prevailing easterly trade winds (e.g., Rankey and Reeder 2010), the western, leeward margin of CAP is most influenced by cold-front associated, long-period swell from the open Atlantic during the winter months, and infrequent but intense hurricanes and tropical storms during the summer months. Qualitative field observations indicate that the swell propagating from the north-northwest during the winter months results in different processes along the margin. In the central and south margin, the upper shoreface includes nearly constant reworking of the sediment-water interface, reflected in the presence of wave ripples and multi-directional current ripples. In contrast, the upper shoreface of the north margin is characterized by current ripples and nearshore bars as a result of southward-directed longshore currents.

Hydrodynamics change seasonally. During the summer months, the hydrodynamic processes on the leeward margin are relatively subdued, interrupted only episodically by storm activity. The sediment-water interface typically is stabilized by surficial microbial mats and devoid of ripple marks or bedforms in the summer. During the winter months (December–March), distal swell propagates from the NNW, and most influences the southern (northwest-facing) part of the arcuate margin (Fig. 1C; Tables 1–2).

North Margin.—The shelf of this margin (Fig. 1C) faces southwest, and is up to 1.9-km wide from the backshore berm to the shelf-slope break (Fig. 3A; Tables 1, 2). Low rocky cliffs (< 4-m above mean water level) of Pleistocene strata form the northernmost shoreline, extending

south ~6 km from Landrail Point. Modern borings are present in the Pleistocene outcrops along the length of the margin. Borings include *Entobia* and *Typanites*. South of the cliffs, Pleistocene outcrops pass inland (location of transect A–A' in Fig. 1C), and the shoreline is rocky (Holocene beachrock) and devoid of sediment (Fig. 4A). Sediment is thin (< 15-cm thick) to absent over beachrock or Pleistocene exposures in the foreshore, but where present, forms a gently sloping (≤ 5° gradient), narrow (~7-m wide) beach. The narrow beach is bounded landward by mature vegetation of the backshore, or rarely, by low-relief (≤ 0.3 m) sandy backshore berms. Sediment of the foreshore, backshore, and backshore berm is composed of well-sorted, medium skeletal-peloid sand. Skeletal grains are predominantly undifferentiated, rounded and abraded skeletal fragments with grain microstructures including microborings and thick micritic rims. Other skeletal grains include whole benthic foraminifera and rare, micritized *Halimeda* (Fig. 6A). Ooids are not present in the backshore or foreshore sediment in this northernmost area of the north margin. Tracemakers of the backshore and beach (upper foreshore) include ghost crabs (Ocypodidae), land crabs (e.g., *Cardisoma* sp.), land snails (e.g., *Cerion* sp.), and such terrestrial macrofauna as amphipods (e.g., Talitridae), arachnids, hermit crabs (e.g., Coenobitidae), lizards, and insects. Mottled fabric associated with pervasive bioturbation by amphipods and other meiofauna (cf. cryptobioturbation, Howard and Frey 1975) is common in the foreshore, backshore, and backshore berm. Discrete traces are sparse in the foreshore and backshore berm, and include J- and Y-shaped, ghost-crab burrows (*Polykladichnus*, *Psilonichnus*) as well as rare trackways of land snails, ghost crabs, and hermit crabs (*Archaeonassa*, *Diplichnites*, and *Coenobichnus*, respectively). Less common traces include feeding burrows (*Macaronichnus*), and dwelling burrows (e.g., *Arenicolites*, *Macanopsis*, *Skolithos*) with or without wall linings.

Seaward of the sediment-barren swash zone, the upper shoreface extends ~1 km (55% of the shelf width), and is relatively flat (~0.2° gradient), with large (up to 150-m diameter, 3-m relief) patch reefs in the shallow nearshore (4-m water depth, within 500 m of shore). Bottom types include a mixture of rocky bottom, active rippled bottom, bioturbated bottom (Fig. 4B), biofilm-stabilized sand, sparse seagrass, and patch reefs. Sediment cover is thin, and progressively thickens seaward, based on observations made by SCUBA of changes from rocky bottom to sediment bioturbation patterns with abundant large mounds from the foreshore to the shelf break and dropoff. Sediment is moderately sorted, coarse, composite grain-skeletal-peloid sand (Fig. 6B), with < 1% mud and rare ooids. Skeletal grains are pervasively micritized, undifferentiated skeletal fragments, as well as mollusk fragments, *Halimeda*, and foraminifera (e.g., *Miliolina* sp., *Peneroplis* sp.) with microborings and little skeletal ornamentation. Ooids are rare, in most cases composing < 3% of the sediment. Tracemakers include callianassid shrimp (Callianassidae), gastropods, goby fish (Gobiidae), and polychaete worms. Traces include abundant sinuous, surficial trackways up to 2 m long and 1–20 cm wide with raised edges (Fig. 4B), formed by echinoids (*Scolicia;* e.g., *Clypeaster* sp., *Mellita* sp.) and gastropods (*Archaeonassa;* e.g., *Xancus* sp.). Also common are hollow, vertical to subvertical tubes (up to 1-cm diameter, 8-cm long), with or without a ≤ 1-mm-thick lining of very fine sand and silt (*Skolithos*; e.g., Fig. 5F), and are attributed to polychaete worms (e.g., Gingras et al. 2008). At the surface, paired openings (≤ 2 cm in diameter and 7-cm apart) form U-shaped burrows (*Arenicolites*; Fig. 5E) attributed to interface feeding by nereid (Nereididae) polychaete worms, whereas Y-shaped burrows of similar surficial expression (*Polykladichnus*) are attributed to filter feeding by arenicolid (Arenicolidae) polychaete worms (e.g., Gingras et al. 2008). Ichnodiversity ranges from low (≤ 3 ichnogenera per m^2) in the proximal nearshore to moderate (4–5

ichnogenera per m^2) near the upper shoreface–bioturbated upper shoreface transition, and bioturbation intensity is ii2–3.

The upper shoreface–bioturbated upper shoreface transition in this northern area occurs at water depths of 5–6 m, and is marked by broad, margin-parallel barforms. The bioturbated upper shoreface covers ~50% (~0.9 km) of the shelf width, sloping up to 1.1° gradient towards the shelf-slope break at ~18 m depth. Bottom types include patchy distribution of sediment among rocky bottoms colonized by abundant corals, sponges, and gorgonians. The bioturbated upper shoreface is characterized by small-diameter patch reefs with relief ≤ 2.5-m. Sediment is typically biofilm-stabilized and thoroughly bioturbated (ii6), poorly sorted, very fine and medium sand with variable amounts of peloids, composite grains, and skeletal grains (Table 2). Mud content ranges from 2% at the upper shoreface–bioturbated upper shoreface transition to 34% at the shelf-slope break (Fig. 6C). Burrow density can exceed 1,000 traces/m^2 and ichnodiversity is high (≥ 8 ichnogenera). Discrete traces visible on the sediment-water interface include paired cylindrical openings (*Arenicolites*, *Polykladichnus*), pock marks ~3 cm in diameter and 1-cm deep (fish-feeding traces; *Piscichnus*), vertical tubes and cylindrical apertures 2 mm in diameter (*Skolithos*), along with cone-shaped mounds of varying sizes. Formed by callianassid shrimp, cone mounds typically have paired pits (Fig. 5G), and may be isolated or grouped with multiple, similarly sized mounds, each displaying a central, vertical shaft that extends below the sediment-water interface and (presumably) branches at depth to form a burrow network (*Ophiomorpha*, *Thalassinoides*).

Central Margin.—This margin shelf faces west, and is up to 2.6-km wide (Fig. 3B; Tables 1, 3). Shorelines are characterized by wide (up to 30 m), gently graded (≤ 5° gradient) sandy beaches, with discontinuous outcrops of poorly indurated Holocene strata and no

Pleistocene rocky cliff exposures (Fig. 4D). Up to 1.5 m in height, the backshore berm includes poorly cemented, vegetation-stabilized sand, or imbricated, cobble to boulder-size clasts of planar-laminated, fenestral grainstone. Up to 1 km of westward progradation is evident in Holocene beach-ridge sets near French Wells tidal inlet (Fig. 2A; Rankey 2014). Foreshore sediment is moderately well-sorted, fine–medium ooid-peloid-composite grain sand with varying amounts of skeletal fragments (Fig. 6D). Ooids have peloid nuclei and generally display ≤ 3 well-preserved laminae. Tracemakers include ghost crabs and terrestrial hermit crabs. Traces include rare (1/5 m^2), J- and Y-shaped burrows (*Psilonichnus*) with paired openings of identical aperture diameters (1.5–3 cm) located above the upper swash zone (Fig. 5A, B) where burrow depths extend down to cemented beachrock. Scratch marks and excavated sediment may be present surrounding the burrow opening on the sediment surface (Fig. 5A).

At the toe-of-beach, sediment is slightly coarser and more poorly sorted than beach sediment and the shallow nearshore is marked locally by a lag of rounded, pebble- to cobble-size intraclasts of coral rubble, beachrock, and grainstone lithoclasts. Shovel sampling revealed blood worms (Glyceridae) within the interstices of toe-of-beach sediment. Though no discrete traces were observed in this environment, such bioturbation may produce cryptobioturbation or indiscrete, mottled sedimentary fabric (i.e., *Macaronichnus*; Pemberton et al. 2008).

Outboard of the toe-of-beach, the upper shoreface slopes gently (≤ 0.3° gradient) to water depths up to 5 m. The upper shoreface covers ~50% (~1.1 km) of the shelf width, and bottom types include patch reefs and active wave and current ripples (Fig. 4E). The upper shoreface is characterized by moderately sorted, fine–medium, ooid-composite grain-skeletal sand (Fig. 6E). Shoreline-oblique barforms (Fig. 3A) have up to 1-m relief, with superimposed, small (20-cm spacing, 8-cm height) current or wave ripples (variable, depending on ambient conditions). Bar

crests exhibit little to no bioturbation (ii1–2). Off the crests of nearshore bars, in slightly deeper water, unidirectional current ripples exhibit higher amplitudes and spacing, and sediment is sparsely to moderately bioturbated (ii2–3) by bivalves, echinoids, and polychaete worms. Traces include U-shaped burrows (*Arenicolites*), shallow, cone-shaped resting traces 4–10 cm in diameter (*Conichnus*), as well as large, dish-shaped pits (up to 1-m diameter, 20-cm deep; *Piscichnus*). Lined and unlined vertical tubes (*Skolithos*) are also common. In general, ichnodiversity is low (≤ 3 ichnogenera per m^2), and bioturbation intensity is ii1–3.

The upper shoreface–bioturbated upper shoreface transition in this area occurs at ~5-m water depth. Reefs are most common along this margin and form elongate, margin-normal patch reefs up to 250-m long. In water depths ≥ 5 m, the gradient of the bioturbated upper shoreface increases to 1.1° toward the shelf-slope break at around 17-m water depth. The bioturbated upper shoreface covers ~55% (~1.2 km) of the shelf width, and is characterized by small (≤ 20-m diameter), low relief (up to 1.5 m) patch reefs, bioturbated and biofilm-stabilized sediment, and rocky bottom; active physical sedimentary structures are absent (Fig. 4F). Sediment is poorly sorted, trimodal, very fine, medium, and coarse peloid-ooid-skeletal sand with 4–17% mud (Fig. 6F). Ooids display < 4 laminae, and skeletal abundance increases toward the shelf-slope break, with grains displaying well-preserved ornamentation. Near the shelf-slope break, the seafloor is characterized by sparse, thin sediment cover among low-relief (up to 1 m) reefs composed of massive, encrusting, and platy corals, as well as soft corals and sponges. The shelf-slope break is oversteepened (> 70° gradient) in some areas, and is characterized by rocky bottom colonized by sponges, coral, and low-relief reefs, with localized patches of thin sediment. Tracemakers of the bioturbated upper shoreface include callianassids, gastropods, goby fish, polychaete worms, and rays. Small, cone-shaped divots (≥ 12-cm diameter, 3-cm deep; *Conichnus*) are the most

abundant of all traces. Also common are cone-shaped mounds (6–40-cm diameter, 2–20-cm relief) that may display apertures (0.8–1.5-cm diameter) and paired pits (Fig. 5G). Associated with cone-shaped mounds are surficial trackways 0.8–25 mm wide, 3 mm deep, and up to 80-cm long, with raised ridges ~8-mm wide on each side (*Archaeonassa*, *Scolicia*). Polychaete worms form open, vertical tubes ≤ 12-mm in diameter (*Polykladichnus*, *Skolithos*), and the feeding activity of rays produce wide, shallow (< 1-m diameter, 20-cm deep) dish-shaped impressions (*Piscichnus*). Where sediment cover is substantial, pervasive to complete bioturbation (ii5–6) is characterized by diverse trace assemblages (≥ 8 ichnogenera per m^2) and high burrow density.

South Margin.—This margin faces NW and includes the narrowest shelf on the leeward margin, ranging from 0.4–1.2-km wide (Figs. 2B, 3C; Tables 1, 4). Vegetation-stabilized backshore berm is the tallest on the leeward margin (up to 4-m relief), located at the crest of narrow (4–25-m wide; typically 10-m wide) and steeply dipping (> 7° gradient; Fig. 4G) sandy beaches, which progressively narrow to the south. In the southernmost part of Long Cay, sandy beaches are absent and Pleistocene outcrops form much of the shoreline. Beach sediment (Fig. 6G) ranges from well-sorted, fine ooid-composite grain-skeletal sand on the northern extent of the south margin, to moderately sorted, medium–coarse ooid-peloid-skeletal sand on the southern portion of the south margin. Ooids of the foreshore commonly display three or fewer laminae. Further south, the shelf orientation arcs from NW to NNW (Fig. 1C), and sediment composition changes to the south, as composite grains become less prevalent, abraded and rounded skeletal grains become more common. Tracemakers in the foreshore include ghost crabs, which produce rare (~3/5 m^2) J-shaped burrows (*Psilonichnus*) at the crest of the beach, usually within ~2 m of beachrock exposure.

At the base of the relatively steep swash zone water depths can drop to as much as 3.4 m, producing the most pronounced beach step observed on the leeward margin. Sediment of the toe-of-beach is poorly sorted, medium to very coarse skeletal sand. Shovel sampling found blood worm (Glyceridae) within sediment interstices. No discrete traces were observed due to constant reworking by swash and breaking waves, though indiscrete mottling is likely (i.e., *Macaronichnus*).

Seaward of the toe-of-beach, the upper shoreface extends westward to ~17-m water depth. The upper shoreface is ~0.6-km wide, and the shelf gradient is 1.3°. The upper shoreface composes ~85% of the total shelf width. Bottom types vary considerably along and across this part of the shelf (Fig. 2B). Here, a substantial portion of the upper shoreface is a flat, rocky bottom, with little to no relief (< 50 cm) covered by individual corals and patch reefs (Fig. 4I). Rocky bottom and patch reefs alternate with rippled areas in water depth ≤ 10 m. Local, sinuous-crested, three-dimensional subaqueous dunes up to 0.8-m high, display superimposed current ripples (Fig. 4H). Sediment is moderately sorted, medium–coarse skeletal-peloid sand that includes *Halimeda,* foraminifera, mollusk, sponge, and coralline algae fragments. Skeletal grains are rounded and lack grain ornamentation. In contrast, sediment in the subaqueous dunes consists of moderately well-sorted, fine ooid-skeletal sand (Fig. 6H), but a lag of boulder-size clasts of coral rubble are present in lows between subaqueous dunes. Polychaete worms and goby fish are the only tracemakers evident in the subaqueous dunes, with rare fish burrows (e.g., Fig. 5H) present at the interface of rocky bottom and sediment. Traces within sediment-filled lows include 6-mm-diameter, ~40-cm-long agglutinated worm tubes (*Skolithos*) on ripple crests that can extend up to 8 cm above the sediment-water interface (Fig. 5F). Bioturbation is sparse to absent (ii1–2), composed of low-diversity assemblages dominated by *Skolithos*. The most pronounced

break in slope occurs in the upper shoreface at ~13-m depth (Figs. 2B; 3C) and is characterized by bare rocky bottom (Fig. 4I). Outboard of the break, the shelf gradient increases considerably to ~19° in a series of 5-m-scale steps with low-relief (≤ 0.5 m) patch reefs (Fig. 3C).

The bioturbated upper shoreface occurs outboard of the shelf-slope break at water depths ≥ 17 m, and covers an area ~0.1 km wide, composing only 10% of the shelf width. Sediment is moderately sorted, trimodal, fine, medium, and coarse ooid-skeletal sand with minor composite grains (Fig. 6I), and physical sedimentary structures are rare. Biota include abundant sponges, callianassid shrimp, gastropods, massive corals, polychaete worms, and gorgonians. Traces include paired openings (*Arenicolites*), agglutinated worm tubes (*Palaeophycus*, *Skolithos*; Fig. 5F), small, conical depressions (*Conichnus*; Fig. 5I), cone mounds (*Ophiomorpha*, *Thalassinoides*), dish-shaped depressions (*Piscichnus*; Fig. 5I), surficial trails (*Scolicia*), and unlined vertical burrows with 8-mm-diameter apertures (*Skolithos*). On the flattest part of the steps, callianassid shrimp form localized groupings of 2–3 large (30-cm diameter, 20-cm height) cone-shaped mounds at ~5-m spacing. Cone mounds of such groupings lack paired pits. Ichnodiversity is moderate (typically 2–4 ichnogenera per m^2) and bioturbation is typically sparse to moderate intensity (ii2–3), although localized areas may display high (ii4) bioturbation intensity.

Pleistocene and Holocene Stratigraphy, Sedimentology, and Ichnology

Pleistocene and Holocene strata exposed along western Crooked Island and Long Cay record the evolution of the leeward margin. Strata form subparallel ridges with ridge and swale topography (up to several m of relief, Fig. 2A). Although absolute ages of strata are unknown, geometric and crosscutting relationships (e.g., truncation, onlap, superposition) document at least

seven stages of Pleistocene and Holocene progradational ridge growth on Long Cay (Fig. 7). These relations show that progradation built Long Cay along strike from NE to SW (ridge sets 1–3, Fig. 7B), then prograded to the W (set 4) and N (sets 5–6). Subsequent Holocene progradation occurred in multiple directions. The thickest outcrop successions occur in association with topographic ridge crests (up to 7-m relief) and are best exposed in cliffs along the shoreline.

Pleistocene and Holocene strata are composed of seven lithofacies (LFA–G; Table 5), subdivided based on sedimentary texture, lithology, physical sedimentary structures, ichnologic features, and pedogenic features (Figs. 8–10). Lithofacies form three facies associations (FA1–3), one Holocene and two Pleistocene (Fig. 10), based on stratigraphic relationships and stacking patterns. The relatively thin (≤ 3 m) exposures of Holocene successions are comprised of only the most proximal lithofacies (LFE, LFF) with superimposed LFG, compared to the full range of lithofacies represented in the thicker (up to 7-m relief above mean water level) Pleistocene successions.

Holocene Facies Association (HFA).—Holocene strata only outcrop on the central and south margins, forming stratigraphically and sedimentologically distinct facies successions. Holocene successions consist of two to three lithofacies, and exposures are low relief (≤ 3-m relief above mean water level), typically outcrop in the modern foreshore and backshore, and strike parallel to the present shoreline (Fig. 4G).

Central-margin successions are characteristically low exposures (< 1-m relief above mean water level) of poorly-indurated strata (LFE), composed of moderately well- to well-sorted, ooid-skeletal grainstone with gently seaward-dipping laminations of alternating medium and fine sand, fenestrae, and interbedded, cobble-sized intraclasts of coral rubble and grainstone (Fig. 8A, B). Laminae are variably cemented by meniscus blocky calcite cement (Fig. 8C). The lithofacies

is sparsely to moderately bioturbated (ii2–3) with low-diversity trace-fossil assemblages with *Asterosoma*, *Bergaueria*, *Conichnus*, *Cylindrichnus*, *Macaronichnus*, *Ophiomorpha*, *Psilonichnus*, and *Skolithos.* Lithofacies F (LFF) is rare in the central margin (and so is described in detail below), and Lithofacies G (LFG) is characterized by ubiquitous rhizoliths (e.g., molds, casts, rhizocretions). In parts of the central margin, Holocene successions are capped by coarse blocks of fenestral, laminated grainstone, which are locally imbricated and analogous in size, position, and geometry to modern hurricane deposits (Rankey 2014).

The character of Holocene strata changes toward the south margin (Fig. 1C), where outcrops are more continuous and better cemented, with greater relief (up to 3-m above mean water level) and more variable stratigraphy. Successions consist of two lithofacies (LFE and LFF), overlain by a diagenetically altered strata below a discontinuity surface (LFG). The base of the succession is characterized by a 1–2-m-thick unit of ooid-skeletal grainstone with low-angle, cross- and planar-laminations and fenestrae (LFE). The lithofacies may contain rounded, cobble-size clasts of well-sorted, fine–medium fenestral ooid-peloid grainstone. Within LFE, bioturbation intensity is ii2–3, and trace-fossil assemblages include simple planiform burrows (i.e. *Macaronichnus*, *Palaeophycus*, and *Planolites*), as well as large-scale (up to 8-cm diameter), penetrative, dissolution-widened burrows (Fig. 8A) similar to *Psilonichnus* and *Skolithos*. Lithofacies E is typically overlain by LFF, a unit of laterally discontinuous, swaley bedsets with topset-to-toeset relief up to 2 m. Bedset-dip direction and angle are spatially variable, and internal stratification is typically weak to absent. Within LFF, intense to complete bioturbation (ii5–6) is associated with the presence of indistinct mottled texture, ubiquitous rhizoliths, and preservation of few discrete trace fossils including *Psilonichnus* and *Skolithos*. Resistant calcareous crusts, referred to as hardpans, characterize LFG (e.g., James 1972; Esteban and

Klappa 1983), as well as well-developed laminated crusts and autoclastic brecciation. These deposits form topographic ridges (1–3-m relief), which roughly parallel the trend of the modern shoreline, and compose the ridge and swale topography observed in satellite images of islands (Rankey, 2014).

Interpretation.—Holocene strata on the central margin are interpreted as a foreshore (LFE) deposits, capped by subaerial exposure surfaces with pedogenesis (LFG), by analogy to sedimentologic and ichnologic characters of modern sediment. These are preserved as beachrock (e.g., Ginsburg 1953; Inden and Moore 1983; Scoffin and Stoddart 1983; Curran and White 1987; Rankey 2014). Holocene strata on the south margin are interpreted to represent shallowing-upward successions deposited in foreshore (LFE) and backshore (LFF) environments, capped by surfaces of subaerial exposure and pedogenesis (LFG).

Pleistocene Facies Association 1 (FA1).—Pleistocene FA1 successions consist of five lithofacies, and are typical of the north margin, where exposures generally have ≤ 4-m relief above mean water level (Fig. 10). The base of the succession is characterized by LFB, which forms a ≤ 2-m-thick unit of moderately sorted, bimodal, very fine- and medium-grained, ooid-composite grain-skeletal grainstone (Fig. 9D–F). The lithofacies is intensely bioturbated (ii4–6), with vaguely preserved trough cross-stratification. Some outcrops contain interbedded unit(s) of cobble-size intraclasts (Fig. 9E) of the same lithofacies. Ooids are superficial, with few poorly preserved laminae, and micritization and partial dissolution result in poorly preserved grain microstructures. Diverse, multi-tier trace-fossil assemblages (Fig. 9F, 11E) include *Cylindrichnus*, *Ophiomorpha*, *Palaeophycus*, *Planolites, Scolicia*, *Skolithos*, and *Thalassinoides*.

Stratigraphically above LFB, LFC consists of a ≤ 1-m-thick unit defined by sharp-based, medium to thick (30–80 cm) trough cross-stratification bedsets composed of poorly to

moderately well-sorted, ooid-peloid-skeletal grainstone. In plan view, trough cross-stratification bedsets display rib and furrow features, the majority of which indicate a southward paleocurrent direction (Fig. 9H). Bimodal grain-size distributions of very fine to coarse sand are common, and bioturbation intensity varies from ii2 to ii5, but typically is ii3. Trace-fossil assemblages are moderately diverse, including *Cylindrichnus*, *Diplocraterion, Lingulichnus, Ophiomorpha*, and *Skolithos.* Burrows penetrate up to 80 cm, and can extend through several bedsets.

Above LFC strata, LFD is typically composed of three subunits with a total unit thickness of ≤ 2 m. The lithofacies is characterized by an upward transition from 1) bidirectional, decimeter-scale, planar crossbeds; to 2) trough cross-stratification beds with toesets of poorly sorted, coarse-sand to gravel-size skeletal grainstone with rounded, cobble-size intraclasts; and overlain by 3) thin (2–5 cm) bedsets of multidirectional current ripple, climbing ripple, and trough cross-stratification with abundant internal scour surfaces (Figs. 9J–L). Bioturbation intensity is ii3–5, and diverse trace-fossil assemblages comprise two suites: 1) cm-scale *Conichnus*, *Cylindrichnus*, *Ophiomorpha*, *Piscichnus*, *Polykladichnus*, *Rosselia*, and *Skolithos*, within planar crossbeds; and 2) *Conichnus*, *Ophiomorpha*, and *Skolithos* of varying size and tiering depth within rippled bedsets.

Near the top of FA1 successions, LFE is a < 1-m-thick unit of gently (< 10°) seaward-dipping, planar-laminated, fenestral, moderately well-sorted, fine ooid-peloid-skeletal grainstone (Figs. 8A–C). Bioturbation intensity is ii3, with low-diversity, trace-fossil assemblages dominated by *Skolithos* and cm-scale, vertical forms of *Ophiomorpha* and *Thalassinoides* with up to 15 cm of vertical tiering. Less common trace fossils include bedding-plane expressions of *Archaeonassa*, *Bergaueria*, and *Scolicia*.

Swaley bedsets of LFF typically are absent within FA1 deposits of the north margin, where the succession is capped by a discontinuity surface, labeled LFG. Lithofacies G is characterized by the presence of multiple laminated micritic crusts (Fig. 8G), ubiquitous rhizoliths, and autoclastic brecciation (Fig. 8H), as well as blackened grains, calcified fine roots and root hairs, moldic porosity, microspar cement, and multiple generations of micritic cement with some alveolar textures (Fig. 8I).

The macro- and microstructures that define LFG are indicative of subaerial exposure and pedogenic processes, which are unique to terrestrial settings (e.g., Esteban 1974; Strasser 1984; Goldstein 1988; Bain and Foos 1993; Hasiotis 2007; Hasiotis et al. 2007, Hasiotis and Platt 2012). Lithofacies G is interpreted to represent a pedogenec overprint of the original sedimentary fabric, resulting from subaerial exposure. Laminated micritic crusts exhibit features similar to those described by Multer and Hoffmeister (1968) and James (1972), and are interpreted as calcrete soils developed under semiarid conditions (e.g., Klappa 1980b; Wright et al. 1988; Rossinsky and Wanless 1992).

Interpretation.—By analogy with the sedimentologic and ichnologic character of modern sediment, FA1 is interpreted to represent shallowing-upward successions of genetically related strata deposited in bioturbated upper shoreface (LFB), upper shoreface (LFC, LFD), and foreshore (LFE) environments (Figs. 8–11) capped by subaerial exposure surfaces with pedogenesis (LFG). Cobble-size intraclasts are interpreted to represent broken beachrock rounded by wave action (e.g., Strasser and Davaud 1986; Aurell et al. 1995).

Pleistocene Facies Association 2 (FA2).—Pleistocene FA2 successions consist of six lithofacies and are common of the south margin, where exposures have up to 7-m relief above mean water level (Fig. 10). At the base of the succession, LFA exhibits localized coral

boundstone and rudstone exposed up to 2 m above mean water level (Fig. 9A). Poorly to moderately sorted, fine to very coarse grained, skeletal-ooid-composite grain grainstone infills the boundstone framework and composes the rudstone matrix. The flanks of the boundstone-rudstone core are interbedded with decimeter-scale, sigmoidal and trough cross-stratification bedsets that dip and pinch out laterally. Rudstone and grainstone are composed of coral rubble as well as whole, abraded, and disarticulated mollusks, foraminifera, *Halimeda*, and coralline algae (Fig. 9B–C). Trace-fossil assemblages are highly variable, with vertical and lateral changes in trace abundance, diversity, and dominant ichnogenera. Bioturbation intensity ranges from ii1–6, but typically ii1–3. Trace fossils include vertical, subvertical, and horizontal burrows that display burrow linings (e.g., *Cylindrichnus*, *Rosselia*), and reinforced walls (e.g., *Ophiomorpha*, *Palaeophycus, Skolithos*). Assemblages are dominated by *Ophiomorpha*, *Palaeophycus*, and *Skolithos* within coral rubble and grainstone, whereas *Thalassinoides* is locally abundant in intervals of fine sand.

Where LFA is not present above water level, the base of FA2 successions are characterized by up to 3 m of LFB, with 0.3–1-m-thick bedsets of multidirectional trough cross-stratification (Fig. 9D). Moderately sorted, bimodal fine sand- to gravel-sized ooid-peloid-composite grain grainstone contains varying amounts of skeletal material. Ooids have thick, well-preserved laminae, and skeletal grains typically are abraded. Bioturbation intensity is ii1–3, with low diversity, shallow-tier, trace-fossil assemblages. Trace fossils include *Macaronichnus*, *Palaeophycus*, and *Planolites*, as well as sparse *Ophiomorpha* and *Skolithos*.

In some outcrops, LFB is overlain by a < 2-m-thick unit of LFD. Lithofacies D is characterized by poorly sorted, coarse-grained, skeletal-ooid-composite grain grainstone with small-scale trough cross-stratification at the base. LFD is commonly interbedded with spatially

discontinuous cobble-rich units (Figs. 9J, 12). Cobbles are rounded and composed of planar-laminated to low-angle, cross-laminated grainstone within a coarse sand to gravel skeletal grainstone matrix. Bioturbation intensity is ii1–3, and trace fossils were observed only in the lower, cross-laminated unit. Trace fossils include cm-scale, vertically oriented *Ophiomorpha*, and small-scale (< 5-mm diameter) *Skolithos* and *Thalassinoides*.

Lithofacies E overlies either LFB or LFD and consists of multiple wedge sets of gently seaward-dipping strata up to 4-m thick. Wedge-set stratification includes low-angle (≤ 10°), cross- and planar-laminated, moderately well- to well-sorted, medium ooid grainstone with peloids and composite grains (Fig. 12). Sharp-based bedsets consist of alternating laminations of coarse and fine sand and fenestrae, and bedding planes may exhibit rill markings. Bioturbation intensity is ii1–3, with moderately diverse trace-fossil assemblages of locally abundant *Macaronichnus*, *Palaeophycus*, and *Planolites*, overprinted by sparse escape traces (fugichnia), as well as *Ophiomorpha*, *Polykladichnus*, and *Skolithos*.

Lithofacies F overlies LFE and forms the uppermost depositional unit within FA2 successions. Up to 3-m thick, LFF consists of large-scale swaley bedsets and gently landward-dipping bedsets of moderately well- to well-sorted, fine-grained ooid-peloid grainstone. High-angle swaley foresets have topset-to-toeset relief up to 2 m and exhibit variable dip directions (Figs. 8D–F; 12). Bedsets are laterally discontinuous, with weak internal stratification and abundant rhizoliths. Planar laminations of coarse and fine sand at the base of bedsets transition upwards to massive, mottled textures with increased rhizolith abundance. Weak internal stratification is interpreted as the combined influence of abundant plant roots and intense bioturbation (ii5–6) by such terrestrial organisms as amphipods, arachnids, and insects. Although

burrow mottling is most common, discrete trace fossils within LFF include *Diplocraterion*, *Palaeophycus*, *Planolites*, and *Skolithos*.

Facies Association 2 is capped by LFG, a discontinuity surface with characteristics similar to LFG as described in FA1 successions (Table 5). Lithofacies G is highly variable, both vertically and laterally, with a gradational lower contact. The lithofacies is characterized by ubiquitous rhizoliths, one or more laminated micritic crusts, alveolar textures, blackened grains, and autoclastic brecciation (Fig. G–I; e.g., Stricklin and Smith 1973; Klappa 1980a, 1980b, 1983).

Interpretation.—The sedimentologic and ichnologic character of FA2 suggest shallow-marine deposition in reef (LFA) and upper shoreface (LFB, LFD) settings, as well foreshore (LFE), and backshore (LFF) environments (Figs. 8–11), with each shallowing-upward succession capped by a discontinuity surface (LFG; Fig. 8; Table 5). Lithofacies G is indicative of subaerial exposure with pedogenesis (e.g., Esteban 1974; Esteban and Klappa 1983; Wright et al. 1988; Kraus 1999; Kraus and Hasiotis 2006).

Ichnofabric of Pleistocene Shoreface Strata

As observed on the modern shelf, the burrowing activities of benthic organisms physically and chemically modify the depositional characteristics and sedimentary fabrics of shallow-marine carbonate deposits. Bioturbation produces a range of ichnofabric in Pleistocene and Holocene strata (Fig. 12; Table 6), which reflect the collective ichnologic influence on depositional sedimentary fabric. Ichnofabric is defined based on overall bioturbation intensity, ichnodiversity, and tiering, as well as trace-fossil abundance, distribution, and architectural and surficial morphologies (e.g., Ekdale and Bromley 1983; Hasiotis and Mitchell 1993; Taylor and

Goldring 1993; Hasiotis and Dubiel 1994). Ichnofabric within Pleistocene and Holocene strata are subdivided into six classes that display a range of petrophysical significance (Fig. 13, Table 6).

Ichnofabric I: Nonbioturbated Fabric.—This ichnofabric is characterized by well-preserved primary sedimentary structures with no evidence of biogenic modification. Ichnofabric I is exceedingly rare, and was only observed within the boundstone and pebble-sized rudstone of LFA deposits. Characterization of this ichnofabric is limited, due to the infrequent occurrence in Pleistocene and Holocene strata. Primary sedimentary fabrics unmodified by biogenic processes are attributed to media instability caused by high rates of sedimentation and/or physical reworking, leading to unfavorable conditions for burrowing organisms, or to the poor preservation of traces in the shifting sediment. As CAP shoreface environments are characterized by normal, open-marine conditions with favorable oxygen and nutrient levels, this ichnofabric is strongly influenced by physical reworking by fair-weather waves, and/or high sedimentation rate.

Ichnofabric II: Network Burrow Ichnofabric.—This ichnofabric is characterized by systems of vertical, inclined, and horizontal burrow components that branch and interconnect to form three-dimensional (3D) networks (Fig. 13I–L) . The burrow networks range from simple structures of predominantly horizontal orientation (cf. mazes; Frey and Pemberton 1985) to relatively large (typically cm-scale), well-integrated 3D boxwork structures comprised of intricately branched and interconnected shafts and tunnels (e.g., Frey and Pemberton 1985).

Larger, cm-scale trace fossils that comprise burrow networks overprint a mottled background fabric characterized by few discrete burrow structures (e.g., *Macaronichnus*, *Palaeophycus*, *Planolites*). The burrow-mottled background fabric is interpreted to result from

the dense distribution of shallow-tier traces. The mottled background fabric is overprinted by deep-tier (burrow penetration up to 80-cm), vertical (e.g., *Siphonichnus*) and inclined (e.g., *Cylindrichnus*) burrows as well as boxwork systems of vertical to inclined shafts and chambers (e.g., *Ophiomorpha*, *Thalassinoides*) connected by horizontal components.

This ichnofabric is most common within sharp-based to amalgamated bedsets (5–50-cm thick) of trough-cross stratification and low-angle, cross-stratification. Abundant assemblages of diverse trace fossils with a wide range of morphologies overprint the depositional sedimentary fabric (Fig. 12A–C). Dominant trace fossils include *Ophiomorpha*, *Palaeophycus*, *Rosselia*, *Skolithos*, and *Thalassinoides*. Burrows may exceed 3 cm in diameter with up to 5-mm-thick wall linings. Burrow walls can be unlined (e.g., *Thalassinoides*), lined with organic matter (e.g., *Cylindrichnus*, *Rosselia*), or lined with round, cylindrical, or irregular pellets to produce a mammillated exterior (e.g., *Ophiomorpha*; Häntzschel 1975; Frey et al. 1978). The vague preservation of physical sedimentary structures, combined with the dense distribution of abundant and diverse trace fossils reflect the high to intense bioturbation (ii4–5). Compared with the surrounding host rock, burrow fill is commonly less well cemented, with coarser grained, more loosely packed sediment than the matrix (Fig. 12C). Burrow fills can be structureless or show slight grain-size alignments indicating active backfill by the tracemaker. Porosity is primary interparticle porosity, with abundant macroporosity in some samples. Some burrows are surrounded by a narrow ($\leq$ 8 mm), low-porosity zone where interparticle pores are occluded by blocky calcite cement. Preserved porosity in the matrix between burrows is dominantly intraparticle microporosity, with primary interparticle porosity occluded by isopachous fibrous and interparticle mosaic blocky calcite cement.

Ichnofabric III: Spreiten and Nonspreiten Ichnofabric.—This ichnofabric is characterized by diverse assemblages of minute (≤ 5-mm diameter), horizontal, subvertical, and U-shaped burrows that overprint and crosscut one another (Fig. 12D–F). Due to the small size of the individual trace fossils, this ichnofabric is best observed in polished slabs and thin section. Though present in all lithofacies, this ichnofabric is most prevalent within the upper units of shallowing upwards successions (LFD, LFE, LFF), with bedsets typically displaying upward increase in both bioturbation intensity and ichnodiversity. Ichnofabric III displays a range of tiering, from bedding-parallel, planiform burrows, to vertical U-shaped burrows that may crosscut, branch, or exhibit spreiten (e.g., *Diplocraterion*, *Polykladichnus*, *Scolicia*, *Skolithos*). The diverse architectural morphologies, crosscutting relationships, and tiering of trace fossils are interpreted to reflect multiple generations of burrowing organisms.

Ichnofabric IV: Discrete Planiform-Burrow Ichnofabric.—This ichnofabric is defined by low-diversity trace-fossil assemblages of simple, bedding-parallel planiform burrows with bioturbation intensity ii2–3 (Fig. 12G–I). Although a minor component of all lithofacies, this ichnofabric is characteristic of parallel-laminated to low-angle, cross-laminated LFE deposits. Burrows are 0.1–2 cm in diameter, and typically do not branch or exhibit significant vertical tiering. The ichnofabric reflects the spatial variability in uniformity of burrowing and bioturbation intensity, and typically displays an upwards increase within individual bedsets.

Discrete trace fossils are differentiated from the matrix by the presence of a thin lining on the burrow wall (e.g., *Palaeophycus*), burrow fill that is sedimentologically or diagenetically different than the matrix (e.g., *Planolites*), or fill of similar composition to the matrix, delineated by subtle grain alignment (e.g., *Macaronichnus*). Burrow abundance and distribution are highly

variable, with greater bioturbation intensity present in coarser intervals, resulting in modification of grain-size distribution and depositional laminations.

Ichnofabric V: Reinforced Vertical-Burrow Ichnofabric.—This ichnofabric is defined by low-diversity assemblages of sparse to locally abundant, vertical and inclined burrows with reinforced walls (Fig. 12J–L). This ichnofabric is typical of crossbedded, medium- to coarse-grained oolitic and skeletal grainstone deposits with low–moderate bioturbation intensity (ii2–3) (Fig. 13E–H). Ichnofabric V is common within the upper lithofacies of FA1 (LFC–E) and the lower lithofacies of FA2 (LFA, B, D) (Fig. 10). Burrow-wall linings stabilize and reinforce the structures and are indicative of unstable, shifting media conditions. Burrow walls are reinforced with thin linings of mucus and trapped sediment (i.e., agglutinated sand; *Palaeophycus* and *Skolithos*) or linings of ovoid to spherical sand pellets (e.g., *Ophiomorpha*). *Ophiomorpha* burrows (2–4-cm in diameter) are characterized by smooth interior walls, and mammillated exterior walls with regular (*O. nodosa*) or irregular (*O. irregulaire*) distribution of pellets. Burrows may cross or interpenetrate, especially common within LFD of FA1, though sparse distribution of burrows is typical. Burrow fill varies by lithology and facies association, and includes structureless, loosely packed coarse skeletal sand as well as very fine to fine peloidal sand. *Ophiomorpha* are dominated by vertical burrow components, but may also branch to form irregular boxworks (Fig. 12J). Overall, burrow connectivity is highly variable, ranging from isolated shafts to locally interconnected mazes and boxworks.

Ichnofabric VI: Cryptobioturbated Ichnofabric.—Ichnofabric VI is distinguished by intense to complete bioturbation (ii5–6) by exceedingly abundant, indistinct trace fossils to produce a mottled fabric with few discrete traces (Fig. 12M–O, Fig. 13A–D). This ichnofabric is prevalent in crossbedded strata of FA1 (LFB and LFC), and planar-laminated and low-angle

cross-laminated strata (LFE) and swaley crossbeds (LFF) of FA2 (Fig. 12M–O). The burrow-mottled fabric, referred to as cryptobioturbation (e.g., Pemberton et al. 2008), is the result of the dense distribution of cylindrical, bedding-parallel burrows (≤ 2-mm diameter), which may preserve, alter, or destroy physical sedimentary structures. Where identifiable, discrete trace fossils include *Macaronichnus*, *Palaeophycus*, and *Planolites*. Cryptobioturbation of this ichnofabric reflects trace-fossil assemblages of monospecific to low ichnodiversity, and is interpreted to represent deposit-feeding by marine polychaete worms (e.g., Clifton and Thompson 1978).

DISCUSSION

Controls on Spatial Variability of Sedimentary Facies and Bioturbation

Observations from the modern leeward shelf margin of CAP reveal geomorphic, sedimentologic, and ichnologic variability, changes that also are reflected in both Holocene and Pleistocene strata. The nature and distribution of sediment, benthic organisms, and modern traces vary within and among shoreface subenvironments along the length of the leeward margin, and demonstrate links among geomorphic setting, sedimentary facies, and trace assemblages (Fig. 14). Research results indicate that the hydrodynamics and platform orientation play a major role in the spatial distribution of sediment and bioturbation. The following sections discuss the controls on the variability of bioturbation and resultant ichnofabrics in modern settings, and how they are used to interpret similar controls in the Holocene and Pleistocene.

Sediment and Bottom Types of the Modern Shelf.—The low-energy shoreface system of the SW-facing north margin lies just south of rocky Pleistocene cliffs and is flanked by a narrow, patch reef to rocky shelf. The north margin is protected from the distal swell from the

north or northwest, and likely has a low rate of sediment supply from the north. These dynamics are reflected in several sedimentologic patterns. Nearshore, the rocky shoreline, paucity of backshore berms, vegetated backshore, and the southward-widening wedge of Holocene beach ridges (Fig. 2A) are all consistent with the low rate of sediment supply on the north margin. The influence of southward-directed longshore currents (Rankey 2014) is reflected in the shallow, proximal upper shoreface by the shoreline-oblique, low subaqueous barforms. Aside from these barforms, and at water depths > ~5 m, the sediment-water interface typically exhibits a microbial mat or intense bioturbation, indicative of infrequent disturbance by waves or currents relative to the rate of reworking. Overall, the fine-grained sediment on the north shelf and the mud content (2–34%) higher than areas further south reflect the lower energy setting.

These patterns are distinct from areas further south along the margin. For example, the west-facing central margin shoreline includes laterally discontinuous, low-relief backshore berms and wide, gently sloping sandy beaches (foreshore), although local beachrock exposures are present. The upper shoreface here includes well-developed shoreline-oblique barforms, and an ebb tidal delta near French Wells. These accumulations, dominated by physical energy, pass outboard to the bioturbated upper shoreface at depths > 5 m. This bioturbated upper shoreface includes stabilized, flat to bioturbated bottom with scattered patch reefs, and between 4–17% mud.

Differences are even greater on the south margin, an area that faces into the brunt of waves generated by winter cold fronts and which is exposed to open-ocean swell. There, the shoreline includes higher relief and more continuous backshore berms, flanked by steeper and coarser beaches. Outboard of the foreshore, the upper shoreface in water depths up to 17 m is characterized by a mix of bare rocky bottom, subaqueous dunes and wave-rippled sediment,

scattered patch reefs, and a paucity of biogenic structures, all of which reflect consistent high energy conditions. The bare rocky bottom of the outer upper shoreface indicates off-bank sediment transport caused by offshore currents. The narrow bioturbated upper shoreface, at water depths > 17 m, includes fine to coarse, ooid-skeletal sand with rare physical sedimentary structures.

Distribution of Bioturbation.—Although the study area extends for < 35 km along strike, it includes highly variable ichnologic assemblages and ichnofabrics at varied depths along the margin. The rocky shores of the north shelf, exposed as cliffs or low rocky outcrops include only borings. Sandy beaches of the central and south margin upper foreshore display moderate bioturbation intensity (typically ii3), with sparse ghost crab burrows (*Psilonichnus*), as well as dwelling and locomotion traces of echinoids, crustaceans, and polychaete worms. Such assemblages are assigned to the Psilonichnus Ichnofacies (upper foreshore and backshore berm) and archetypal Skolithos Ichnofacies (lower foreshore and toe-of-beach). The modern borings in the Pleistocene and Holocene outcrops along the margin are assigned to the Trypanites Ichnofacies.

One upper shoreface end member, the north shelf, includes ichnologic characteristics indicative of low-energy conditions. The upper shoreface here includes moderate bioturbation intensity (ii3), with a low-diversity Scolicia-Skolithos assemblage representing predominantly filter- and deposit-feeding (with minor predation and locomotion) behaviors of callianassids, echinoids, mollusks, and polychaetes. The moderate degree of bioturbation is evident in the presence of burrow-modified ripples, reflecting a high rate of biologic reworking of sediment, relative to physical reworking at the sediment-water interface. Trace assemblages represent the proximal Cruziana Ichnofacies (Fig. 15). In contrast, trace assemblages of the central and south

margin upper shoreface are characterized by rare to sparse distribution of simple dwelling and predation burrows with bioturbation intensity ii2 (central margin) and ≤ ii3, though ii1 (south margin) are typical. Thus, the upper shoreface of the north margin is considerably more bioturbated, with greater ichnologic and ethologic diversity, than the upper shoreface of the central or south margins.

The character and depth of the bioturbated upper shoreface also varies along strike. In the bioturbated upper shoreface, the position, depth range, and characteristic trace assemblages are generally similar on the north and central margins. There, at water depths generally > 17 m, abundant tracemakers produce diverse traces of high to complete bioturbation intensity (ii4–6; Tables 2, 3). In contrast, the bioturbated upper shoreface of the south margin is present only at water depths > 17 m, and comprises a much smaller portion of the shelf. The bioturbated upper shoreface of the south margin is characterized by sparse to moderate bioturbation intensity (ii2–3) with low-diversity assemblages dominated by vertical burrows with reinforced walls (e.g., *Ophiomorpha*, *Skolithos*). This assemblage is similar to the archetypal Skolithos Ichnofacies.

Synthesis.—Regional changes in margin orientation result in along-strike variability in depositional energy from tides, waves from passage of cold fronts, and open-ocean swell. These dynamics are interpreted to influence sediment and organism distribution, bottom-type changes along and across strike, beach ridge progradation patterns, and the relative rates of physical versus biological reworking.

The north margin is largely protected from storm waves and swell due to the Crooked Island shoreline, which creates the embayed, protected margin (Fig. 1C). This SW-facing north margin is most influenced by weak, southward longshore currents, reflected in the fine sediment, low sediment supply, and rare ooids. The transitional central margin, with low backshore berms,

gently dipping beaches, broader Holocene beach ridges, and abundant nearshore oolitic bars, reflects an intermediate energy level. The south margin, which faces into storm waves generated by the passage of winter cold fronts and open-Atlantic swell, includes tall backshore berms, steep beaches, and a deep upper shoreface, and represents the highest energy setting along this margin.

Neoichnology of the modern shelf displays comparable along- and across-strike variability. The general patterns of diverse and intense biotic activity to the north and minimal bioturbation to the south reflect changes in the distribution and constituents of benthic organisms, behaviors, and hence, the resulting ichnofabrics. Trace abundance and distribution record changes in the distribution of benthic organisms and behaviors consistent with depositional conditions associated with the progressive, north to south increase in hydrodynamic energy.

Pleistocene and Holocene Strata

The orientation, spatial distribution, and crosscutting relationships of topographic beach ridges reveal the progradation history and evolution of the leeward margin, and provide a framework for interpreting vertical stacking patterns and stratigraphy of FA1 and FA2 successions. Crosscutting relationships of beach ridges (Fig. 7) evident in satellite images of Crooked Island and Long Cay reveal diverse progradation patterns. In the north margin area of Crooked Island, progradation of Pleistocene ridges are characterized by few, laterally continuous beach-ridge sets which arc oriented south to southeast, and beach-ridge orientation shows at least two stages of progradation (Fig. 1C). In contrast, spatial relationships between topographic ridge sets of the south margin reveal complex patterns of progradation, longshore accretion, and erosional truncation (Fig. 7).

Within this larger-scale framework, Pleistocene and Holocene strata form shallowing-upward successions interpreted to represent deposition in upper shoreface (LFA–D), foreshore (LFE), and backshore berm (LFF) environments, broadly similar to those observed on the modern shelf. These strata exhibit along-strike changes in sedimentologic, stratigraphic, and ichnologic characteristics that are broadly comparable to trends observed on the modern shelf, and which define the two distinct Holocene and Pleistocene facies associations (FA1, FA2; Fig. 10).

The FA1 strata of the north margin are characterized by intensely bioturbated (≥ ii4) shallowing-upward successions of poorly sorted, very fine- to course-grained peloid-ooid-skeletal sand. At the base of FA1 successions, LFB deposits typically are trough-cross stratified, but display ii5-6, with poor preservation of physical sedimentary structures due to the mottled fabric. Trace-fossil assemblages are diverse, with high burrow density indicated by the abundance of crosscutting burrows. The mottled fabric and discrete trace fossils (ii5–6), result in the preservation of Ichnofabrics II and VI. Above LFB, deposits interpreted as upper shoreface in FA1 (LFC, LFD) are moderately to poorly sorted, very fine-grained grainstone consisting of peloids, ooids, composite grains, and skeletal fragments of varying abundance, similar to sediment of the modern north-margin upper shoreface. Physical sedimentary structures are generally dm-scale (0.1–0.5-m thick) crossbedding and range from poorly preserved (ii4) to completely reworked (ii6) by burrowing organisms, indicating that the rate of biological reworking was greater than the rate of physical reworking for much of this segment of the shelf. Composite grains are abundant, and most ooids display few (generally < 3) thin laminae. Skeletal grains are predominantly whole and unbroken, with well-preserved ornamentation, indicating

limited physical abrasion. Limited physical abrasion, combined with prevalent microborings and pervasive micritization of grains suggest low-energy conditions.

These bioturbated upper shoreface and upper shoreface strata (LFB, LFC, LFD) exposed along this northern margin exhibit the greatest bioturbation intensity (ii3–6) of Pleistocene strata in the area. The abundance and density of tracemakers, and the diverse nature of the trace-fossil assemblages indicate that, although infrequently influenced by wave and current agitation, these shoreface deposits reflect a greater rate of bioturbation relative to the rate of physical reworking of the sediment, and dominant influence of biologic processes.

Several attributes of FA2 successions of the south margin contrast with the shelf further north, including: 1) laterally continuous, high-relief backshore berm deposits up to several meters thick; 2) thick (up to 4 m) foreshore successions; 3) thick upper shoreface deposits dominated by dm- to m-scale trough cross-strata; and 4) upper shoreface and toe-of-beach deposits (LFA, LFB, LFD) with limited ichnodiversity and sparse distribution of vertical to inclined burrows with or without reinforced walls (ii1–3; Ichnofabric V). The preservation of physical sedimentary structures in these ridges to the south suggest deposition in a higher energy, wave-dominated shoreface system, and reflect a rate of physical reworking higher than the rate of biological reworking.

Similarly, patterns of bioturbation intensity (ii5–6) and ichnofabrics (Ichnofabrics III and VI) of Pleistocene and Holocene LFF and LFG (backshore berm and subaerial exposure intervals) are consistent with the processes observed in modern backshore and backshore berm environments. Where discrete traces are preserved, assemblages are assigned to the Psilonichnus Ichnofacies. The backshore and backshore berms of the central and south margin include intense

to complete bioturbation (ii5–6) by meiofauna, macrofauna, and plant roots, resulting in cryptobioturbation preserved as Ichnofabric VI.

Synthesis.—Ancient and modern deposits illustrate along-strike variations in grain type, size, and sorting, as well as trace-fossil associations, ichnofabric, and ichnodiversity similar to their character and distribution on the modern shelf. By analogy with the present-day margin, along-strike changes are interpreted to be controlled by margin orientation relative to the direction of dominant wave energy, and result in progressive increase in depositional energy from north to south (Fig. 14). Akin to deposits of the modern north-margin shelf, Pleistocene FA1 strata more common to the north are interpreted as deposits of a shoreface system sheltered from local, wind-generated waves, storm waves, and distal swell. Physical oceanographic processes governing the deposition of FA1 strata were dominated by generally weak, southward longshore currents and broad periods of stasis, and biological reworking. Analogously, the patterns of the Pleistocene FA2 strata are interpreted to represent a higher energy shoreface, with conditions favoring a rate of physical reworking greater than the rate of biological reworking. This shoreface likely reflects exposure to waves of cold fronts and distal swell.

Sedimentologic, Ichnologic, and Diagenetic Influences on Petrophysical Heterogeneity

Understanding controls on spatial patterns of sedimentary facies and bioturbation within carbonate shoreface systems can provide new insights into controls on petrophysical heterogeneity within subsurface grainstone deposits and analog reservoirs. The results of this study show several scales of variability that could influence the thickness and quality of reservoir analogs.

Regional scale.—At the largest scale, along-strike changes in sedimentologic character, stratal successions, and ichnofabric are marked by the differences between FA1 (more common

to the north) and FA2 (more common to the south) successions in the Pleistocene. Several patterns are observed. First, the stratigraphic succession and most individual facies are thicker to the south. For example, the upper shoreface grainstones are < 3-m thick in FA1, but can be 4-m thick in FA2. Second, bioturbation is more intense and deeper to the north. For example, some grainstones are completely bioturbated; primary physical sedimentary structures within them are difficult to discern or are absent. Third, the continuity of the beach ridges—and presumably the underlying upper shoreface—is greater along strike in the north, where individual ridges can extend more than 10 km. To the south, ridge sets are more complex, and can be discontinuous across several km strike.

Outcrop scale.—The distribution, behaviors, and tiering of tracemakers are recorded in the ichnologic character (trace-fossil assemblages, ichnofabrics, ichnofacies) of Pleistocene strata. Carbonate shoreface deposits of CAP are characterized by six ichnofabrics (Table 6) that reflect the biological modification of the primary sedimentary fabric. The six ichnofabrics reflect the burrowing activity of individuals (i.e., ethology and trophic structure) as well as the epifaunal and infaunal community as a whole (i.e., bioturbation intensity, burrow crosscutting, tiering). Ichnofabrics range from no bioturbation (Ichnofabric I), to complete burrow mottling and homogenization of the depositional fabric to produce cryptobioturbation (Ichnofabric VI; Figs. 12, 13).

Facies associations within Pleistocene and Holocene shallowing-upward successions display systematic vertical changes in sediment, physical sedimentary structures, bioturbation intensity, ichnodiversity, tiering, and ichnofabric (Fig. 10). For example, upper shoreface strata commonly are more bioturbated than the overlying foreshore deposits, and exhibit greater burrow penetration and connectivity. Thus, the ichnology and depositional facies vary

considerably at the scale of a single shallowing-upward succession, resulting in m-scale vertical heterogeneity.

Hand sample scale.—Micro- and macro-CT data reveal density heterogeneities in 2D and 3D, which are interpreted to reflect the patterns of trace-fossil distribution, architectural morphology, connectivity, and crosscutting relationships of the ichnofabric. Petrophysical and CT-scan data reveal a range of burrow orientation and connectivity. Ichnofabric II (Sample 3) shows the greatest cm- and sub-cm-scale variability in rock fabric, pore networks, and porosity, interpreted to reflect vertical and horizontal burrow connectivity and associated cement haloes. Ichnofabric VI (Sample 1) shows the least spatial variability, reflecting a relatively homogeneous rock fabric interpreted to reflect complete bioturbation by ubiquitous meiofauna and macrofauna. Ichnofabric V (Sample 2) represents a transition between the spatial complexity and high-burrow connectivity in Ichnofabric II and the more-or-less homogeneous fabric, complete bioturbation, and ubiquitous burrow connectivity of Ichnofabric VI.

Thus, at the scale of an individual core or hand sample, trace fossils influence carbonate sedimentary textures and porosity in a variety of ichnofabrics (Figs. 12, 13): 1) millimeter- to centimeter-scale, bedding-parallel planiform trace fossils with burrow fill that is coarser grained and more porous than the host rock; 2) complete bioturbation by meiofauna to produce mottled, cryptobioturbate textures; 3) discrete vertical, subvertical, and U-shaped trace fossils that display less well-sorted, loosely packed burrow fill with considerably less cement than the host rock, and cement linings and hollow interiors that may act as conduits between units; and 4) 3D burrow networks characterized by poorly sorted, loosely packed peloidal fill, surrounded by a halo of pore-occluding, sparry calcite cement.

Integrated Ichnofacies Model for Carbonate Shoreface Systems

Integration of ichnologic and sedimentologic characteristics of Pleistocene, Holocene, and modern shoreface deposits on the leeward margin of CAP lead to the development of a new ichnofacies model specific to wave-dominated carbonate shoreface systems (Fig. 15). A conceptual ichnofacies model specific to wave-dominated carbonate shoreface systems (Fig. 15) includes synthesis of ichnologic and sedimentologic characteristics of Pleistocene and Holocene shallowing-upward successions, informed by parallels with the hydrodynamic conditions and geomorphic elements on the modern shelf. This model (Fig. 17) provides the framework for interpreting the controls on sedimentological, ichnological, and petrophysical variability within shallow-marine carbonate depositional systems. The trace-fossil assemblages and ethological groups of modern and ancient deposits include four ichnofacies: Trypanites Ichnofacies, Psilonichnus Ichnofacies, Skolithos Ichnofacies, and Cruziana Ichnofacies.

The Psilonichnus Ichnofacies is characteristic of such geomorphic elements as the backshore and foreshore within the uppermost intertidal and supratidal environments of coastal settings. Consistent with the traditional Seilacherian ichnofacies model, the Psilonichnus Ichnofacies of CAP is best expressed in deposits of the backshore and backshore berm. Such environments are subject to eolian and other continental processes (e.g., pedogenesis; Hasiotis 2007; Hasiotis et al. 2007; Hasiotis and Platt 2012; Hasiotis et al. 2013), with marine processes dominant during perigean spring tide and storm conditions (Fig. 15). Bioturbation is dominated by terrestrial plants and organisms in the backshore and backshore berm settings, including terrestrial meiofauna and macrofauna (e.g., amphipods, snails, arachnids, insects, lizards), which form trackways and trails and burrow through the interstitial sediment, producing ubiquitous mottled texture. The mottling may preserve or destroy the primary sedimentary fabric,

commonly resulting in preservation of Ichnofabrics VI, III, and IV. In the upper foreshore, bioturbation is dominated by marine macrofauna and meiofauna. Terrestrial organisms, such as lizards, amphipods, and insects, form surficial trackways, as well as vertical to inclined burrows in the backshore environments on the leeward margin.

The backshore is characterized by terrestrial plants and organisms that produce surficial tracks, trackways, and burrows. Trace-fossil assemblages are characterized by sparse distribution of vertical, inclined, and U-shaped dwelling burrows attributed to insects (*Arenicolites*, *Macaronichnus*, *Macanopsis*, *Polykladichnus*, *Skolithos*), as well as sparse J- and Y-shaped fiddler- and ghost-crab burrows (*Psilonichnus*). Less common traces include bird tracks, and rare trackways of land snails, hermit crabs, and ghost crabs (*Archaeonassa*, *Coenobichnus*, and *Diplichnites*, respectively). Cryptobioturbation is also prevalent, attributed to the burrowing activity of meiofauna (e.g., amphipods). Bioturbation intensity (ii2–6) and sedimentary processes result in preservation of Ichnofabrics III, IV, and VI.

The Skolithos Ichnofacies is characteristic of high energy, shifting sandy media in intertidal to shallow subtidal settings. On the modern shelf, the Skolithos Ichnofacies extends from the lower foreshore (swash zone) to the upper shoreface–bioturbated upper shoreface transition zone, within high-energy, marine environments influenced by waves, currents, and storms. Although variable along the margin, the Skolithos Ichnofacies is typical of moderately sorted, medium-grained sand with well-preserved physical sedimentary structures (ii1–2). Actively migrating, sinuous-crested subaqueous dunes (preserved as trough cross-strata, Fig. 9) include conditions favorable to habitation by certain groups of macrofauna (e.g., suspension-feeders and passive carnivores). As a result, trace-fossil assemblages are dominated by vertical dwelling burrows (e.g., *Ophiomorpha*, *Skolithos*) and display a wider range of bioturbation

intensity (ii1–5). Together, the physical sedimentary processes and bioturbation of such carbonate shoreface environments result in the preservation of Ichnofabrics I–IV.

The Cruziana Ichnofacies is characteristic of lower energy, subtidal settings with limited influence by waves. This setting is comparable to the lower shoreface of Kamola and Van Wagoner (1995), in that it lies below fairweather wave base but is likely subject to disturbance during distal swell and extreme wave events or storms. On the modern shelf, the Cruziana Ichnofacies extends seaward from the upper shoreface–bioturbated upper shoreface transition zone on the north and central margins, and is indicative of low-energy, permanently subtidal marine environments that experience infrequent high-energy events. The Cruziana Ichnofacies is typical of poorly-sorted, very fine to coarse sand with variable amounts of mud (up to 34%) and poor preservation of physical sedimentary structures. Bioturbation by surficial epifaunal deposit feeders (e.g., sea biscuits, gastropods), predators (sting rays) along with dwelling structures of polychaete worms and callianassid shrimp, result in intense to complete bioturbation (ii5–6). Trace-fossil assemblages are dominated by locomotion, and surficial deposit-feeding traces (e.g., *Archaeonassa*, *Scolicia*), as well as *Thalassinoides* and *Ophiomorpha*, and dwelling burrows of suspension feeders or passive carnivores (e.g., *Cylindrichnus*, *Conichnus*, *Skolithos*). Together, the paucity of physical sedimentary structures and intense bioturbation by diverse and abundant trace fossils results in preservation of Ichnofabrics II, III, and IV.

CONCLUSIONS

This study characterizes the geomorphology, sedimentology, and ichnologic variability within shoreface deposits along the western, leeward margin of Crooked-Acklins Platform, southern Bahamas. Evaluation of bottom types, geomorphic features, and remote-sensing data along with analysis of neoichnology and sediment distribution on the modern shelf provide the

framework for outcrop analyses. Integration of modern and outcrop data illustrate how hydrodynamic and biologic processes influence the nature and distribution of sedimentary facies and biogenic structures within carbonate shoreface systems. Results include a conceptual model for the controls on spatial variability, and provide insight that can be applied to better understand heterogeneous subsurface analogs.

Bioturbation within carbonate shoreface deposits reflects the large-scale changes in energy and hydrodynamic conditions along the western leeward margin. These changes are analogous to those in the Holocene and Pleistocene outcrops on the margin. The interaction between physicochemical and biogenic controls results in preservation as one of six ichnofabrics, representing the range of ichnologic features observed on the modern shelf and in the Pleistocene outcrops. Descriptions of ichnofabrics in hand sample, slabbed sample, and thin section demonstrate the influence of bioturbation on grain-size distributions, grain packing and sorting, and cementation patterns. Vertical and lateral changes in both character and intensity of bioturbation are evident at several scales: 1) regional (along-strike); 2) lithofacies (within shallowing-upward successions); 3) hand sample (stratigraphic position and geomorphic setting); and 4) thin section (mm-scale variations in cementation, grain size distribution, and grain packing). Bioturbation alters pore distributions, and porosity and CT scan data reveal that ichnofabric-associated textural variability can have a considerably influence on petrophysical heterogeneity. These insights provide a conceptual model for controls on sedimentological and ichnological heterogeneity in carbonate shoreface systems, and may be applicable to understanding similar systems in the subsurface.

REFERENCES

AURELL, M., MCNEILL, D.F., GUYOMARD, T., and KINDLER, P., 1995, Pleistocene shallowing-upward sequences in New Providence, Bahamas: Signature of high-frequency sea-level fluctuations in shallow carbonate platforms: Journal of Sedimentary Research, v. 65, p. 170–182.

BAIN, R.J., and FOOS, A.M., 1993, Carbonate microfabrics related to subaerial exposure and paleosol formation, *in* Rezak, R., and Lavoie, D., eds., Carbonate Microfabrics: Frontiers in Sedimentology: New York, Springer-Verlag, p. 19–27.

BANIAK, G.M., GINGRAS, M.K., and PEMBERTON, S.G., 2013, Reservoir characterization of burrow-associated dolomites in the Upper Devonian Wabamun Group, Pine Creek gas field, central Alberta, Canada: Marine and Petroleum Geology, v. 48, p. 275–292.

BANIAK, G.M., GINGRAS, M.K., BURNS, B.A., and PEMBERTON, S.G., 2015, Petrophysical characterization of bioturbated sandstone reservoir facies in the Upper Jurassic Ula Formation, Norwegian North Sea, Europe: Journal of Sedimentary Research, v. 85, p. 62–81.

BEN-AWUAH, J., and PADMANABHAN, P., 2015, Effect of bioturbation on reservoir rock quality of sandstones: A case from the Baram Delta, offshore Sarawak, Malaysia: Petroleum Exploration and Development, v. 42, p. 223–231.

BLOTT, S.J., and PYE, K., 2001, Gradistat: a grain-size distribution and statistics package for the analysis of unconsolidated sediments: Earth Surface Processes and Landforms, v. 26, p. 1237–1248.

BROMLEY, R.G., 1996, Trace Fossils: Biology, Taphonomy and Applications: London, Chapman & Hall, 280 p.

BUDD, D.A., 2002, The relative roles of compaction and early cementation in the destruction of permeability in carbonate grainstones: a case study from the Paleogene of west-central Florida, U.S.A.: Journal of Sedimentary Research, v. 72, p. 116–128.

BURCHETTE, T.P., and WRIGHT, V.P., 1992, Carbonate ramp depositional systems: Sedimentary Geology, v. 79, p. 3–57.

CLIFTON, E.H., and THOMSON, J.K., 1978, Macaronichnus segregatis: a feeding structure of shallow marine polychaetes, Journal of Sedimentary Petrology, v. 48, p. 1293–1302.

CUNNINGHAM, K.J., SUKOP, M.C., 2012, Megaporosity and permeability of Thalassinoides-dominated ichnofabrics in the Cretaceous karst-carbonate Edwards-Trinity aquifer system, Texas: U.S. Geological Survey Open-File Report 2012-1021, 4 p.

CUNNINGHAM, K.J., SUKOP, M.C., HUANG, H., ALVAREZ, P.F., CURRAN, H.A., RENKEN, R.A., and DIXON, J.F., 2009, Prominence of ichnologically influenced macroporosity in the karst Biscayne aquifer: stratiform "super-K" zones: Geological Society of America, Bulletin, v. 121, p. 164–180.

CURRAN, H.A., 1994, The palaeobiology of ichnocoenoses in Quaternary, Bahamian-style carbonate environments: the modern to fossil transition, *in* Donovan, S.K., ed., The Palaeobiology of Trace Fossils: New York, Wiley, p. 83–104.

CURRAN, H.A., and WHITE, B., 1987, Trace fossils in carbonate upper beach rocks and eolianites: Recognition of the backshore to dune transition, *in* Curran, H.A., ed.,

Proceedings of the Third Symposium on the Geology of the Bahamas CCFL Bahamian Field Station, Ft. Lauderdale, Florida, p. 243–254.

CURRAN, H.A., and WHITE, B., 1991, Trace fossils of shallow subtidal to dunal ichnofacies in Bahamian Quaternary carbonates: Palaios, v. 6, p. 498–510.

DASHTGARD, S.E., GINGRAS, M.K., and MACEACHERN, J.A., 2009, Tidally modulated shorefaces: Journal of Sedimentary Research, v. 79, p. 793–807.

DAWSON, W.C., 1978, Improvement of sandstone porosity during bioturbation: American Association of Petroleum Geologists, Bulletin, v. 62, p. 508–509.

DROSER, M.L., and BOTTJER, D.J., 1986, A semiquantitative field classification of ichnofabrics: Journal of Sedimentary Petrology, v. 56, p. 558–559.

DUNHAM, R.J., 1962, Classification of carbonate rocks according to depositional texture, *in* Ham, W.E., ed., Classification of Carbonate Rocks—A Symposium: American Association of Petroleum Geologists, Memoir 1, p. 108–121.

EKDALE, A.A., and BROMLEY, R.G., 1983, Trace fossils and ichnofabrics in the Kjølby Gaard Marl, uppermost Cretaceous, Denmark: Bulletin of the Geological Society of Denmark, v. 31, p. 107–119.

EKDALE, A.A., BROMLEY, R.G., and PEMBERTON, S.G., 1984, Shallow Marine Carbonate Environments, *in* Ekdale, A.A., Bromley, R.G., and Pemberton, S.G., eds., Ichnology--The Use of Trace Fossils in Sedimentology and Stratigraphy, SEPM Short Course Notes 15: Tulsa, Oklahoma, SEPM, p. 199–213.

ELTOM, H. and HASIOTIS, S.T., 2019, Lateral and Vertical Trends of Preferred Flow Pathways Associated with Bioturbated Carbonate: Examples from Middle to Upper Jurassic Strata, Central Saudi Arabia: Carbonate Pore Systems: New Development and Case Studies. SEPM Special Publication No.112, p. 1–15.

ELTOM, H., HASIOTIS, S.T., and RANKEY, E.C., 2019, Effect of Bioturbation on Petrophysical Properties of Shelf Carbonates: Geostatistical Modeling Approach, the Ulayyah Member of the Hanifa Formations, Central Saudi Arabia: Marine and Petroleum Geology Bulletin, v. 104, p. 259–269.

ENOS, P., 1977, Holocene sediment accumulations of the Florida shelf margin, *in* Enos, P., and Perkins, R.D., eds., Quaternary Sedimentation in South Florida, Geological Society of America Memoir 147, p. 1–130.

ESTEBAN, M.C., 1974, Caliche textures and "Microcodium": Bollettino della Societa Geologica Italiana, v. 92, p. 105–125.

ESTEBAN, M.C., 1976, Vadose pisolite and caliche: American Association of Petroleum Geologists, Bulletin, v. 60, p. 2048–2057.

ESTEBAN, M.C., and KLAPPA, C.F., 1983, Subaerial Exposure Environment, *in* Scholle, P.A., Bebout, D.G., and Moore, C.H., eds., Carbonate Depositional Environments: AAPG Memoir 33, p. 1–54.

FARROW, G.E., 1971, Back-reef and lagoonal environments of Aldabra Atoll distinguished by their crustacean burrows: Symposium of the Zoological Society of London, v. 28, p. 455–500.

FLUGEL, E., 2004, Microfacies of Carbonate Rocks: Analysis, Interpretation and Application: Berlin, Springer-Verlag, 976 p.

FOLK, R.L., and WARD, W.C., 1957, Brazos river bar: a study of significance of grain size parameters: Journal of Sedimentary Petrology, v. 27, p. 3–26.

FREY, S.E., and DASHTGARD, S.E., 2011, Sedimentology, ichnology and hydrodynamics of strait-margin, sand and gravel beaches and shorefaces: Juan de Fuca Strait, British Columbia, Canada: Sedimentology, v. 58, p. 1326–1346.

FREY, R.W., and PEMBERTON, S.G., 1985, Biogenic structures in outcrops and cores, I. Approaches to ichnology: Bulletin of Canadian Petroleum Geologists, v. 33, p. 72–115.

FREY, R.W., HOWARD, J.D., and PRYOR, W.A., 1978, *Ophiomorpha*: its morphologic, taxonomic, and environmental significance: Palaeogeography, Palaeoclimatology, Palaeoecology, v. 23, p. 199–229.

GINGRAS, M.K., BANIAK, G., GORDON, J., HOVIKOSKI, J., KONHAUSER, K.O., LA CROIX, A., LEMISKI, R., MENDOZA, C., PEMBERTON, S.G., and POLO, C., 2012, Porosity and permeability in bioturbated sediments, *in* Knaust, D., and Bromley, R.G., eds., Trace Fossils as Indicators of Sedimentary Environments: Developments in Sedimentology 64, p. 837–868.

GINGRAS, M.K., DASHTGARD, S.E., MACEACHERN, J.A., and PEMBERTON, S.G., 2008, Biology of shallow marine ichnology: a modern perspective: Aquatic Biology, v. 2, p. 255–268.

GINGRAS, M.K., MACMILLAN, B., and BALCOM, B.J., 2002, Visualizing the internal physical characteristics of carbonate sediments with magnetic resonance imaging and petrography: Canadian Society of Petroleum Geologists, Bulletin, v. 50, p. 363–369.

GINGRAS, M.K., MENDOZA, C.A., and PEMBERTON, S.G., 2004, Fossilized worm burrows influence the resource quality of porous media: American Association of Petroleum Geologists, Bulletin, v. 88, p. 875–883.

GINGRAS, M.K., PEMBERTON, S.G., HENK, F., MACEACHERN, J.A., MENDOZA, C., ROSTRON, B., O'HARE, R., SPILA, M., and KONHAUSER, K., 2007, Applications of ichnology to fluid and gas production in hydrocarbon reservoirs, *in* MacEachern, J.A., Bann, K.L., Gingras, M.K., and Pemberton, S.G., eds., Applied Ichnology: SEPM Short Course Notes 52, p. 131–145.

GINGRAS, M.K., PEMBERTON, S.G., MENDOZA, C.A., and HENK, F., 1999, Assessing the anisotropic permeability of Glossifungites surfaces: Petroleum Geoscience, v. 5, p. 349–357.

GINSBERG, R.N., 1953, Beachrock in south Florida: Journal of Sedimentary Research, v. 23, p. 85–92.

GOLDRING, R., TAYLOR, A.M., and HUGHES, W.G., 2005, The application of ichnofabrics towards bridging the dichotomy between siliciclastic and carbonate shelf facies: examples from the Upper Jurassic Fulmar Formation (UK) and the Jubaila Formation (Saudi Arabia): Proceedings of the Geologists' Association, v. 116, p. 235–249.

GOLDSTEIN, R.H., 1988, Paleosols of Late Pennsylvanian cyclic strata, New Mexico: Sedimentology, v. 35, p. 777–804.

GRANT, C.W., GOGGIN, D.J., and HARRIS, P.M., 1994, Outcrop analog for cyclic-shelf reservoirs, San Andres Formation of Permian Basin: Stratigraphic framework, permeability distribution, geostatistics, and fluid-flow modeling: American Association of Petroleum Geologists, Bulletin, v. 78, p. 23–54.

HANTZSCHEL, W., 1975, Trace fossils and problematica, *in* Teichert, C., ed., Treatise on Invertebrate Paleontology, Part W. Miscellanea, Supplement I. Geological Society of America and University of Kansas Press, 269 p.

HARRIS, P.M., 1979, Facies anatomy and diagenesis of a Bahamian ooid shoal: Sedimenta VII: Miami, Florida, The Comparative Sedimentology Laboratory, 164 p.

HARRIS, P.M., and WEBER, L.J., eds., 2006, Giant hydrocarbon reservoirs of the world: From rocks to reservoir characterization and modeling: AAPG Memoir 88, 469 p.

HARRIS, P.M., KERANS, C., and BEBOUT, D.G., 1993, Ancient outcrop and modern examples of platform carbonate cycles--implications for subsurface correlation and understanding reservoir heterogeneity, *in* Loucks, R.G., and Sarg, J.F., eds., Carbonate Sequence Stratigraphy--Recent Developments and Applications: AAPG Memoir 57, p. 475–492.

HASIOTIS, S.T., 2007. Continental ichnology: fundamental processes and controls on trace-fossil distribution. In, Miller, W. III (ed.), Trace Fossils—Concepts, Problems, Prospects, Elsevier Press, p. 268-284.

HASIOTIS, S.T., and MITCHELL, C.E., 1993, A comparison of crayfish burrow morphologies: Triassic and Holocene fossil, paleo- and neo-ichnological evidence, and the identification of their burrowing signatures: Ichnos, v. 2, p. 291–314.

HASIOTIS, S.T., KRAUS, M.J., and DEMKO, T.M., 2007, Climate controls on continental trace fossils, in Miller, W, III, ed., Trace Fossils: Concepts, Problems, Prospects: Amsterdam, Elsevier Press, p. 172–195.

HASIOTIS, S.T., and PLATT, B.F., 2012, Exploring the sedimentary, pedogenic, and hydrologic factors that control the occurrence and role of bioturbation in soil formation and horizonation in continental deposits: An integrative approach: The Sedimentary Record, v. 10, p. 4–9.

HASIOTIS, S. T., MCPHERSON, J., and REILLY, M., 2013. Using Ichnofossils to Reconstruct the Depositional History of Sedimentary Successions in Alluvial, Coastal Plain, and Deltaic Settings. 2013 International Petroleum Technical Conference Proceedings, Beijing, China, p. 1-48.

HEINE, J.N., 2000, Scientific diving techniques: Marine Technology Society Journal, v. 34, p. 23–37.

HILL, G.W., 1985, Ichnofacies of a modern size-graded shelf, northwestern Gulf of Mexico, *in* Curran, H.A., ed., Biogenic Structures: Their Use in Interpreting Depositional Environments, SEPM Special Publication 35, p. 195–210.

HINE, A.C., 1979, Mechanism of berm development and resulting beach growth along a barrier spit complex: Sedimentology, v. 26, p. 333-351.

HINE, A.C., and MULLINS, H.T., 1983, Modern carbonate shelf-slope breaks, *in* Stanley, D.J., and Moore, G.T., eds., The Shelfbreak: Critical Interface on Continental Margins, SEPM Special Publication 33, p. 169–188.

HINE, A.C., and NEUMANN, A.C., 1977, Shallow carbonate-bank-margin growth and structure, Little Bahama Bank, Bahamas: American Association of Petroleum Geologists, Bulletin, v. 61, p. 376–406.

HINE, A.C., WILBER R.J., and NEUMANN, A.C., 1981, Carbonate sand bodies along contrasting shallow bank margins facing open seaways in northern Bahamas: American Association of Petroleum Geologists, Bulletin, v. 65, p. 261–290.

HOLLIS, C., 2011, Diagenetic controls on reservoir properties of carbonate successions within the Albian–Turonian of the Arabian Plate: Petroleum Geoscience, v. 17, p. 223–241.

HOWARD, J.D., 1971, Comparison of the beach-to-offshore sequence in modern and ancient sediments, *in* Howard, J.D., Valentine, J.W., and Warme, J.E., eds., Recent Advances in Paleoecology and Ichnology, American Geological Institute, Short Course Lecture Notes, p. 148–183.

HOWARD, J.D., and FREY, R.W., 1975, Estuaries of the Georgia Coast, U.S.A.: Sedimentology and Biology. II Regional Animal-Sediment Characteristics of Georgia Estuaries: Senckenbergiana Maritima, v. 7, p. 33–103.

HOWARD, J.D., and FREY, R.W., 1984, Characteristic trace fossils in nearshore to offshore sequences, Upper Cretaceous of east-central Utah: Canadian Journal of Earth Sciences, v. 21, p. 200–219.

INDEN, R.F., and MOORE, C.H., 1983, Beach Environment, *in* Scholle, P.A., Bebout, D.G., and Moore, C.H., eds., Carbonate Depositional Environments, AAPG Memoir 33, p. 211–265.

JACKSON, A.M., HASIOTIS, S.T., and FLAIG, P.P., 2016, Ichnology of a paleopolar, river-dominated, shallow marine deltaic succession in the Mackellar Sea: Mackellar Formation (Lower Permian), central Transantarctic Mountains, Antarctica: Palaeogeography, Palaeoclimatology, Palaeoecology, v. 441, p. 266–291.

JACKSON, C.A., MODE, A.W., OTI, M.N., ADEJINMI, K., OZUMBA, K., OSTERLOFF, P., 2013, Effects of bioturbation on reservoir quality: an integration in reservoir modeling of selected fields in the Niger Delta Petroleum Province: Nigerian Association of Petroleum Explorationists, Bulletin, v. 25, p. 29–42.

JAMES, N.P., 1972, Holocene and Pleistocene calcareous crust (caliche) profiles: criteria for subaerial exposure: Journal of Sedimentary Research, v. 42, p. 817–836.

JAMES, N.P., 1983. Reef environment, *in* Scholle, P.A., Bebout, D.G., and Moore, C.H., eds., Carbonate Depositional Environments: AAPG Memoir 33, p. 345–440.

Kamola, D.L., and Van Wagoner, J.C., 1995, Stratigraphy and facies architecture of parasequences with examples from the Spring Canyon Member, Blackhawk Formation, Utah, *in* Van Wagoner, J.C., and Bertram, G.T., eds., Sequence Stratigraphy of Foreland Basin Deposits: Outcrop and Subsurface Examples from the Cretaceous of North America: AAPG Memoir 64, p. 27–54.

KENNEDY, W.J., 1975, Trace fossils in carbonate rocks, *in* Rey, R.W., ed., The Study of Trace Fossils: New York, Springer, p. 377–398.

KERANS, C., and LOUCKS, R.G., 2002, Stratigraphic setting and controls on occurrence of high-energy carbonate beach deposits: Lower Cretaceous of the Gulf of Mexico: Transactions of the Gulf Coast Association of Geological Societies, v. 52, p. 517–526.

KESWANI, A.D., 1999, An integrated ichnological perspective for carbonate diagenesis [unpublished M.S., thesis]: University of Alberta, 124 p.

KESWANI, A.D., and PEMBERTON, S.G., 2007, Applications of ichnology in exploration and exploitation of Mississippian carbonate reservoirs, Midale Beds, Weyburn Oilfield, Saskatchewan (abs.): Canadian Society of Petroleum Geologists and Canadian Society of Exploration Geophysicists Conference, Calgary, Alberta, Canada, May 14–17, 2007, 28 p.

KLAPPA, C.F., 1980a, Brecciation textures and tepee structures in Quaternary calcrete (caliche) profiles from eastern Spain: the plant factor in their formation: Geological Journal, v. 15, p. 81–89.

KLAPPA, C.F., 1980b, Rhizoliths in terrestrial carbonates: classification, recognition, genesis, and significance: Sedimentology, v. 27, p. 613–629.

KLAPPA, C.F., 1983, A process-response model for the formation of pedogenic calcretes, *in* Wilson, R.C.L., Residual Deposits: Geological Society, London, Special Publications, 11, Geological Society of London Special Publication 11, p. 211–220.

KNAUST, D., 2007, Invertebrate trace fossils and ichnodiversity in shallow-marine carbonates of the German Middle Triassic (Muschelkalk), *in* Bromley, R.G., Buatois, L.A., Mángano, M.G., Genise, J.F., Melchor, R.N. (Eds.), Sediment–organism interactions: A multifaceted ichnology: SEPM Special Publication 88, pp. 223–240.

KNAUST, D., 2009, Ichnology as a tool in carbonate reservoir characterization: A case study from the Permian-Triassic Khuff Formation in the Middle East: GeoArabia, v. 14, p. 17–38.

KNAUST, D., 2010, Meiobenthic trace fossils comprising a miniature ichnofabric from Late Permian carbonates of the Oman Mountains: Palaeogeography, Palaeoclimatology, Palaeoecology, v. 286, p. 81–87.

KNAUST, D., 2014, Classification of bioturbation-related reservoir quality in the Khuff Formation: towards a genetic approach, in Pöppelreiter, M.C., (Ed.), Permo-Triassic Sequence of the Arabian Plate, EAGE, Amsterdam, p. 247–267.

KRAUS, M.J., 1999, Paleosols in clastic sedimentary rocks: their geologic applications: Earth-Science Reviews, v. 47, p. 41–70.

KRAUS, M.J., and HASIOTIS, S.T., 2006, Significance of different modes of rhizoliths preservation to interpreting paleoenvironmental and paleohydrologic settings: examples from Paleogene paleosols, Bighorn Basin, Wyoming, U.S.A.: Journal of Sedimentary Research, v. 76, p. 633–646.

LA CROIX, A.D., GINGRAS, M.K., PEMBERTON, S.G., MENDOZA, C.A., MACEACHERN, J.A., and LEMISKI, R.T., 2013, Biogenically enhanced reservoir properties in the Medicine Hat gas field, Alberta, Canada: Marine and Petroleum Geology, v. 43, p. 464–477.

LLOYD, R.M., PERKINS, R.D., and KERR, S.D., 1987, Beach and shoreface ooid deposition on shallow interior banks, Turks and Caicos Islands, British West Indies: Journal of Sedimentary Research, v. 57, p. 976–982.

LUCIA, F.J., 1995, Rock-fabric/petrophysical classification of carbonate pore space for reservoir characterization: American Association of Petroleum Geologists, Bulletin, v. 79, p. 1275–1300.

MACEACHERN, J.A., and BANN, K.L., 2008, The role of ichnology in refining shallow marine facies models, *in* Hampson, G.J., Steel, R.J., Burgess, P.M., and Dalrymple, R.W., eds., Recent Advances in Models of Siliciclastic Shallow-Marine Stratigraphy: SEPM, Special Publication 90, p. 73–116.

MACEACHERN, J.A., and PEMBERTON, S.G., 1992, Ichnological aspects of Cretaceous shoreface successions and shoreface variability in the Western Interior Seaway of North America, *in* Pemberton, S.G., ed., Applications of Ichnology to Petroleum Exploration, SEPM Core Workshop 17, p. 57–84.

MACEACHERN, J.A., PEMBERTON, S.G., GINGRAS, M.K., and BANN, K.L., 2010, Ichnology and facies models, *in* James, N.P., and Dalrymple, R.W., eds., Facies Models 4, Geological Association of Canada, p. 19–58.

MASSELINK, G., and SHORT, A.D., 1993, The effect of tide range on beach morphodynamics and morphology: a conceptual beach model: Journal of Coastal Research, v. 9, p. 785–800.

MCILROY, D., 2004. Some ichnological concepts, methodologies, applications, and frontiers, *in* McIlroy, D., ed., The Application of Ichnology to Palaeoenvironmental and Stratigraphic Analysis: Geological Society, London, Special Publications, 228, p. 3–27.

MIERAS, B., SAGEMAN, B., and KAUFFMAN, E., 1993, Trace fossil distribution patterns in Cretaceous facies of the Western Interior Basin, North America: Evolution of the Western Interior Basin: Geological Association of Canada, Special Paper, v. 39, p. 585–620.

MONACO, P., and GIANNETTI, A., 2002, Three-dimensional burrow systems and taphofacies in shallowing-upward parasequences, Lower Jurassic carbonate platform (Calcari Grigi, Southern Alps, Italy): Facies, v. 47, p. 57–82.

MORGAN, W.A., 2008, Holocene sediments of northern and western Caicos platform, British West Indies, *in* Morgan, W.A., and Harris, P.M., eds., Developing Models and Analogs for Isolated Carbonate Platforms—Holocene and Pleistocene Carbonates of Caicos Platform, British West Indies, SEPM Core Workshop 22, p. 75–104.

MULTER, H.G., and HOFFMEISTER, J.F., 1968, Subaerial laminated crusts of the Florida Keys: Geological Society of America, Bulletin, v. 79, p. 183–192.

O'LEARY, M.J., PERRY, C.T., BEAVINGTON-PENNEY, S.J., and TURNER, J.R., 2009, The significant role of sediment bio-retexturing within a contemporary carbonate platform system: implications for carbonate microfacies development: Sedimentary Geology, v. 219, p. 169–179.

PEMBERTON, S.G., and FREY, R.W., 1984, Ichnology of storm-influenced shallow marine sequence: Cardium Formation (Upper Cretaceous) at Seebe, Alberta, *in* Stott, D.F., and Glass, D.J., eds., The Mesozoic of Middle North America: Canadian Society of Petroleum Geologists, Memoir 9, p. 281–304.

PEMBERTON, S.G., and GINGRAS, M.K., 2005. Classification and characterizations of biogenically enhanced permeability: American Association of Petroleum Geologists, Bulletin, v. 89, p. 1493–1517.

PEMBERTON, S.G., MACEACHERN, J.A., GINGRAS, M.K., and SAUNDERS, T.D., 2008, Biogenic chaos: Cryptobioturbation and the work of sedimentologically friendly organisms: Palaeogeography, Palaeoclimatology, Palaeoecology, v. 270, p. 273–279.

PEMBERTON, S.G., VAN WAGONER, J.C., and WACH, G.D., 1992, Ichnofacies of a wave-dominated shoreline, *in* Pemberton, S.G., ed., Applications of Ichnology to Petroleum Exploration: SEPM Core Workshop 17, p. 339–382.

PERKINS, R.D., 1977, Depositional Framework of Pleistocene Rocks in South Florida, Geological Society of America Memoir 147, p. 131–198.

POLLARD, J., GOLDRING, R., and BUCK, S., 1993, Ichnofabrics containing *Ophiomorpha*: significance in shallow-water facies interpretation: Journal of the Geological Society, v. 150, p. 149–164.

POMAR, L., and WARD, W., 1999, Reservoir-scale heterogeneity in depositional packages and diagenetic patterns on a reef-rimmed platform, Upper Miocene, Mallorca, Spain: American Association of Petroleum Geologists, Bulletin, v. 83, p. 1759–1773.

RANKEY, E.C., 2014, Contrasts between wave- and tide-dominated oolitic systems: Holocene of Crooked-Acklins Platform, southern Bahamas: Facies, v. 60, p. 405–428.

RANKEY, E.C., and REEDER, S.L., 2010, Controls on platform-scale patterns of surface sediments, shallow Holocene platforms, Bahamas: Sedimentology, v. 57, p. 1545–1565.

RANKEY, E.C., GUIDRY, S.A., REEDER, S.L., and GUARIN, H., 2009, Geomorphic and sedimentologic heterogeneity along a Holocene shelf margin: Caicos Platform: Journal of Sedimentary Research, v. 79, p. 440–456.

READ, J.F., 1985, Carbonate platform facies models: American Association of Petroleum Geologists, Bulletin, v. 69, p. 1–21.

REINSON, G.E., 1984, Barrier-island and associated strand-plain systems, *in* Walker, R.G., ed., Facies models, Geoscience Canada Reprint Series 1, p. 119–140.

RODUIT, N., 2008, JMicroVision: Image analysis toolbox for measuring and quantifying components of high-definition images. Version 1.2.7. Software available for free download at http://jmicrovision.com.

ROSSINSKY, V., JR., and WANLESS, H.R., 1992, Topographic and vegetative controls on calcrete formation, Turks and Caicos Islands, British West Indies: Journal of Sedimentary Research, v. 62, p. 84–98.

SAUNDERS, T., and PEMBERTON, S.G., 1986, Trace fossils and sedimentology of the Appaloosa Sandstone Bearpaw-Horseshoe Canyon Formation transition, Dorothy, Alberta: Canadian Society of Petroleum Geologists Field Trip Guide Book, 117 p.

SCOFFIN, T., and STODDART, D., 1983, Beachrock and intertidal cements, *in* Goudie, A.S., and Pye, K., eds., Chemical Sediments and Geomorphology, Academic Press, London, p. 401–425.

SEILACHER, A., 1953, Studien zur palichnologie. I. Über die methoden der palichnologie: Neues Jahrbuch für Geologie und Paläontologie, Abhandlungen, v. 96, p. 421–452.

SEILACHER, A., 1967, Bathymetry of trace fossils: Marine geology, v. 5, p. 413–428.

SHINN, E.A., 1968, Burrowing in recent lime sediments of Florida and the Bahamas: Journal of Paleontology, v. 42, p. 879–894.

SHINN, E.A., 1980, Geologic history of Grecian Rocks, Key Largo coral reef marine sanctuary: Bulletin of Marine Science, v. 30, p. 646–656.

SHINN, E.A., LIDZ, B.H., and HOLMES, C.W., 1990, High-energy carbonate-sand accumulation, The Quicksands, southwest Florida Keys: Journal of Sedimentary Petrology, v. 60, p. 952–967.

SIMO, J.A., GUIDRY, S.A., IANNELLO, C., RANKEY, G., HARRIS, C.E., GUARIN, H., RUF, A., HUGHES, T., DEREWETZKY, A.N., and PARKER, R.S., 2008, Holocene-Pleistocene Geology of a Transect of an Isolated Carbonate Platform, NW Caicos Platform, British West Indies, *in* Morgan, W.A., and Harris, P.M., eds., Developing Models and Analogs for Isolated Carbonate Platforms—Holocene and Pleistocene Carbonates of Caicos Platform, British West Indies: SEPM Core Workshop 22, p. 111–118.

SPILA, M.V., PEMBERTON, S.G., ROSTRON, B., and GINGRAS, M.K., 2007, Biogenic textural heterogeneity, fluid flow and hydrocarbon production: Bioturbated facies Ben Nevis Formation, Hibernia Field, offshore Newfoundland, *in* MacEachern, J.A., Bann, K.L., Gingras, M.K., and Pemberton, S.G., eds., Applied Ichnology: SEPM Short Course Notes 52, p. 363–380.

STRASSER, A., 1984, Black-pebble occurrence and genesis in Holocene carbonate sediments (Florida Keys, Bahamas, and Tunisia): Journal of Sedimentary Research, v. 54, p. 1098–1109.

STRASSER, A., and DAVAUD, E., 1986, Formation of Holocene limestone sequences by progradation, cementation, and erosion: two examples from the Bahamas: Journal of Sedimentary Research, v. 56, p. 422–428.

STRICKLIN, F., and SMITH, C.I., 1973, Environmental reconstruction of a carbonate beach complex: Cow Creek (Lower Cretaceous) Formation of central Texas: Geological Society of America, Bulletin, v. 84, p. 1349–1368.

TANNER, W.F., 1995, Origin of beach ridges and swales: Marine Geology, v. 129, p. 149–161.

TAYLOR, A.M., and GOLDRING, R., 1993, Description and analysis of bioturbation and ichnofabric: Journal of the Geological Society of London, v. 150, p. 141–148.

TEDESCO, L.P., and WANLESS, H.R., 1991, Generation of sedimentary fabrics and facies by repetitive excavation and storm infilling of burrow networks, Holocene of South Florida and Caicos Platform, BWI: Palaios, v. 6, p. 326–343.

TONKIN, N.S., MCILROY, D., MEYER, R., and MOORE-TURPIN, A., 2010, Bioturbation influence on reservoir quality: A case study from the Cretaceous Ben Nevis Formation, Jeanne d'Arc Basin, offshore Newfoundland, Canada: American Association of Petroleum Geologists, Bulletin, v. 94, p. 1059–1078.

TUCKER, M.E., 1985, Shallow-marine carbonate facies and facies models, *in* Brenchley, P.J., and Williams, B.P.J., eds., Sedimentology: Recent Developments and Applied Aspects, Geological Society of London Special Publication 18, p. 147–169.

WALKER, R.G., and PLINT, A.G., 1992, Wave and storm-dominated shallow marine systems, *in* Walker, R.G., and James, N.P., eds., Facies Models: Response to Sea-Level Change, Geological Association of Canada, p 219–238.

WILSON, J.L., 1975, Carbonate Facies in Geologic History: New York, Springer-Verlag, 471 p.

WRIGHT, V., PLATT, N., and WIMBLEDON, W., 1988, Biogenic laminar calcretes: evidence of calcified root-mat horizons in paleosols: Sedimentology, v. 35, p. 603–620.

ZENGER, D.H., 1992, Burrowing and dolomitization patterns in the Steamboat Point Member, Bighorn Dolomite (Upper Ordovician), northeast Wyoming: Northwest Wyoming Contributions to Geology, v. 29, p. 133–142.

ZENGER, D.H., 1996, Dolomitization patterns in widespread "Bighorn Facies" (Upper Ordovician), western craton, USA: Carbonates and Evaporites, v. 11, p. 219–225.

FIGURE CAPTIONS

Key of Ichnogenera Abbreviations used in figures, tables, and captions:

Ac = *Archaeonassa*	Di = *Diplocraterion*	Rz = Rhizoliths
Ar = *Arenicolites*	Fu = Fugichnia	Ro = *Rosselia*
As = *Asterosoma*	Li = *Lingulichnus*	Ru = *Rusophycus*
Bg = *Bergaueria*	Ma = *Macaronichnus*	Sc = *Scolicia*
Bi = *Bichordites*	Mc = *Macanopsis*	Si = *Siphonichnus*
Ce = *Coenobichnus*	Op = *Ophiomorpha*	Sk = *Skolithos*
Co = *Conichnus*	Pa = *Palaeophycus*	Ta = *Taenidium*
Cr = Cryptobioturbation	Ph = *Phycosiphon*	Te = *Teichichnus*
Cy = *Cylindrichnus*	Pc = *Piscichnus*	Th = *Thalassinoides*
Dc = *Diplichnites*	Pl = *Planolites*	
Di = *Diplocraterion*	Pk = *Polykladichnus*	
Fu = Fugichnia	Ps = *Psilonichnus*	

FIG. 1.—Study area. **A)** Google Earth image of Crooked-Acklins Platform (CAP), southeastern Bahamas. Yellow star is Nassau; red box shows location of B. **B)** Remote sensing image of CAP with study area (red box) highlighted on the arcuate, leeward margin, detailed in C. **C)** QuickBird NIR-G-B image of study area on leeward margin, indicating the three study regions. White star is location of shoreface hydrodynamic data (Rankey 2014).

FIG. 2.—QuickBird remote sensing images showing variability of geomorphic features and bottom types (white text) on the central- and south-margin shelf, as well as along-strike changes in shelf-margin bathymetry (red lines show the shelf break) and distribution of geomorphic elements (yellow text). The grey area within the black dashed lines represents the transitional area between the upper shoreface (USF) and the bioturbated upper shoreface (bUSF). Major ridge sets (black lines) on Crooked Island and Long Cay illustrate along-strike variability of Pleistocene and Holocene progradation. **A)** Central margin shelf (transect B–B', Fig. 1C). Note that the transitional area is deflected seaward near the tidal delta. **B)** South margin shelf (transect C–C', Fig. 1C).

FIG. 3.—Shoreface profiles of transects A–A', B–B', and C–C' (locations in Fig. 1C). Each profile shows the distribution of geomorphic elements on the shelf (grey = transitional boundaries); blue letters correspond to the location of sediment samples shown in Fig. 6. The scale horizontal scale is the same for A–A' and B–B'; note the change in horizontal scale in transect C–C', reflecting the narrow shelf-width. The shelf gradient steepens distally, with the upper shoreface (USF) to bioturbated upper shoreface (bUSF) transition marked by a slight increase in gradient on all three margins. Note the ratio of USF to bUSF increases as the shelf gradient becomes progressively steeper from north to south.

FIG. 4.—Field photos of bottom-type variability among geomorphic elements of the modern leeward shelf. **A–C)** North margin. **D–F)** Central margin. **G–I)** South margin. **A, D, G)** Bottom types of the backshore berm and foreshore. **B, E, H)** Bottom types of the upper shoreface (USF). **C, F, I)** Bottom types of the bioturbated upper shoreface (bUSF). **A)** Rocky shoreline characteristic of the north margin foreshore. **B)** Asymmetrical wave ripples modified by burrowing activities of echinoids and other benthic fauna (*Archaeonassa*, *Scolicia*; arrows and dotted lines). **C)** Patch reefs (up to 2.5 m relief) and bioturbated sediment typical of the north margin bUSF. **D)** Wide, gently sloping sandy beaches characteristic of the central margin. **E)** Current-modified wave ripples with little bioturbation, typical of the central margin USF. **F)** Thoroughly bioturbated sediment of the central margin bUSF with scattered low patch reefs in the distance. **G)** Narrow, steeply sloping beaches and Holocene outcrops of the south margin. **H)** Flood-oriented, 3D subaqueous dunes (height up to 0.8 m) with superimposed current ripples, typical of the USF; note boulder-size clasts in lows between dune crests (arrow). **I)** Rocky bottom zone devoid of sediment.

FIG. 5.—Modern traces of the leeward margin, arranged proximally–distally. **A–C** are common in the backshore (BS) and foreshore (FS), **D–F** in the upper shoreface (USF), and **G–I** in the bioturbated upper shoreface (bUSF). **A**) Plan-view photo showing paired apertures of a ghost-crab burrow (*Psilonichnus*) in the upper FS. **B**) Cast of a ghost crab burrow assignable to *Psilonichnus*; note the upwards branching to form Y-shaped burrow morphology near the sediment surface (yellow line). **C)** Crab trackways up to 5-cm in diameter are typical of the upper FS and BS, and may be surrounded by sediment expelled from the burrow. **D)** Fecal mound common of the central-margin USF; **E)** Paired openings to burrows common of ghost shrimp *Alpheus sp.* **F)** Vertical tube (cf. *Skolithos*) with lining of agglutinated sediment, prevalent in the USF of all three margins. **G)** Cone-shaped mound (white arrow) and paired pit (black arrow) mark the entrance and exit to burrow systems formed by Thalassinid and Callianassid shrimp, prevalent in the bUSF of the central and south margins. **H)** Goby fish burrow in the bUSF. Vial cap is 4.6 cm in diameter. **I)** Sting ray deposit-feeding pit similar in morphology to *Piscichnus*, common from the USF–FS transition to the bUSF.

FIG. 6.—Thin-section photomicrographs showing sedimentologic variability of the leeward margin of CAP, locations shown on Fig. 3. **A–C** are from the north margin, **D–F** from the central margin, and **G–I** from the south margin. **A)** Well-sorted, medium skeletal-peloid sand from the foreshore (FS); note the micritic rims on the undifferentiated skeletal fragments, foraminifera, and *Halimeda* grains. **B)** Moderately-sorted, coarse composite grain-skeletal sand with micritic rims, from the upper shoreface (USF) (5-m water depth). **C)** Poorly sorted, bimodal, very fine peloid-skeletal sand with 33% mud from the bioturbated upper shoreface (bUSF) (18-m water depth). **D)** Moderately-sorted, fine–

medium ooid-peloid-skeletal sand from the FS. **E)** Moderately-sorted, medium ooid-composite grain-skeletal sand of the USF (4-m water depth). **F)** Poorly-sorted, trimodal, very fine, medium, and coarse skeletal-composite grain-ooid sand from the shelf-slope bUSF (31-m water depth). **G)** Moderately-sorted, medium–coarse ooid-composite grain-skeletal sand from the FS; undifferentiated skeletal fragments are rounded and abraded with micritic rims, microborings, and poor preservation of ornamentation. **H)** Moderately-sorted, medium–coarse skeletal-composite grain-ooid sand from the USF (7-m water depth). Skeletal and composite grains comprise the coarse sand fraction; skeletal grains include whole *Halimeda* and foraminifera, and mollusk, sponge, and red algal fragments with preserved ornamentation as well as micritic rims; rare ooids are fine sand-size superficial ooids with peloid nuclei and ≤ 3 oolitic laminae. **I)** Moderately-sorted, trimodal, fine, medium, and coarse ooid-skeletal sand from the bUSF (27-m water depth).

FIG. 7.—QuickBird remote-sensing image and interpreted diagram of beach ridges of southern Long Cay, illustrating progradation patterns. **A)** Quickbird image of southern Long Cay. Beach ridges are the linear, margin-parallel, lighter-colored features. **B)** Interpretation of beach-ridge set progradation, which first occurred from NE to SW (ridge sets 1–3), then proceeded to the W (set 4) and N (sets 5–6) before Holocene progradation began in multiple directions.

FIG. 8.—Outcrop photos and thin-section photomicrographs illustrating the character of Pleistocene Lithofacies (LF) E, F, and G. **A)** Low-relief (< 75 cm) Holocene LFE deposit from the central margin; note the abundance of *Psilonichnus* burrows and rhizoliths. **B)** Fenestral ooid grainstone with alternating laminations of coarse and fine sand (LFE); **C)** Moderately-sorted, bimodal fine- to medium-grained ooid-peloid-skeletal grainstone

typical of south margin LFE strata; note the vague preservation of coarse–fine laminae, and presence of meniscus calcite cement. **D)** Holocene LFF deposit from the south margin; swaley bedsets are laterally discontinuous, and exhibit steep, seaward-dipping foresets as well as landward-dipping bedsets that flatten and become tangential towards the backshore. **E)** Swaley LFF bedsets separated by internal truncation surfaces (arrows). **F)** Poorly-sorted, fine-grained ooid-skeletal-composite grain grainstone of a FA1 berm deposit; note the incipient dissolution, as well as the presence of secondary micrite that coats grains and fills interparticle pores. **G)** Irregular, laminated micritic crusts of LFG (arrows), overlain by a ≤ 30-cm-thick unit angular breccia. **H)** Caliche crust and overlying breccia, typical of LFG from both FA1 and FA2 successions; note the irregular laminations within the micritic crust, as well as the arrangement of the angular clasts within the breccia. **I)** Oolitic grainstone, illustrating petrographic characteristics associated with subaerial exposure; note the secondary micrite and subtle laminations that compose the crust, as well as the aligned, downward-bifurcating moldic pores interpreted as rhizoliths.

FIG. 9.—Outcrop photos and thin-section photomicrographs illustrating the character of Pleistocene Lithofacies (LF) A through D. **A)** LFA deposit from the south margin composed of coral rubble rudstone and coralline boundstone with rare *in situ* coral; above, a sharp contact (red arrow) separates LFA from the overlying seaward-dipping, planar and low-angle cross-laminated strata of LFE. **B)** Bedding-plane of coral rubble rudstone. **C)** Moderately-sorted, coarse-grained skeletal-ooid grainstone matrix, which infills and overlies the boundstone and rudstone of LFA; note the abundance of micritic cement that partially occludes interparticle pores. **D)** LFB deposit from the south margin,

showing well-preserved TCS (ii2); note the sharp, erosive contacts both above and below each bedsets (red arrows). **E)** Decimeter-scale TCS bedsets of FA1 (ii5), with interbedded cobble-size intraclasts (red arrow). **F)** LFB deposit from FA1, illustrating mm-scale variability; red line marks the edge of a subvertical trace fossil (cf. *Bergaueria).* Note the looser packing and coarser sediment in the burrow interior. **G)** Thick, southward-dipping trough cross-stratified bedsets with sharp, parallel bedset boundaries (red arrows), common in north margin LFC strata from a north margin outcrop. **H)** Plan-view of southward-dipping LFC strata showing rib and furrow paleocurrent indicators (white arrows). **I)** LFC, composed of bimodal, poorly sorted very fine to medium-grained skeletal-ooid-composite grain grainstone, showing the fill of an unlined, subvertical burrow, with coarser fill and looser sediment packing than the matrix. **J)** Rounded, cobble-size intraclasts of planar-laminated grainstone (red arrow) within FA2 toe-of-beach (LFD) strata. **K)** LFD displaying coarse grain size, poor to moderate sorting, and climbing ripples, typical of toe-of-beach deposits on the north margin. **L)** Moderately-sorted, fine-grained, ooid-composite grain grainstone from a south margin LFD deposit; note the patchy distribution of cement and paucity of laminations or other physical sedimentary structures.

FIG. 10.—Representative measured sections of Pleistocene facies associations with stratigraphic, sedimentologic, and ichnologic data, and interpreted environments of deposition. **A)** Succession common of Facies Association 1; note the thinner overall section and higher bioturbation intensity throughout as well as the thin foreshore. **B)** Succession common of Facies Association 2. Where all six lithofacies are present, FA2 is characterized by a discontinuous, basal unit of boundstone-rudstone, upper shoreface deposits with thick

trough cross-stratified bedsets and low bioturbation intensity (≤ ii3), cryptobioturbated foreshore deposits up to 2-m thick, and swaley-bedded berm deposits up to 2-m thick. The measured section is < 4 m, the succession lacks both reef (LFA) and berm (LFF) facies, grain size is much finer, and bioturbation intensity (ii) is much greater than Facies Association 1.

FIG. 11.—Outcrop photos of trace fossils. **A)** Plant root molds preserved in concave hyporelief; note the Y-shaped branching pattern and associated change in trace diameter. **B)** *Psilonichnus* preserved within LFE of a south-margin succession. **C)** Planiform traces preserved within fenestral, moderately well-sorted, medium-grained ooid grainstone of LFE; note the subtle nature of the horizontal burrow (*Planolites*), which lacks a defined burrow lining. **D)** *Piscichnus* within LFB of a north-margin succession. **E)** *Skolithos* common of LFB and LFD deposits of FA1. **F)** *Conichnus* within LFD. **G)** Vertical transition from *Rosselia* (lower) to *Cylindrichnus* (upper). **H)** *Thalassinoides* in LFB deposits of FA1. I) Horizontally oriented *Ophiomorpha* burrow network within LFD; note the branching pattern and hollow interior of the burrow shafts.

FIG. 12.—Representative outcrop, hand sample, and thin section photos of Ichnofabrics II–VI. **A–C**) Ichnofabric II, illustrating tiering of trace fossils with horizontal, vertical, and boxwork morphologies. Note the intensity of bioturbation, and degree of interpenetration and crosscutting compared to the other ichnofabrics. Also note the porous, loosely packed burrow fill (BF) compared to the cement halo (H) surrounding the burrow (contact marked with red arrows). **D–F**) Ichnofabric III, showing diminutive subvertical and U-shaped trace fossils. Trace fossils of Ichnofabric III typically display protrusive (common) and retrusive (less common) spreiten. **G–I**) Ichnofabric IV, dominated by

planiform, cylindrical trace fossils that intermittently disrupt primary laminations (black arrows). I) Ichnofabric IV expressed in thin section, illustrating the subtle alteration of primary laminae. Small, horizontal burrows are expressed as ovoid disruptions in primary laminae (yellow arrow), with burrow fill that has looser grain packing and less cementation than the surrounding host rock. Note the looser grain packing and diminished cement that define burrow interiors (yellow arrows). **J–L**) Characteristics of Ichnofabric V, with vertically-oriented, reinforced burrows such as *Ophiomorpha* (yellow arrow) and *Skolithos*. Burrow walls are lined with pellets of sand-sized grains to form mammillated textures on exterior walls (dashed lines). Note the coarser grain size and lack of cement within burrow fill (BF) compared to the finer grained matrix (M). **M–O**) Ichnofabric VI, illustrating cryptobioturbation at multiple scales. Dense distribution of mm-scale burrows destroys primary laminations at bioturbation intensity > ii3 (black arrows).

FIG. 13.—Corresponding slab sample, thin section, and CT scan data. Cryptobioturbation (Ichnofabric VI), Vertical Reinforced Burrows (Ichnofabric V), and Network Burrows (Ichnofabric II) ichnofabrics common within carbonate shoreface deposits of CAP. The character of each ichnofabric is displayed in high-resolution digital scans of slabbed samples, whole thin-section scans, and axial images from CT- and Micro-CT scans. Density is represented by color range: black (no density, open pore) to white (highest density) for micro-CT and thin section scans, and from black to dark red in CT scans. Density values are used as a proxy for porosity distribution, in turn correlated to permeability distribution. The three samples represent the spectrum of porosity distribution within shoreface grainstone of CAP. **A–D**) Ichnofabric VI, cryptobioturbated

with density homogenized in both vertical and horizontal directions. This type of porosity distribution is most common within LFE and LFF deposits; **E-H**) Ichnofabric V, characterized by *Ophiomorpha* and *Skolithos* with reinforced, cm-scale burrows. CT scans show sparse distribution of cm-scale density heterogeneities, common in LFA and LFB deposits of FA2. **I–L**) Ichnofabric II, characterized by network burrows with density heterogeneities that form interconnected 3D networks, corresponding to burrow systems with morphologies similar to *Ophiomorpha* or *Thalassinoides*. These porosity distributions are most common within FA1 deposits of the North Margin. For network burrow ichnofabrics, note that the burrow interiors are darker, indicative of porous burrow fill, and are typically surrounded by a lighter colored halo of higher density calcite cement.

FIG. 14.—Schematic summary and conceptual model showing hydrodynamic processes that influence sedimentation and bioturbation on the leeward margin of CAP, the stratigraphic character and preservation of shallowing-upward grainstone successions in the rock record, and the defining characteristics of along-strike variability. Arrows on the modern processes map show schematic direction of currents and sediment transport. Pleistocene sections illustrate the stratigraphic patterns and bioturbation intensity of protected versus open margin shoreface deposits. Defining character summarizes features of along-strike heterogeneity, applicable to predicting variability within analog reservoirs.

FIG. 15.—Ichnofacies model of a carbonate shoreface system with along-strike variability in hydrodynamic conditions and depositional environments. Bathymetric profiles, dominant hydrodynamic processes, depositional environments, abundance and distribution of traces and associated ichnofacies for the north, central, and south margins. The profiles are

derived from bathymetric data collected during scuba transects. For horizontal scale, compare to the bathymetric profiles in Fig. 3. Please refer to the Key of Ichnogenera for abbreviations.

TABLE CAPTIONS

TABLE 1.—Geomorphic characteristics of the north, central, and south margin. Abbreviations are as follows: BCB=boulder clast berm; LSF=lower shoreface; MHT = mean high tide; RC=rocky cliffs, RS=rocky shoreline; SB=sand berm; SS=sandy shoreline; USF=upper shoreface; and VSB=vegetation-stabilized sand berm.

TABLE 2.—Summary table for North Margin Transect A–A', location in Fig. 1C. Abbreviations are as follows: BST = boundstone; GST = grainstone; ii = ichnofabric index; MHT = mean high tide; N/A = not available; PKST = packstone; PR = patch reef; RB = rocky bottom; RC = rocky cliffs; RS = rocky shoreline; RST = rudstone; SB = sand berm; and U. skeletal = unidentified skeletal fragments. Sorting abbreviations: M = moderately; MW = moderately well; P = poorly; VP = very poorly; VW = very well; W = well.

TABLE 3.—Summary table for Central Margin Transect B–B', location in Fig. 1C. Abbreviations are as follows: BCB = boulder clast berm; BST = boundstone; bUSF = bioturbated upper shoreface; GST = grainstone; ii = ichnofabric index; PKST = packstone; PR = patch reef; RC = rocky cliffs; RS = rocky shoreline; RST = rudstone; SB = sand berm; TCS = trough cross-stratification; TOB = toe of the beach; and USF = upper shoreface, and VSB=vegetation-stabilized sand berm.

TABLE 4.—Summary table for South Margin Transect C–C', location in Fig. 1C. Abbreviations are as follows: BST = boundstone; bUSF = bioturbated upper shoreface; GST =

grainstone; ii = ichnofabric index; PR = patch reef; RC = rocky cliffs; RS = rocky shoreline; RST = rudstone; TCS = trough cross-stratification; TOB = toe of the beach; and USF = upper shoreface, and VSB=vegetation-stabilized sand berm.

TABLE 5.—Summary table of Pleistocene and Holocene lithofacies. Abbreviations are as follows: BSB = backshore berm; bUSF = bioturbated upper shoreface; FA1 = Facies Association 1; FA2 = Facies Association 2; FS = foreshore; M = moderately sorted; MHT = mean high tide; MW = moderately well sorted; P = poorly sorted; SL = sea level; TCS = trough cross-stratified; ii = ichnofabric index; USF = upper shoreface; and W = well sorted.

TABLE 6.—Summary table of carbonate shoreface ichnofabrics.

FIGURES

Figure 1:

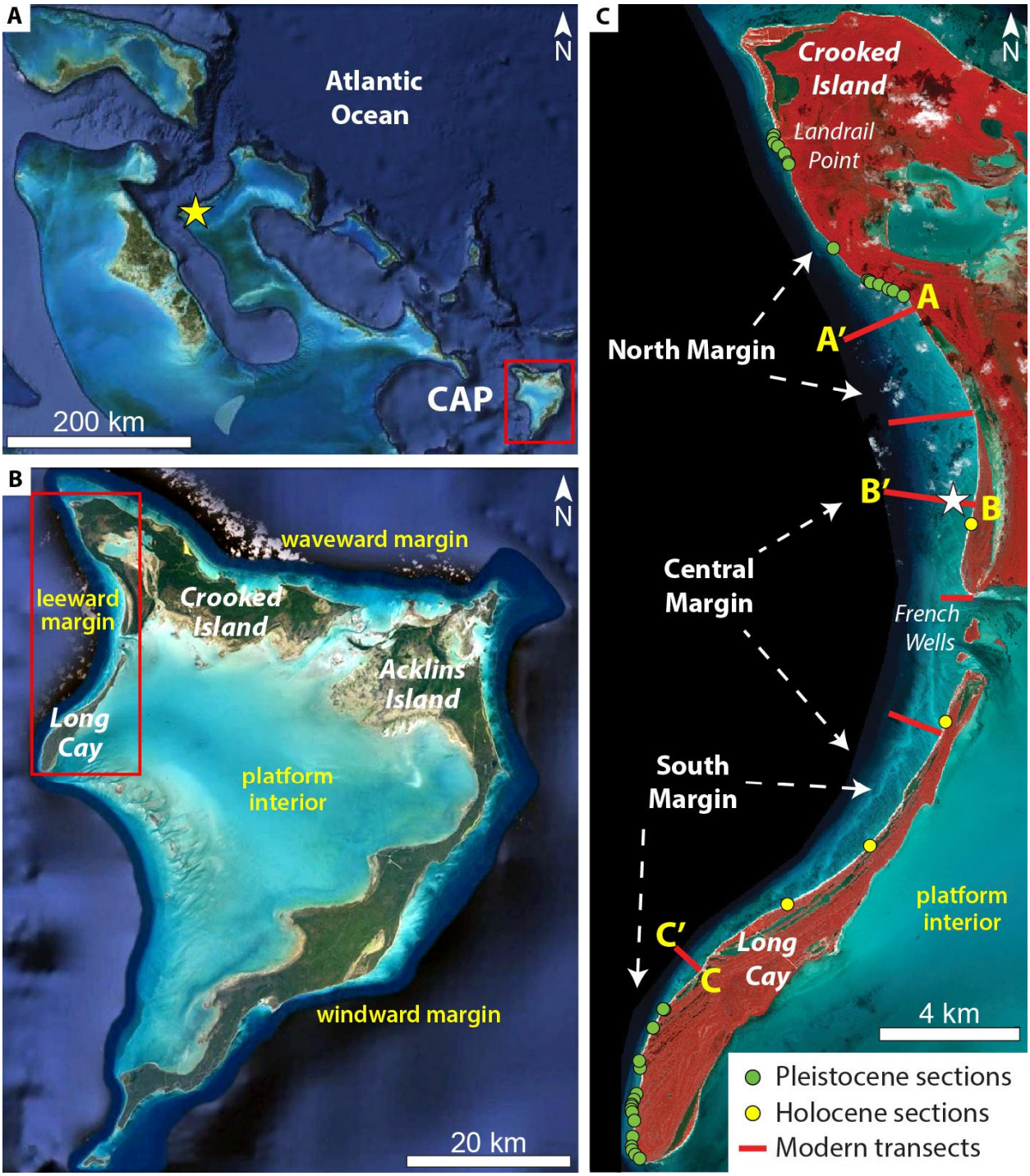

Figure 2:

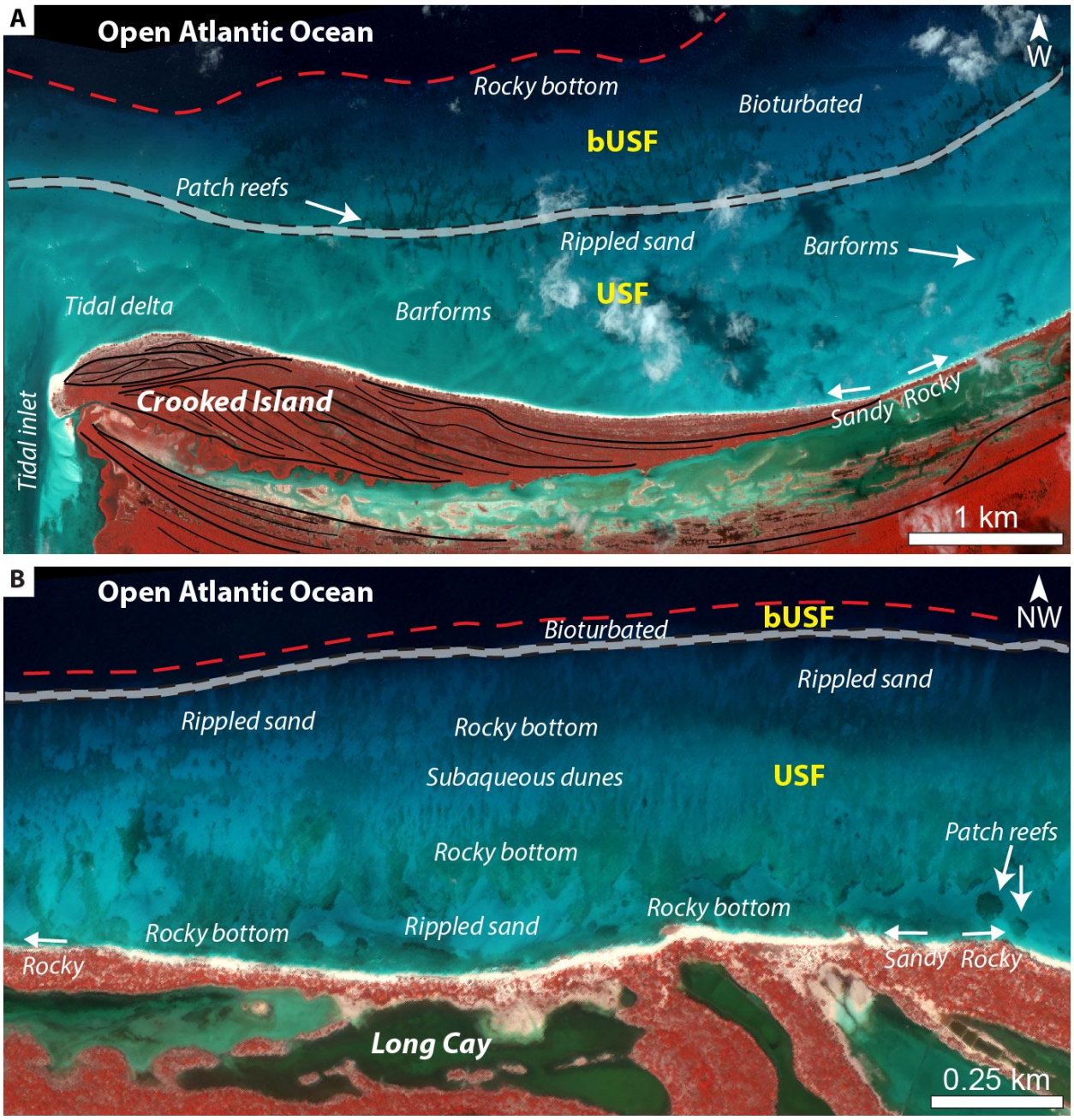
A
Open Atlantic Ocean
W
Rocky bottom
Bioturbated
bUSF
Patch reefs
Rippled sand
Barforms
USF
Tidal delta
Barforms
Crooked Island
Tidal inlet
Sandy
Rocky
1 km
B
Open Atlantic Ocean
NW
Bioturbated
bUSF
Rippled sand
Rippled sand
Rocky bottom
Subaqueous dunes
USF
Patch reefs
Rocky bottom
Rocky bottom
Rocky bottom
Rippled sand
Rocky
Sandy
Rocky
Long Cay
0.25 km

Figure 3:

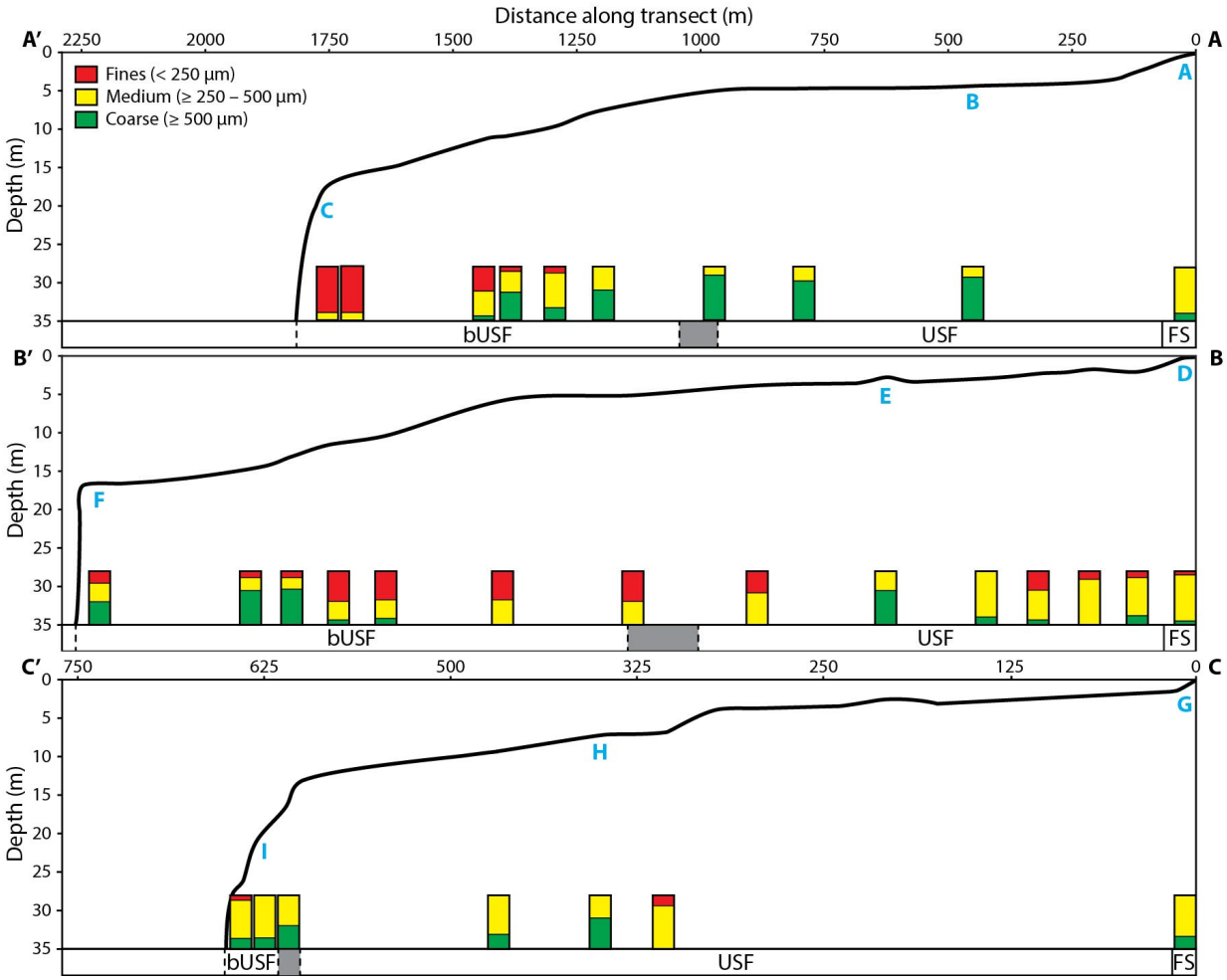
Distance along transect (m)
A′
2250
2000
1750
1500
1250
1000
750
500
250
0
A
Fines (< 250 µm)
Medium (≥ 250 – 500 µm)
Coarse (≥ 500 µm)
Depth (m)
A
B
C
bUSF
USF
FS
B′
B
D
E
F
C′
750
625
500
325
250
125
C
G
H
I

Figure 4:

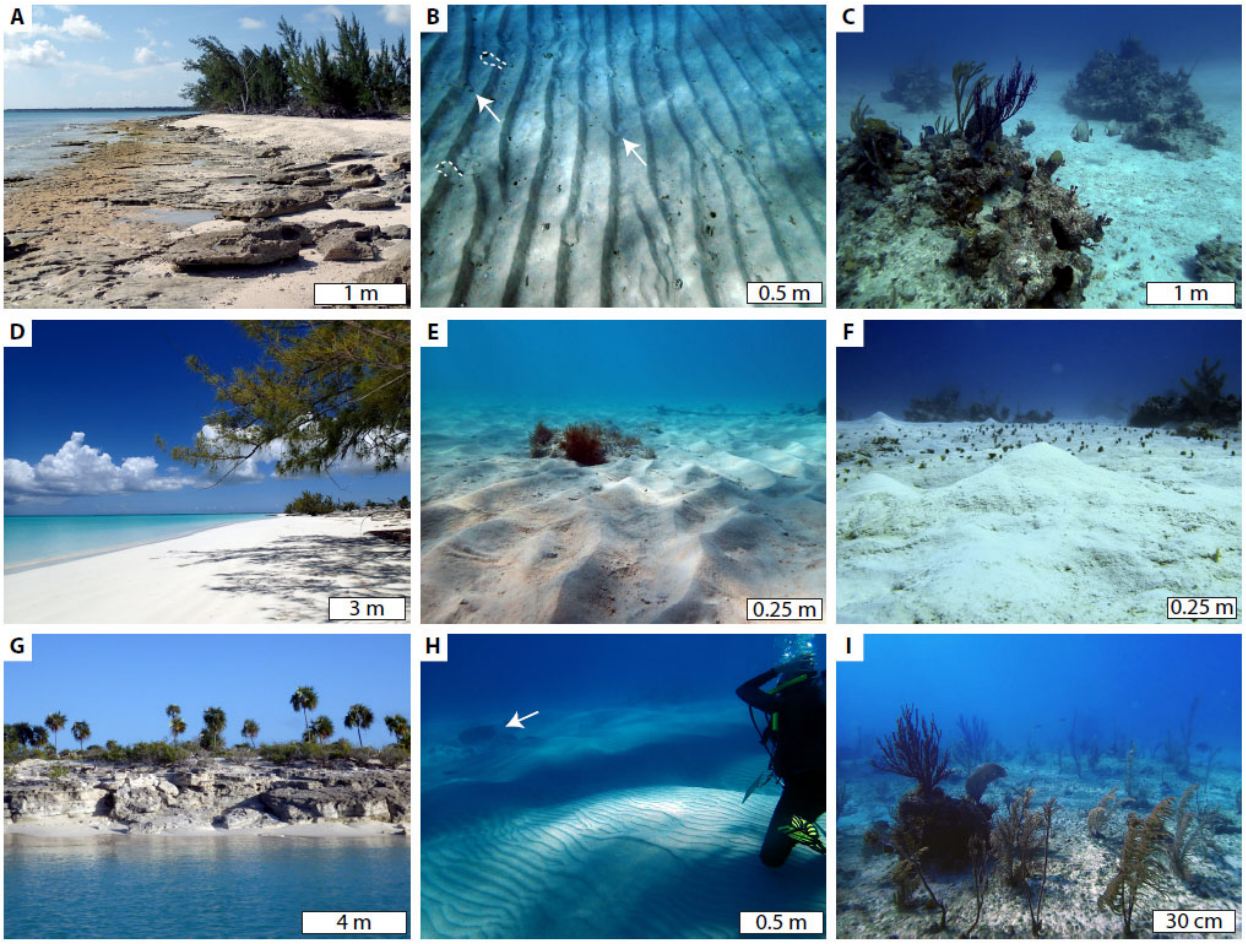

Figure 5:

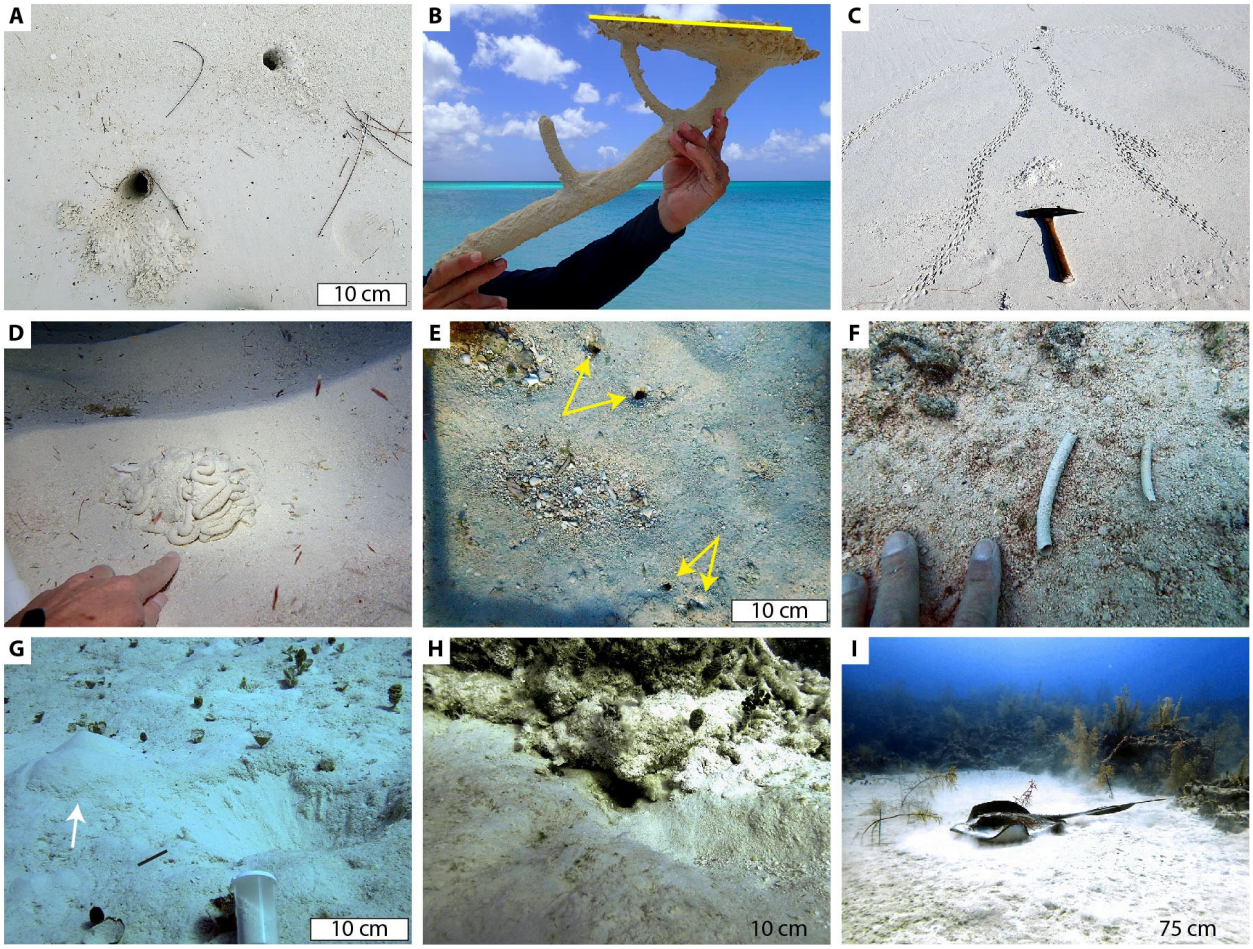

Figure 6:

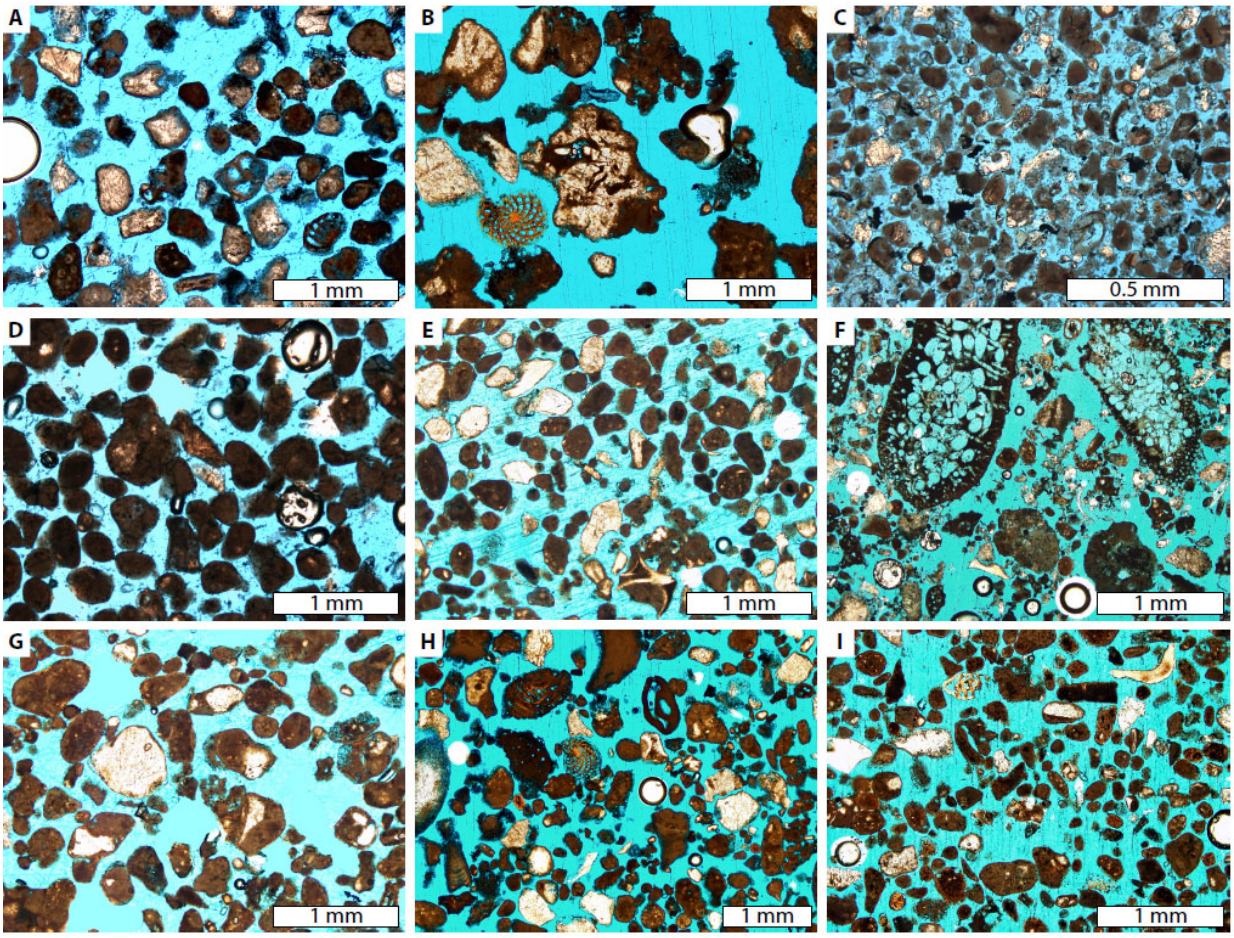

Figure 7:

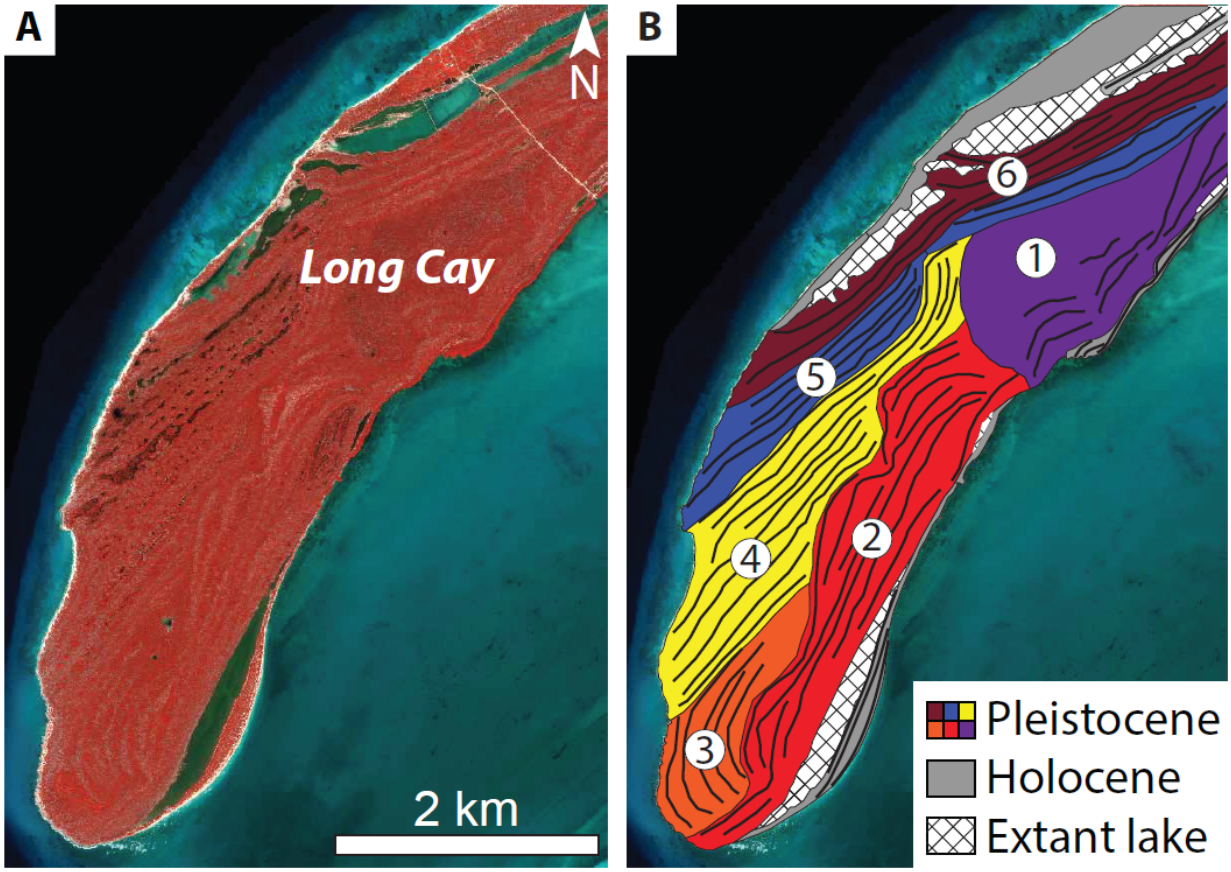

Figure 8:

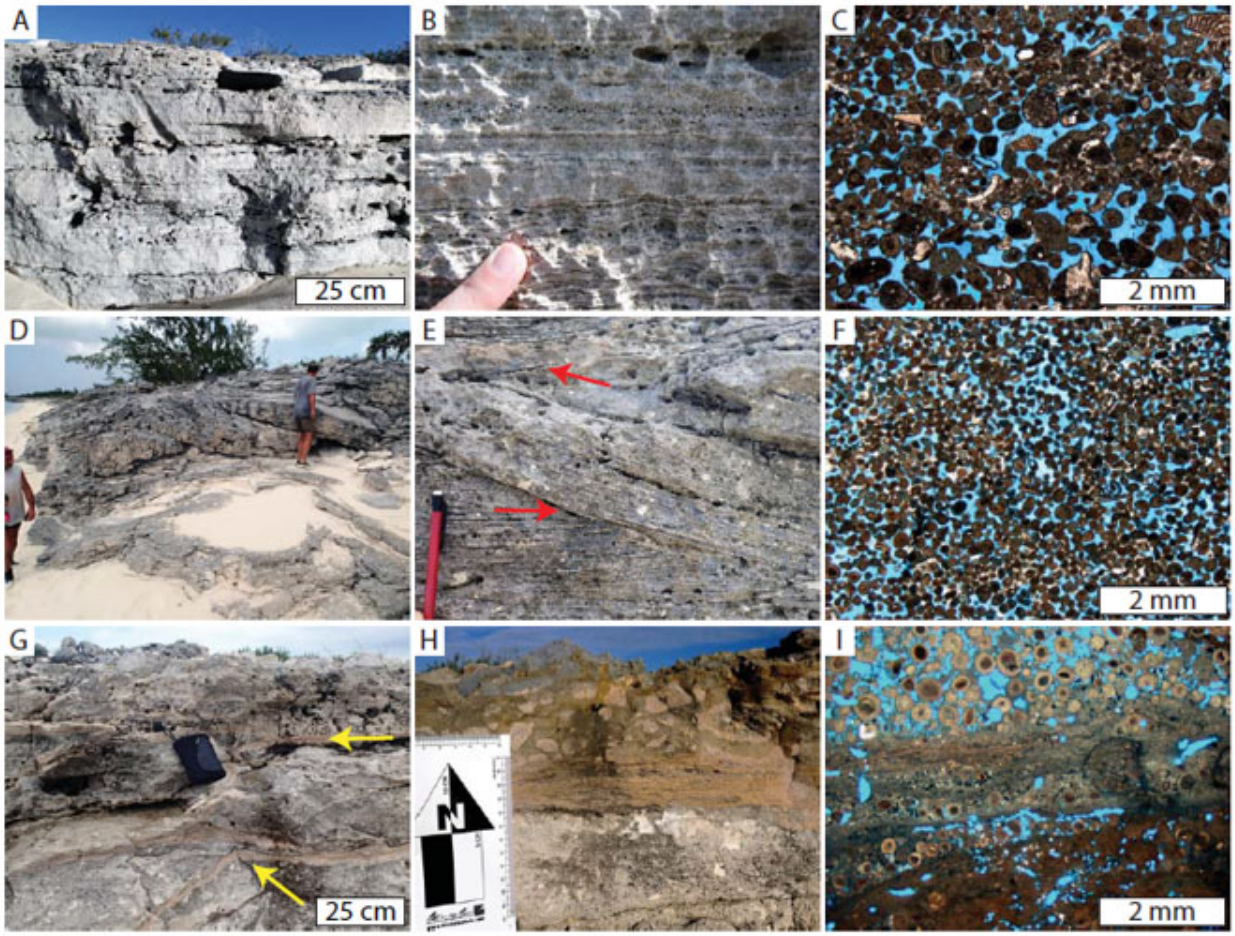

Figure 9:

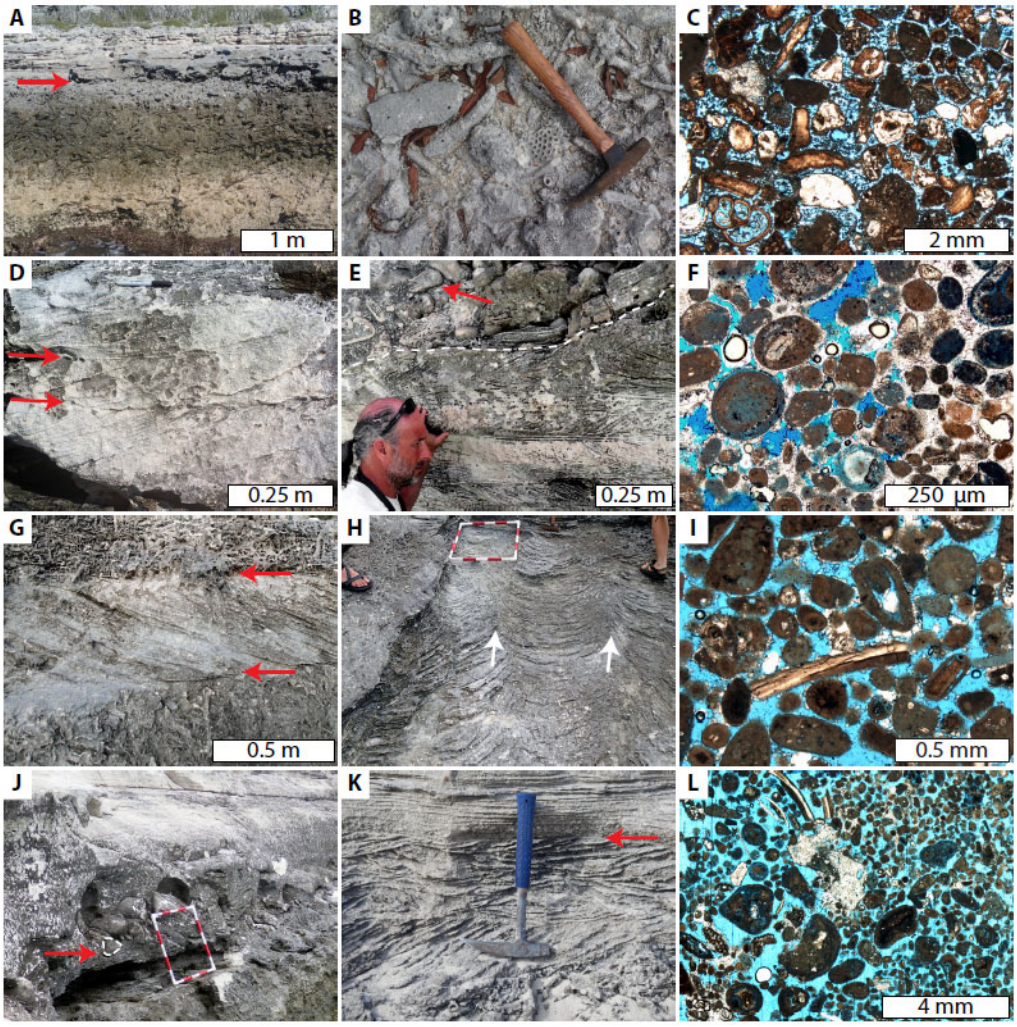

Figure 10:

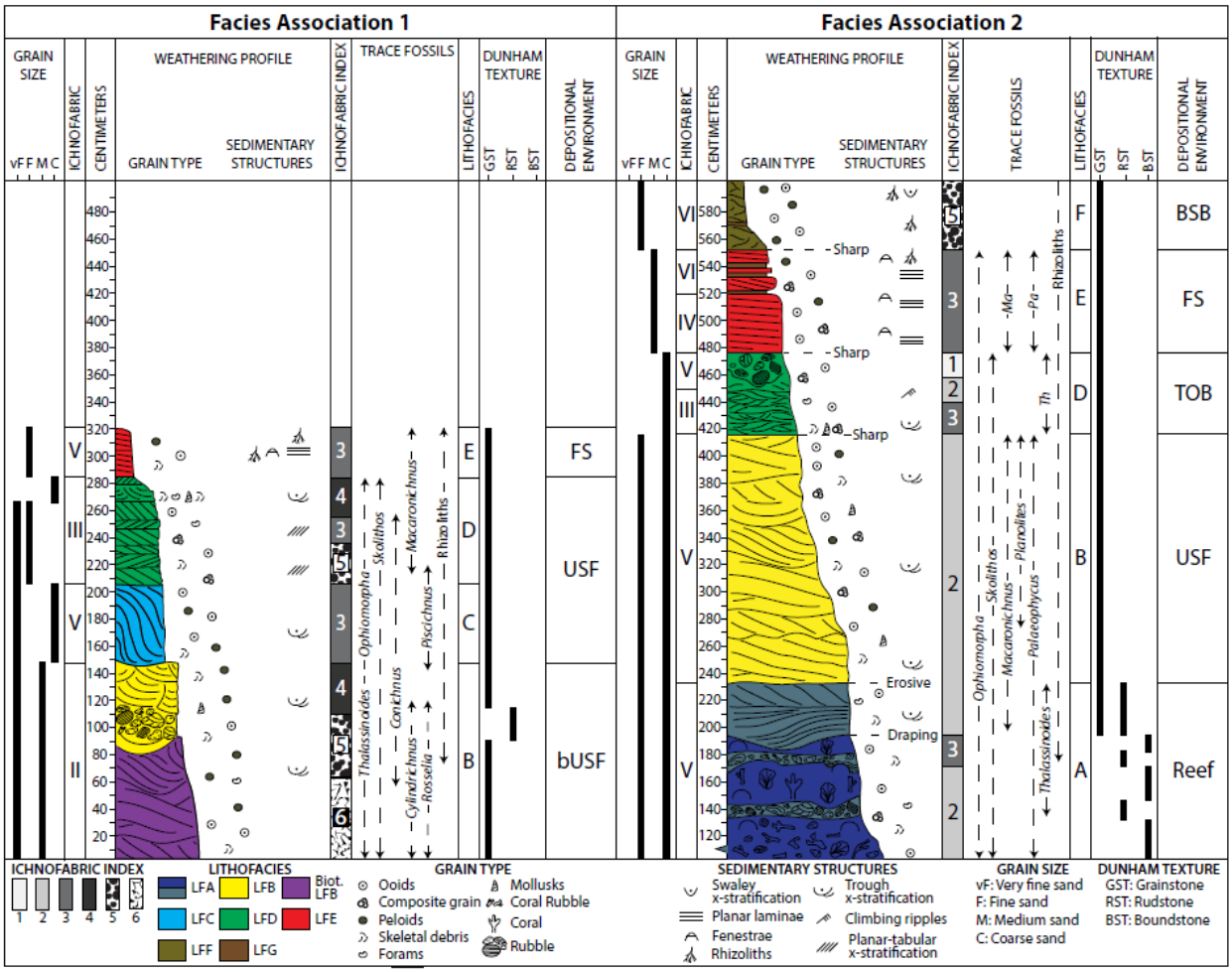
Facies Association 1
Facies Association 2
GRAIN SIZE
ICHNOFABRIC
CENTIMETERS
WEATHERING PROFILE
GRAIN TYPE
SEDIMENTARY STRUCTURES
ICHNOFABRIC INDEX
TRACE FOSSILS
LITHOFACIES
DUNHAM TEXTURE
GST
RST
BST
DEPOSITIONAL ENVIRONMENT
vF F M C
FS
USF
bUSF
BSB
TOB
Reef
Thalassinoides
Ophiomorpha
Skolithos
Conichnus
Cylindrichnus
Macaronichnus
Piscichnus
Rosselia
Rhizoliths
Palaeophycus
Planolites
Sharp
Erosive
Draping
ICHNOFABRIC INDEX
LITHOFACIES
LFA
LFB
Biot. LFB
LFC
LFD
LFE
LFF
LFG
GRAIN TYPE
Ooids
Composite grain
Peloids
Skeletal debris
Forams
Mollusks
Coral Rubble
Coral
Rubble
SEDIMENTARY STRUCTURES
Swaley x-stratification
Planar laminae
Fenestrae
Rhizoliths
Trough x-stratification
Climbing ripples
Planar-tabular x-stratification
GRAIN SIZE
vF: Very fine sand
F: Fine sand
M: Medium sand
C: Coarse sand
DUNHAM TEXTURE
GST: Grainstone
RST: Rudstone
BST: Boundstone

Figure 11:

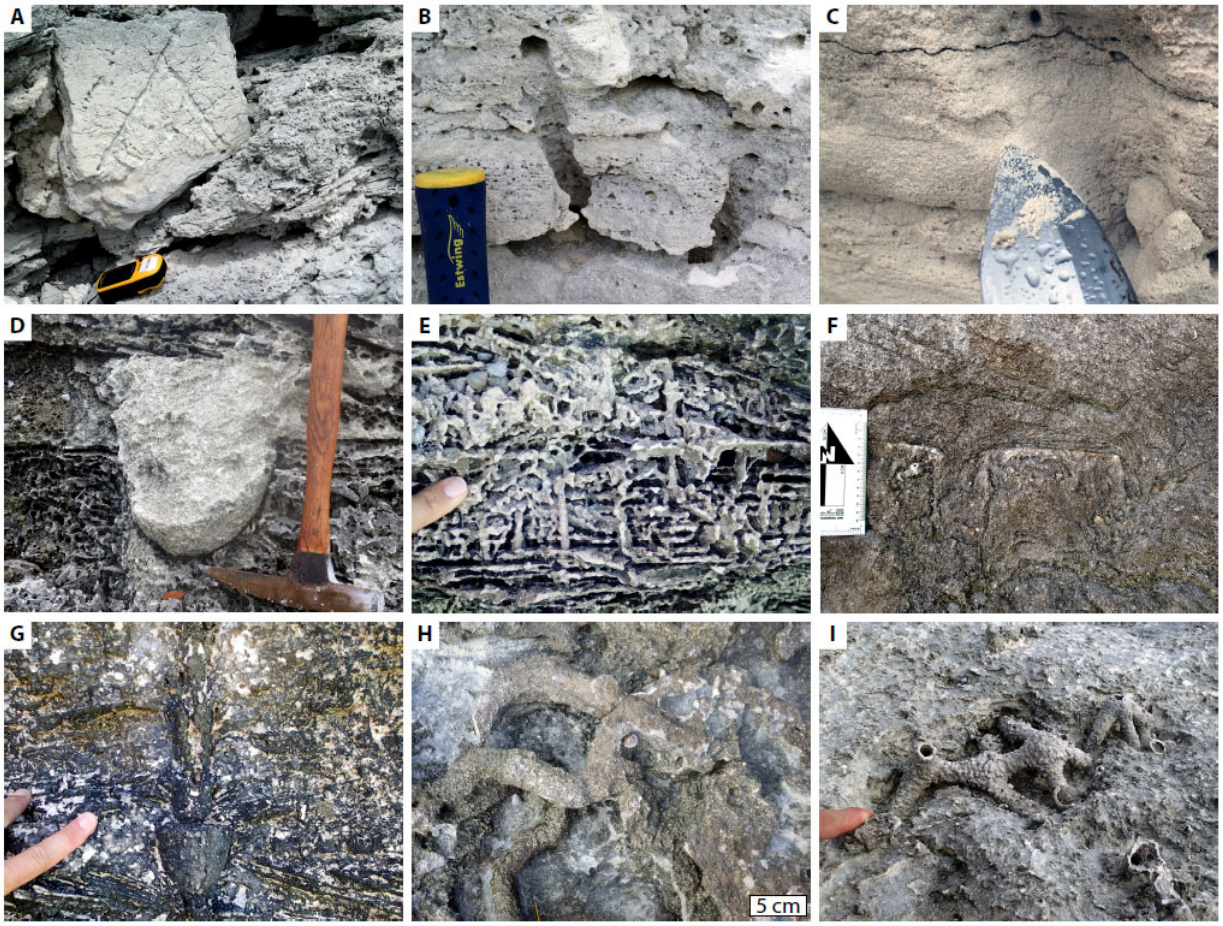

Figure 12:

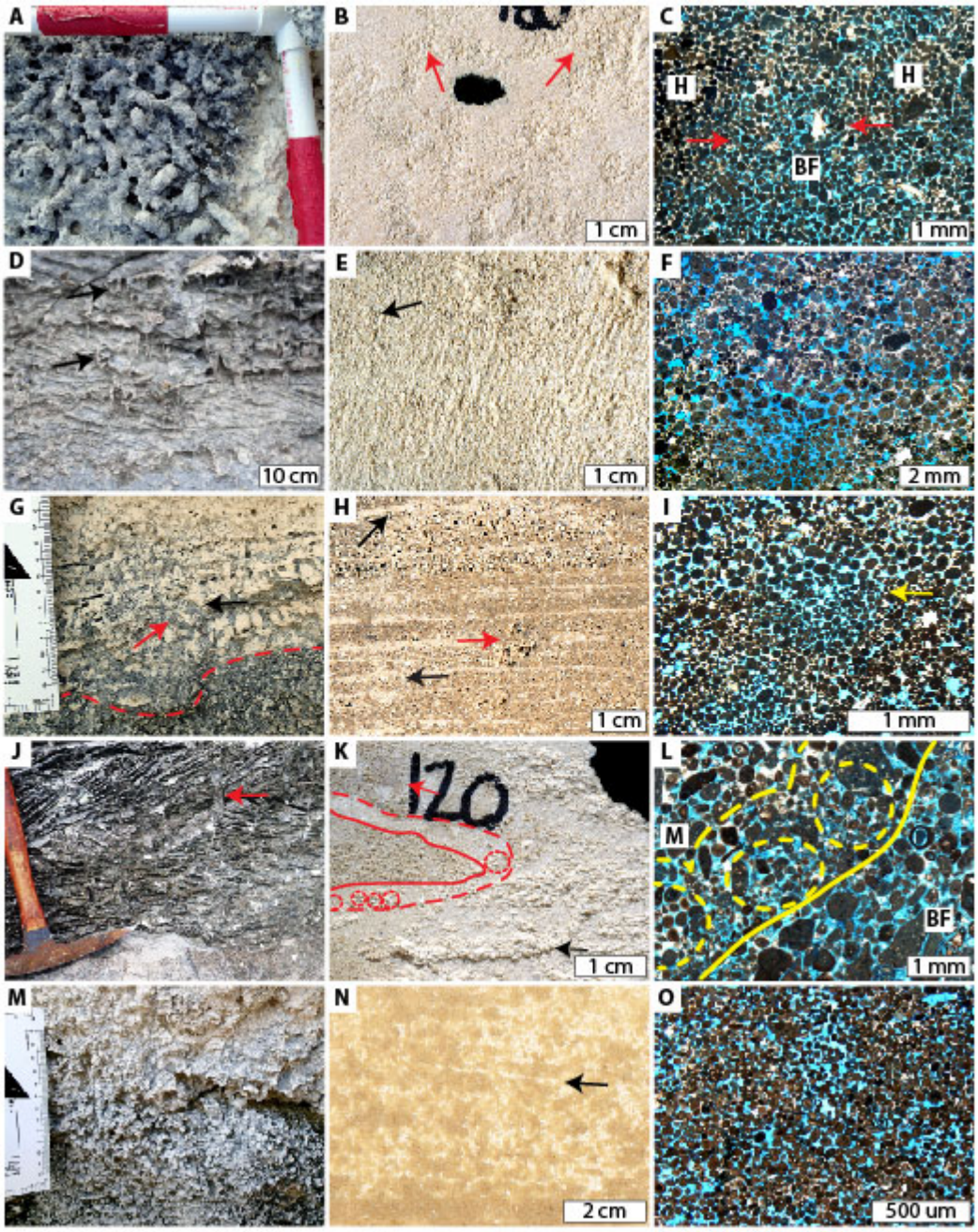
A
B
1 cm
C
H
H
BF
1 mm
D
10 cm
E
1 cm
F
2 mm
G
H
1 cm
I
1 mm
J
K
1 cm
L
M
BF
1 mm
M
N
2 cm
O
500 um

Figure 13:

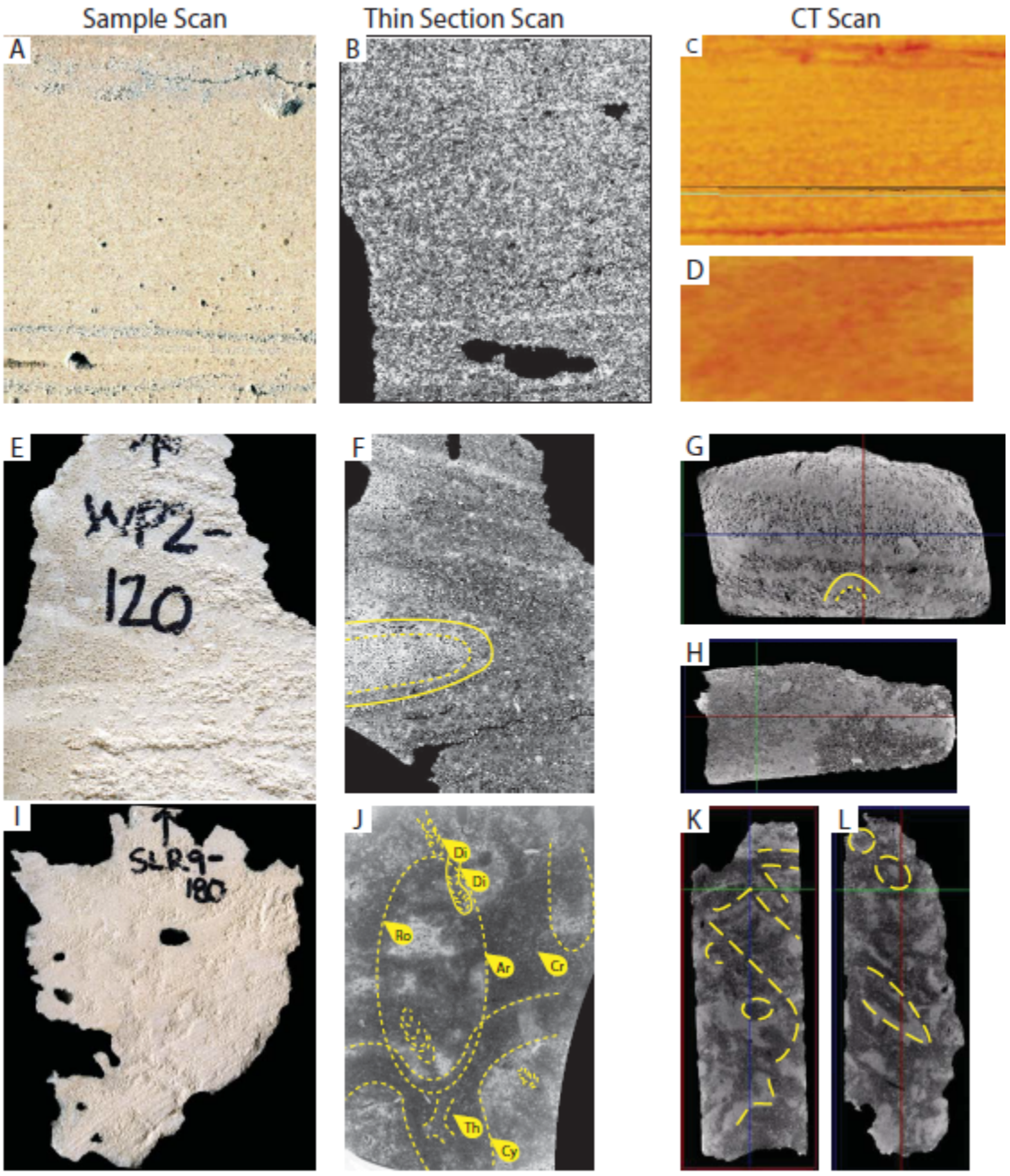
Sample Scan
Thin Section Scan
CT Scan
A
B
C
D
E
WP2-
120
F
G
H
I
SLR9-
180
J
Di
Di
Ro
Ar
Cr
Th
Cy
K
L

Figure 14:

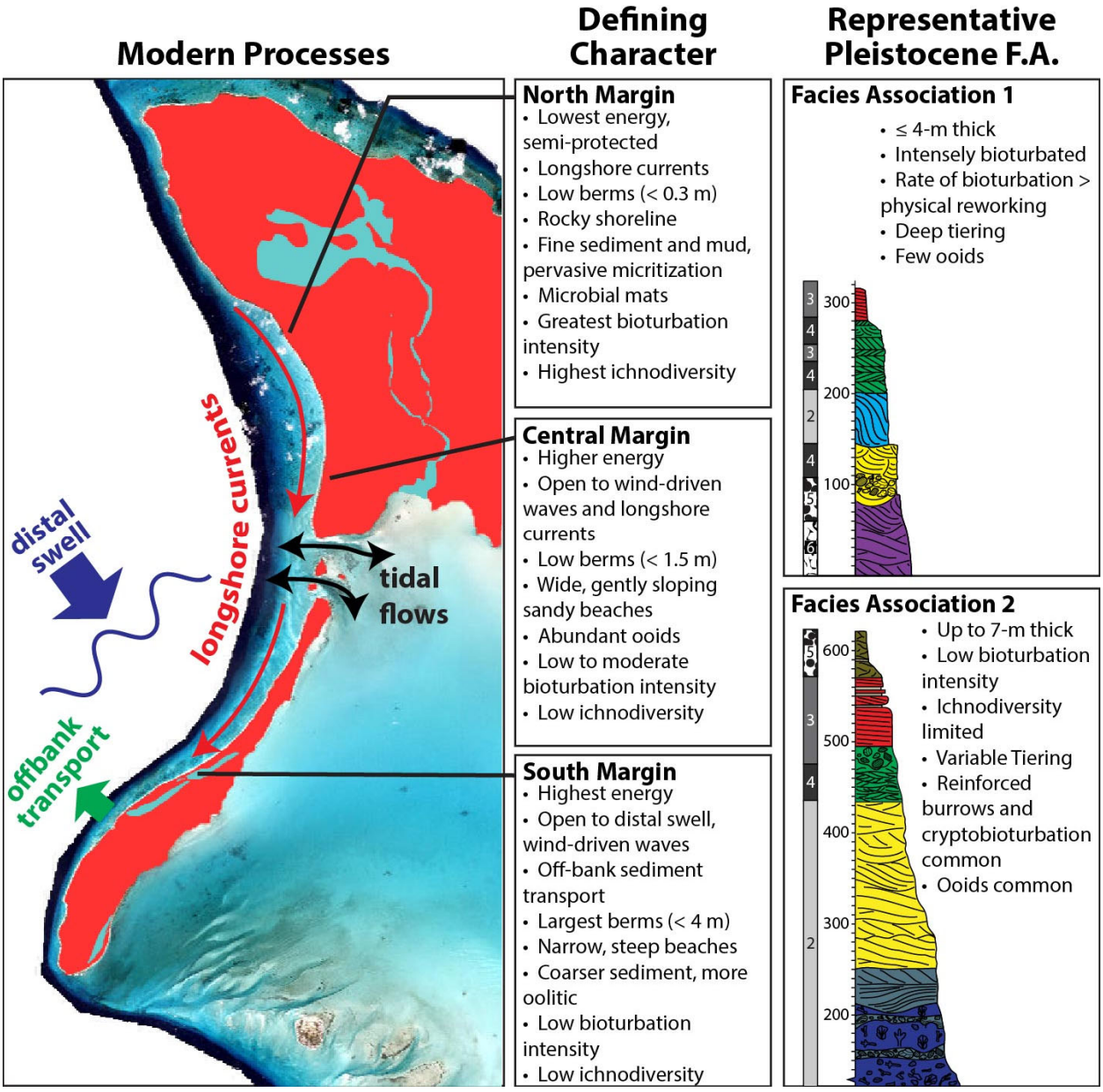
Modern Processes
Defining Character
Representative Pleistocene F.A.
distal swell
longshore currents
tidal flows
offbank transport
North Margin
• Lowest energy, semi-protected
• Longshore currents
• Low berms (< 0.3 m)
• Rocky shoreline
• Fine sediment and mud, pervasive micritization
• Microbial mats
• Greatest bioturbation intensity
• Highest ichnodiversity
Central Margin
• Higher energy
• Open to wind-driven waves and longshore currents
• Low berms (< 1.5 m)
• Wide, gently sloping sandy beaches
• Abundant ooids
• Low to moderate bioturbation intensity
• Low ichnodiversity
South Margin
• Highest energy
• Open to distal swell, wind-driven waves
• Off-bank sediment transport
• Largest berms (< 4 m)
• Narrow, steep beaches
• Coarser sediment, more oolitic
• Low bioturbation intensity
• Low ichnodiversity
Facies Association 1
• ≤ 4-m thick
• Intensely bioturbated
• Rate of bioturbation > physical reworking
• Deep tiering
• Few ooids
300
200
100
Facies Association 2
• Up to 7-m thick
• Low bioturbation intensity
• Ichnodiversity limited
• Variable Tiering
• Reinforced burrows and cryptobioturbation common
• Ooids common
600
500
400
300
200

Figure 15:

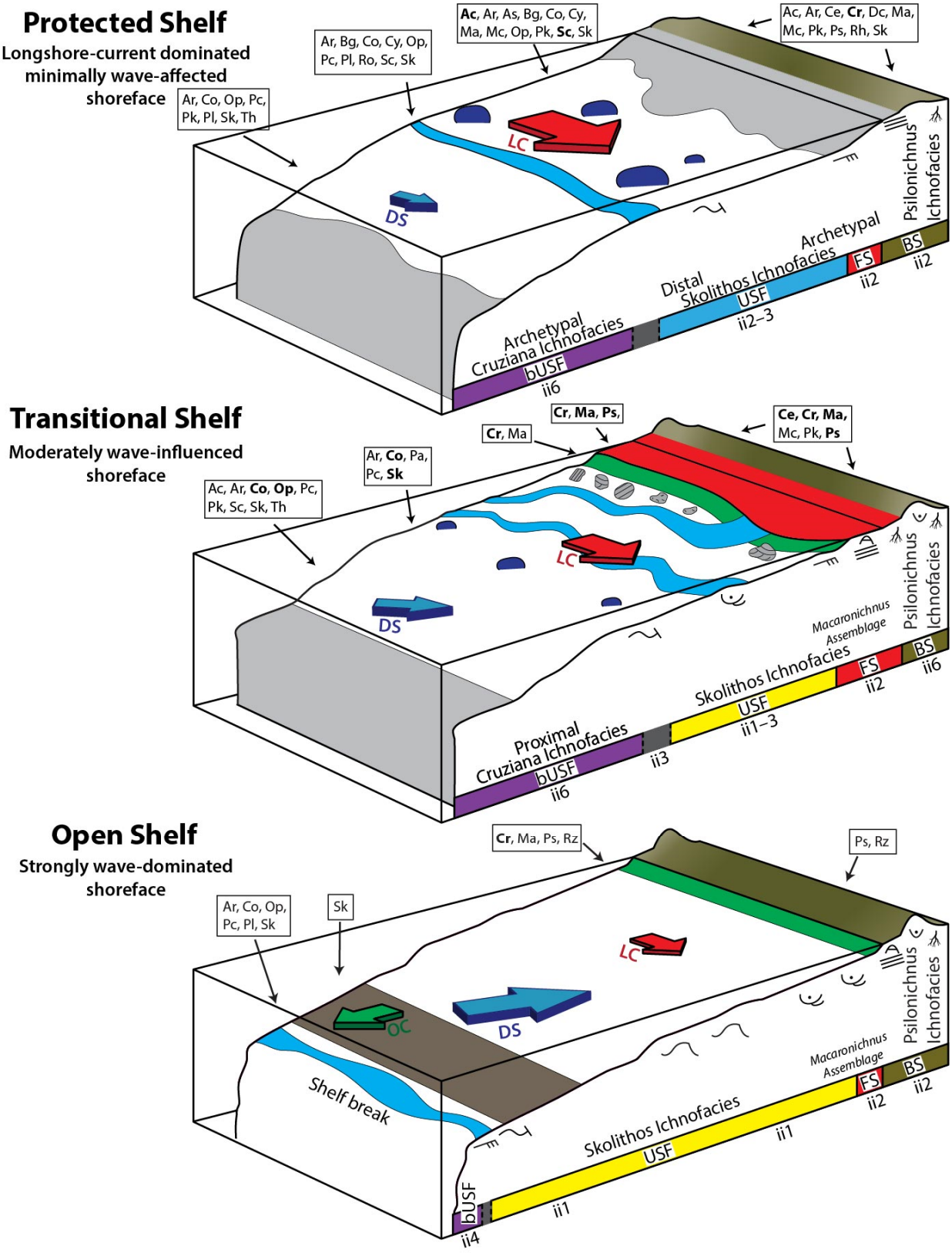
Protected Shelf
Longshore-current dominated minimally wave-affected shoreface
Ar, Co, Op, Pc, Pk, Pl, Sk, Th
Ar, Bg, Co, Cy, Op, Pc, Pl, Ro, Sc, Sk
Ac, Ar, As, Bg, Co, Cy, Ma, Mc, Op, Pk, Sc, Sk
Ac, Ar, Ce, Cr, Dc, Ma, Mc, Pk, Ps, Rh, Sk
LC
DS
Psilonichnus Ichnofacies
Archetypal Skolithos Ichnofacies
BS
FS
USF
ii2
Distal
ii2–3
Archetypal Cruziana Ichnofacies
bUSF
ii6
Transitional Shelf
Moderately wave-influenced shoreface
Ar, Co, Pa, Pc, Sk
Cr, Ma
Cr, Ma, Ps,
Ce, Cr, Ma, Mc, Pk, Ps
Ac, Ar, Co, Op, Pc, Pk, Sc, Sk, Th
Macaronichnus Assemblage
Skolithos Ichnofacies
ii1–3
Proximal
ii3
Open Shelf
Strongly wave-dominated shoreface
Cr, Ma, Ps, Rz
Ps, Rz
Ar, Co, Op, Pc, Pl, Sk
Sk
OC
Shelf break
ii1
ii4

TABLES

Table 1:

Margin Characteristics	North Margin	Central Margin	South Margin
Margin orientation	SW facing	W facing	NW facing
Shelf width (km)	0.7–1.9	1.4–2.6	0.4–1.2
Shelf-break depth (m)	18	17	13
Average shelf gradient	0.5°	0.5°	2.1°
Berm type	SB	BCB; VSB	VSB
Berm height (m)	≤ 0.3	< 1.5	≤ 4
Shoreline type	RC; RS	SS	RC; SS
Beach width (m)	≤ 10	≤ 30	4–25
Beach gradient	≤ 5°	≤ 5°	> 7°
USF depth range (m)	0.7–7.0	1.0–5.0	3.4–17.0
USF width (km)	1.0	1.1	0.6
USF width (% shelf)	55%	50%	85%
USF shelf gradient	0.2°	0.3°	1.3°
bUSF depth range (m)	7–18	5–17	17–27
bUSF width (km)	0.9	1.2	0.1
bUSF width (% shelf)	50%	55%	10%
bUSF shelf gradient	1.1°	1.1°	19°

Zones	Geomorphic Features		Bioturbated Upper Shoreface	Upper Shoreface	Foreshore		Backshore
	Shelf-slope break	Patch Reefs	bUSF	USF	Swash & TOB	Beach	BS & BSB
Dominant Physical Processes	Shoaling waves; Infrequent storm-associated wave-driven currents	Shoaling waves; Infrequent storm-associated waves & currents	Shoaling waves; Infrequent storm-associated wave-driven currents	Southward longshore currents	Fair-weather breaking waves, wave swash and backwash	Wave swash and backwash; Tides; Storm washover (infrequent)	Eolian and terrestrial processes; Storm washover
Geomorphic Features and Bottom Types	High-relief PR (up to 3 m); Sparse, thin sediment cover over RB; up to 35% mud	Rocky bottom; PR up to 250-m diameter, 3-m relief	High-relief PR on RB; Sediment surface intermittently stabilized by 8–15-mm-thick biofilm	Thin sediment cover in shallow, thickens seaward; Margin-parallel barforms; Large, circular high-relief PR	RC (northern) and RS (southern); Devoid of sediment accumulation	Above MHT, narrow beach with thin (≤ 15 cm) sediment cover over Holocene beachrock	Subtle uncemented SB ≤ 0.3-m relief; Thin sediment cover over Holocene beachrock
Physical Sedimentary Structures and Features	Sediment stabilized by up to 10-cm-thick biofilm	N/A	Rare sinous-crested current ripples	Bioturbated wave ripples; Current ripples	Rocky bottom	Seaward-dipping planar bedding, alternating laminae of coarse and fine sand, fenestrae	Landward-dipping bedding
Depositional Texture	PKST	BST; RST	PKST	GST	N/A	GST	GST
Sediment Type	P sorted, bimodal very fine and medium peloid-skeletal sand	P sorted, coarse skeletal-peloid sand	P sorted, trimodal very fine, medium, and coarse peloid-skeletal-composite grain sand	M sorted, coarse composite grain-skeletal-peloid sand	Gravel-size coral rubble, GST intraclasts, beachrock lithoclasts	W sorted, medium skeletal-peloid sand	W sorted, medium skeletal-peloid sand
Grain Constituents	Coral fragments, lithoclasts, *Halimeda*	N/A	Foraminifera, U. skeletal; Few ooids (< 10%)	U. skeletal, *Halimeda*, forams, mollusk fragments; Very few ooids (< 3%)	N/A	U. skeletal, foraminifera, *Halimeda*	U. skeletal, foraminifera, *Halimeda*
Grain Character	N/A	N/A	U. skeletal, foraminifera, and *Halimeda;* Pervasive micritization of skeletal grains	Skeletal grains lack ornamentation, with pervasive micritization and microborings	N/A	Skeletal fragments are rounded and exhibit microborings and micritic rims	Skeletal fragments are rounded and exhibit microborings and micritic rims
Dominant Biota	Callianassid shrimp, goby fish, polychaetes, rays	Sponges, soft coral, sea whips, sea fans	Callianassid shrimp, goby fish, polychaetes	Bivalves, callianassid shrimp, echinoids, gastropods, goby fish, polychaetes	N/A	Amphipods, birds, ghost crabs, insects, land snails, land crabs, terrestrial hermit crabs	Terrestrial organisms; amphipods, birds, ghost and hermit crabs, insects, land snails, land crabs
Bioturbation Intensity	ii6	ii1–2	ii6	ii2–3	ii1	ii2	ii2
Traces	Co, Op, Sk, Th	N/A	Ar, Bg, Co, Op, Pc, Pk, Sc, Sk, Th	Ac, Ar, As, Bg, Bi, Co, Di, Pa, Pc, Pk, Sc, Sk	None	Ac, Ce, cr, Dc, Pk, Ps	Ac, Ar, Ce, Dc, Ma, Mc, Pk, Ps, Sk
Ichnodiversity	High; > 5 ichnogenera	N/A	High; ≥ 8 ichnogenera	Low; ≤ 3 ichnogenera	Absent	Low; ≤ 3 ichnogenera	Low; ≤ 3 ichnogenera
Trace Assemblage	*Skolithos -Conichnus*	N/A	*Skolithos -Conichnus*	*Scolicia -Skolithos-Piscichnus*	N/A	*Psilonichnus*	*Psilonichnus*
Interpretation	Weakly storm-affected shoreface	Weakly storm-affected shoreface	Weakly storm-affected shoreface	Longshore-current dominated USF	Narrow, sediment starved foreshore	Narrow, sediment starved foreshore	Backshore
Ethology				S—C simple feeding and grazing traces (Interface-feeding; Filter-feeding)	N/A	Sparse dwelling and crawling traces	Sparse dwelling and crawling traces
Ichnofacies	Cruziana Ichnofacies	Skolithos Ichnofacies	Cruziana Ichnofacies	Distal Skolithos Ichnofacies	N/A	Psilonichnus Ichnofacies	Psilonichnus Ichnofacies

Table 2

	Geomorphic Features		Bioturbated Upper Shoreface	Upper Shoreface	Foreshore		Backshore
Zones	**Shelf-slope break**	**Patch Reefs**	**bUSF**	**USF**	**Swash & TOB**	**Beach**	**BS & BSB**
Dominant Physical Processes	Shoaling waves; Periodic storm-associated swell	Shoaling waves; Periodic storm-associated swell	Shoaling waves; Periodic storm-associated swell	Local, wind-driven waves; Southward longshore currents	Fairweather breaking waves; Wave swash and backwash	Wave swash and backwash; Tides; Storm washover (periodic)	Storm washover; Eolian and terrestrial processes
Geomorphic Features and Bottom Types	Oversteepened margin; sparse, thin sediment among rocky bottom;	PR ≤ 1.5-m relief, ≤ 150-m diameter	PR ≤ 25-m diameter	Margin-oblique barforms (≤ 1-m relief); Bioturbation is greatest in bar-adjacent troughs	SS; gentle slope (≤ 5°); Rounded cobbles on seafloor (localized)	SS; gentle slope (≤ 5°)	BCB, VSB < 1.5-m relief
Physical Sedimentary Structures and Features	Sediment up to 16% mud	N/A	Bare sediment stablized by a thin, ~3-mm thick biofilm	Active wave and current ripples; barforms exhibit low angle, low period current or wave ripples	Seaward-dipping planar bedding; sinuous-crested ripples; small-scale TCS	Seaward-dipping planar bedding; coarse-fine laminae	BCB composed of imbricated grainstone clasts; landward-dipping planar bedding
Depositional Texture	PKST	BST; RST	PKST	GST	GST	GST	GST
Sediment Type	P sorted, very fine–coarse skeletal-peloid sand	P sorted, very fine–coarse skeletal-peloid-ooid sand	P sorted, very fine–coarse skeletal-composite grain-peloid sand	M sorted, fine–medium ooid-composite grain-skeletal sand	P–M sorted, medium ooid-peloid sand	M–MW sorted, fine–medium ooid-peloid-composite grain sand	M–MW sorted, fine–medium ooid-peloid-composite grain sand
Grain Constituents	*Halimeda*, foraminifera, U. skeletal	U. skeletal, *Halimeda*, foraminifera, coral	Skeletal grains include *Halimeda*, mollusk fragments, foraminifera	U. skeletal, *Halimeda*, foraminifera, mollusk fragments	Pervasively micritized U. skeletal	< 10% U. skeletal with micritic rims and abundant microborings	U. skeletal, mollusk fragments
Grain Character	Abundant microborings, thin micritic rims	Skeletal grains have micritic rims	Microborings and micritic rims common	Pervasively micritized skeletal	Ooids have peloid nuclei, and display < 5 laminae	Ooids have composite grain and skeletal nuclei with concentric laminae, little micritization	Micritzed ooids with peloid and composite-grain nuclei, < 3 laminae
Dominant Biota	Small massive corals, platy corals, sponges, soft corals and other Gorgonians	Small massive corals, platy corals, sponges, soft corals and other Gorgonians	Callianassid shrimp, gastropods, goby fish, polychaete worms	Bivalves, echinoids, polychaete worms, rays	Nereid and other polychaete worms	Ghost crabs	Amphipods, birds, ghost crabs, insects, terrestrial hermit crabs, land crabs, and snails
Bioturbation Intensity	ii6	ii1–2	ii6	ii1–3	ii1–2	ii2	ii1 (BCB) or ii6 (VSB)
Traces	**Pa**, Sk, **Th**	**Pc**	Ac, Ar, **Co**, **Op**, Pc, Pk, Sc, Sk, Th	**Ar**, **Co**, Pa, Pc, **Sk**	**Cr**, Ma	**Cr**, **Ma**, **Ps**	**Ce**, **Cr**, **Ma**, Mc, Pk, **Ps**
Ichnodiversity	Low; ≤ 3 ichnogenera	N/A	High; > 5 ichnogenera	Low; ≤ 3 ichnogenera	Absent–monospecific	Low; ≤ 3 ichnogenera	Low; ≤ 3 ichnogenera
Trace Assemblage	*Skolithos - Thalassinoides*	N/A	*Conichnus-Arenicolites-Thalassinoides*	*Arenicolites -Conichnus - Skolithos*	*Macaronichnus*	*Psilonichnus*	*Psilonichnus - Coenobichnus*
Interpretation	Moderately storm-dominated shoreface	Moderately storm-influenced	Moderately storm-dominated shoreface	Dominated by currents (wave-driven & longshore)	Wide, gently sloping foreshore	Wide, gently sloping foreshore	Backshore Berm
Ethology		Rare				Sparse dwelling and crawling traces	VSB intensely bioturbated by dwelling traces
Ichnofacies	Proximal Cruziana Ichnofacies	Skolithos Ichnofacies	Proximal Cruziana Ichnofacies	Skolithos Ichnofacies	Archetypal Skolithos Ichnofacies	Psilonichnus Ichnofacies	Psilonichnus Ichnofacies

Table 3

	Geomorphic Features		oturbated Upper Shorefa	Upper Shoreface	Foreshore		Backshore
Zones	**Shelf-slope break**	**Patch Reefs**	**bUSF**	**USF**	**Swash & TOB**	**Beach**	**BS & BSB**
Dominant Physical Processes	Shoaling waves; Frequent storm influence, off-bank currents	Shoaling waves; Frequent storm influence, off-bank currents	Shoaling waves; Frequent storm influence, off-bank currents	Breaking waves, Wave surf, Fairweather waves, Off-bank currents	Fairweather breaking waves; wave swash and backwash	Wave swash and backwash; Tides; Storm washover (Frequent)	Extremely variable conditions; Eolian and other terrestrial processes; Storm washover
Geomorphic Features and Bottom Types	Stepped shelf-slope break located within USF	PR relief ≤ 0.5 m	Located outboard of the shelf-slope break	Zone of bare rocky bottom; subaqueous dunes; Lacks barforms	SS; steep slope (up to 15°); Poorly sorted, coarse skeletal lag at TOB	SS; beaches are narrow and steep	VSB ≤ 4-m relief; relict Holocene berm
Physical sedimentary Structures and Features	Slope sediment stabilized by 4-mm thick biofilm	N/A	N/A	Subaqueous dunes, flood-oriented current ripples	Multidirectional cross-bedding and current-modified wave ripples	Seaward-dipping planar wedge-set stratification; coarse-fine laminae	Landward-dipping bedding
Depositional Texture	GST	BST; RST	GST	GST	GST	GST	GST
Sediment Type	P sorted, trimodal fine–coarse ooid-skeletal-composite grain sand	N/A	M sorted, trimodal fine–coarse ooid-skeletal sand	MW sorted, fine ooid-skeletal sand	P sorted, medium ooid-composite grain-skeletal sand	W sorted, medium ooid-skeletal sand	W sorted, fine ooid-composite grain-skeletal to M sorted, medium–coarse ooid-peloid-skeletal sand
Grain Constituents	U. skeletal, foraminifera, mollusk fragments	N/A	U. skeletal, foraminifera, mollusk fragments	U. skeletal	U. skeletal, mollusk fragments	U. skeletal, mollusk fragments	U. skeletal, mollusk fragments
Grain Character	Ubiquitous microborings, thin micritic rims	N/A	Ooid nuclei are peloids; microborings and micritic rims common on skeletal fragments	Ubiquitous microborings, micritic rims thin or absent	Round, abraded skeletal fragments; little to no micritization	Ooids are superficial (< 3 laminae); composite grains decrease south	Ooids are superficial (< 3 laminae); composite grains decrease south
Dominant Biota	Callianassid shrimp, gastropods	Burrowing fish, rays	Bivalves, callianassid shrimp, gastropods, polychaete worms	Goby fish, polychaete worms	Polychaete worms	Ghost crabs	Amphipods, birds, insects, snails, ghost and hermit crabs
Bioturbation Intensity	ii4–6	ii1–2	ii4–6	ii1–2	ii2	ii2	ii6
Traces	Op, Pc, Sk	Pc	Ar, Co, Op, Pa, Pc, Sk, Th	Op, Pa, Sk	cr, Ma	cr, Ps	cr, Ce, Ma, Mc, Ps
Ichnodiversity	Low; ≤ 3 ichnogenera	N/A	Moderate; ≤ 5 ichnogenera	Absent–monospecific	Absent–monospecific	Low; ≤ 3 ichnogenera	Low; ≤ 3 ichnogenera
Trace Assemblage	*Ophiomorpha -Skolithos -Piscichnus*	N/A	*Arenicolites -Skolithos - Ophiomorpha*	*Skolithos*	Cryptobioturbation-*Macaronichnus*	*Psilonichnus*	Cryptobioturbation-*Psilonichnus*
Interpretation	Storm-dominated shoreface; Off-bank transport	Storm-dominated shoreface; Off-bank transport	Storm-dominated shoreface; Off-bank transport	Nearshore, dominated by local- and storm-generated waves	Narrow, steeply sloping foreshore	Wide, gently sloping foreshore	Backshore Berm
Ethology	Dwelling burrows of suspension-feeding organisms	Rare	Rare dwelling traces	Sparse suspension-feeding traces	Intense bioturbation by abundant deposit-feeding traces	Sparse dwelling and crawling traces	VSB intensely bioturbated by dwelling traces
Ichnofacies	Skolithos Ichnofacies	Skolithos Ichnofacies	Archetypal Skolithos Ichnofacies	Skolithos Ichnofacies	Macaronichnus Assemblage	Psilonichnus Ichnofacies	Psilonichnus Ichnofacies

Table 4

Lithofacies	Occurrence	Sedimentological Features	Grain Types and Constituents	Trace fossils	Bioturbation Intensity	Ichnofabric and Ichnofacies	Interpretation
LFA **Coralgal boundstone, coral rudstone, and skeletal-ooid grainstone**	**FA1:** N/A **FA2:** Base of outcrop ≤ 2 m above MHT; Localized distribution (≤ 0.08 km along strike)	Basal coral BST and weakly stratified coralgal RST; P–MW sorted, fine- to very coarse-grained skeletal-ooid-composite grain GST infills reef framework and composes the RST matrix; LFA transitions upward to GST dominated	**BST:** *In situ* and non-growth position corals and encrusting coralline algae **RST:** Coral rubble in fine- to very coarse-grained skeletal grainstone matrix **GST:** P–M sorted, coarse skeletal-ooid grainstone GST; skeletal grains include whole, abraded, and disarticulated mollusks, well-preserved foraminifera, *Halimeda* , and coralline algae.	**FA2:** As, Bg, Co, Cy, Di, Op, Pa, Pl, Sc, Sk, Ta, Te, Th	**FA2:** ii1–6	**FA2:** V; Skolithos Ichnofacies	**FA2:** Patch reefs
LFB **Multidirectional TCS grainstone**	**FA1:** ≤ 2-m thick **FA2:** ≤ 3-m thick; May overlie LFA or form base of outcrop	**FA1:** TCS bedsets ≤ 30-cm thick **FA2:** Multidirectional TCS bedsets 0.3–1 m thick	**FA1:** M sorted, very fine-grained ooid-composite grain-skeletal GST **FA2:** P–MW sorted, fine- to very coarse-grained GST with ooid, peloid, skeletal, and composite grains	**FA1:** Ar, As, Co, Cr, Cy, Di, Ma, Op, Pa, Pk, Pl, Ro, Sc, Si, Sk, Th **FA2:** Ma, Op, Pa, Pl, Sk, Th	**FA1:** ii4–6 **FA2:** ii1–3	**FA1:** II; Cruziana Ichnofacies **FA2:** V; Skolithos Ichnofacies	**FA1:** Low-energy USF protected from storm swell (bUSF) **FA2:** Tidally-influenced USF, open to waves and storm swell
LFC **Southward-dipping, sharp-based TCS**	**FA1:** ≤ 1-m thick; overlies LFB, LFD **FA2:** Absent	≤ 1-m- thick unit of sharp-based, medium to thick (30–80 cm) TCS bedsets with southward paleocurrent indicators	**FA1:** P sorted, very fine- to coarse-grained ooid-peloid-skeletal GST; skeletal grains include whole bivalves, mollusk and coral fragments, and foraminifera	**FA1:** Co, Cr, Cy, Di, Li, Ma, Op, Pa, Pc, Ph, Si, Sk	**FA1:** ii2–5, typically ii3	**FA1:** V; Skolithos Ichnofacies	**FA1:** Longshore-current-dominated USF
LFD **Cross-stratified grainstone with or without cobble interbeds**	Directly below LFE **FA1:** < 2-m thick **FA2:** < 2-m thick	Decimeter-scale bedsets of bi-directional planar cross-stratification are overlain by TCS bedsets with coarse skeletal lag common at toesets. TCS beds thin upward and transition to thin bedsets of current-ripple, climbing-ripple, and wave-ripple cross-stratification with internal truncation.	**FA1 & FA2:** P sorted, very fine sand to coarse gravel-sized skeletal-composite grain GST with variable ooid content Skeletal= *Halimeda* , bivalves, forams, coral fragments, coralline algae; May contain rounded, cobble size clasts of coral and grainstone, whole bivalves	**FA1:** Ar, As, Co, Cy, Di, Li, Ma, **Op**, Pc, Ph, Pk, Pl, Ro, Ru, Sc, Si, Sk, Te, **Th** **FA2:** Ar, As, Di, **Op**, **Pa**, Pc, Pl, Ru, **Sk**, **Te**, Th	**FA1:** ii3–5 **FA2:** ii2	**FA1:** II & III; Skolithos Ichnofacies **FA2:** V; Skolithos Ichnofacies	**FA1 & FA2:** USF–FS transition (TOB)
LFE **Planar laminated to low-angle cross-laminated fenestral grainstone**	**FA1:** < 1-m thick **FA2:** Up to 4-m thick; typically underlies LFF	Gently seaward dipping wedge sets of low-angle (< 10°) cross stratified to planar laminated ooid-grainstone with peloids and skeletal debris; Planar wedge-set stratification, coarse-fine laminae, fenestrae, and rill markings common; May contain gravel–boulder size grainstone lithoclasts	**FA1:** MW sorted, fine-grained ooid-peloid-skeletal grainstone **FA2:** MW–W sorted, bimodal fine and coarse-grained ooid grainstone	**FA1:** Ac, Ar, Bg, Co, cr, Cy, Fu, Ma, **Op**, Pa, Pc, Pl, Ps, Sc, Sk, Th **FA2:** Co, cr, **Fu**, **Ma**, Op, **Pa**, Pc, Pk, **Pl**, Sc, Si, Sk	**FA1:** ii2–5 **FA2:** ii1–3, typically ii3	**FA1:** IV & V; Skolithos–Psilonichnus Ichnofacies **FA2:** IV & VI; Skolithos Ichnofacies	**FA1 & FA2:** FS
LFF **Swaley cross-stratified grainstone**	**FA1:** Absent **FA2:** ≤ 3-m thick; top of succession	Laterally discontinuous swaley bedsets with weak internal stratification and variable dip direction; Where preserved, laminae are upward-coarsening	**FA2:** MW–W sorted, fine ooid-skeletal grainstone	**FA2:** Ac, Ar, Bi, Dc, **Di**, **Ma**, Mc, **Pa**, Pk, **Pl**, Ps, Sc, Sk	**FA2:** ii2–6, typically ii4–6	**FA2:** III & VI; Psilonichnus Ichnofacies	**FA2:** BSB and washover fan
LFG **Discontinuity surface**	Caps shallowing-upwards successions	Surface denoted by presence of laminated micritic crust(s), extensive leaching, blackened grains, needle-fiber calcite, alveolar texture, and rhizoliths; Penetration depth of diagenetic alteration is highly variable	N/A Spatially variable, dependent on nature of underlying lithofacies	Abundant rhizoliths, root density, distribution, and vertical penetration are variable	N/A	N/A	Subaerial exposure surface and associated pedogenesis marking the top of shallowing-upward successions

Table 5

Ichnofabric	Description	Bioturbation Intensity	Occurrence	Architectural Morphology	Trace Fossils & Ichnodiversity	Burrow density and abundance	Tiering and Cross-cutting	Burrow Connectivity (Degree and type)
Ichnofabric I: Nonbioturbated Fabric	Physical sedimentary structures are preserved, with no indication of bioturbation at outcrop, hand-sample, or thin-section scale.	ii1	**FA1**: Not observed **FA2**: LFA, LFB, LFD	N/A	N/A	N/A	N/A	N/A
Ichnofabric II: Network-Burrow Ichnofabric	Mottled background fabric of indistinct, shallow-tier traces overprinted by large (1–10-cm diameter), deep-tier vertical burrows and boxwork systems of branching and interconnected burrows.	ii4–6	**FA1**: LFB, LFD **FA2**: Not observed	Uniform, dense distribution of diverse trace fossils branch and interpenetrate to form 3D burrow networks. Vertical, inclined, or horizontal burrows may display wall linings (up to 5-mm thick) composed of organic matter, mud, or pelleted sand.	Co, **Cy**, Ma, **Op**, Pa, Pk, Pl, Ro, Sk, **Th** High Ichnodiv.	Densely populated and multi-tier organism communities produce abundant trace fossils with high burrow densities	Shallow-tier traces overprinted by deep-tier burrow systems of vertical to horizontally inclined shafts and chambers	High degree of burrow connectivity both vertically and laterally
Ichnofabric III: Vertical, Horizontal, and U-shaped Spreiten-Burrow Ichnofabric	Abundant subvertical, cylindrical to U-shaped burrows, many with spreite; Burrow walls may be lined or unlined; Multi-tier systems are characterized by cross-cutting and overprinting	ii2–6	Most prevalent in LFD, LFE, and LFF; Commonly intergradational with Ichnofabric VI	Minute (1–2-mm diameter) vertical, inclined, and U-shaped trace fossils with or without wall linings; Spreiten and meniscate burrows common	Ar, **Di**, **Pa**, Pk, Sc, **Sk**, Ta, Te Moderate–High Ichnodiv.	Burrow density, trace-fossil abundance, and ichnodiversity are spatially variable, but typically increase upwards within individual bedsets	Tiering is highly variable; Shallow, planiform traces are crosscut and overprinted by penetrative vertical burrows; Tiering and spreite together result in a high degree of burrow connectivity	Diverse morphologies and penetrative burrows result in high degree of cross-cutting and overprinting
Ichnofabric IV: Discrete Planiform-Burrow Ichnofabric	Moderate bioturbation intensity, low ichnodiversity assemblages of discrete planiform traces	ii2–3	Characteristic of LFE	Bedding-parallel, planiform to inclined burrows of 0.1–2 cm diameter; Burrows do not branch or exhibit vertical tiering	**Ma**, **Pa**, **Pl**, Sc Low Ichnodiv.	Burrows may be isolated or exhibit dense concentration; Primary lamination disrupted by subcircular to cylindrical burrows	Bedding-parallel burrows produce shallow-tier, planiform ichnofabric; Paucity of branching morphologies and planiform distribution result in low degree of vertical connectivity; horizontal connectivity is variable	Planiform distribution and paucity of branching morphologies result in low degree of vertical connectivity; Horizontal connectivity is spatially variable
Ichnofabric V: Reinforced Vertical-Burrow Ichnofabric	Sparse to locally abundant distribution of vertical and inclined burrows with reinforced walls	ii2–3	**FA1**: LFC, LFD, LFE **FA2**: LFA, LFB, LFD	Horizontal to inclined burrows (< 1-cm diameter) are overprinted by mid- to deep-tier vertical burrows (< 3-cm diameter) with	As, Co, Fu, **Op**, Pa, Si, **Sk** Low Ichnodiv.	Burrow connectivity is highly variable, ranging from isolated shafts to locally interconnected mazes and boxworks.	Horizontal to inclined burrows (Pa) overprinted by mid- to deep-tier Co, Fu, Op, Si, Sk	Sparse distribution results in low degree of burrow connectivity Moderate degree of vertical connectivity where locally abundant
Ichnofabric VI: Cryptobioturbated Ichnofabric	Minute disruptions of depositional laminae associated with dense concentration of small (typically ≤ 2 mm diameter) indistinct trace fossils. The small cylindrical, bedding-parallel burrows do not destroy primary sedimentary structures, resulting in cryptobioturbated fabric.	ii5–6	**FA1**: LFB, LFC, LFF **FA2**: LFE, LFF Characteristic of LFF; Commonly intergradational with Ichnofabric III	Bedding-parallel (subhorizontal) cylindrical, meandering, or spiraled burrows ≤ 2-mm in diameter; Burrows do not branch or crosscut	**cr**, **Ma**, **Mc**, Pa, **Pl** Low to monospecific Ichnodiv.	Extremely high burrow density produces mottled fabric with few discrete burrows Dense concentration of cylindrical, bedding-parallel burrows produce mottled fabric that may preserve (< ii3) or destroy (> ii3) bedding	May preserve (≤ ii3) or destroy (≥ ii4) primary sedimentary fabrics	Complete bioturbation results in universal burrow connectivity, effectively homogenizing the primary sedimentary fabric to reduce spatial variability and, subsequently, permeability heterogeneity

Table 6

APPENDIX A

Porosity and Permeability in Carbonate Shoreface Strata

Shoreface strata of CAP are largely characterized by grainstone depositional textures that exhibit considerable sedimentologic and ichnologic variability (Fig. 10), and a wide range of petrophysical properties. Shoreface deposits show porosity that ranges from 3–34% (N = 76) and permeability that varies from 0.011–317 D (N = 910). Integration of thin-section petrography, CT scans, and porosity and permeability data from three representative samples (Fig. 13; Table A) explore the relationship between sedimentologic and ichnologic variability and petrophysical heterogeneity.

Spot-permeametry testing on 21 unpolished slab samples used a New England Research TinyPerm II portable handheld air permeameter. The device measures air permeability ranging from 1 millidarcy (mD) to 5,000 Darcy (1–10,000 mD with the highest accuracy), through a probe tip with an internal diameter of 9.27 mm. Spot-permeability measurements (N = 910) obtained on the cut face of slabbed samples used a grid pattern with 2-cm spacing, supplemented by additional grid points to capture large (> 9.27 mm) discrete traces. Following standard procedures (e.g., Gingras et al. 2012), five permeability measurements were recorded at each grid point, with datasets ranging from 30–80 measurements per sample, depending on the number of grid points. Due to the size of the probe tip, spot-permeametry data of burrows ≤ 9.27 mm in size are representative of both original (depositional) sedimentary fabric, as well as burrow-modified fill. Conversely, spot-permeametry data do not include any contribution from fractures or vugs > 9.27 mm. The large size of the probe tip relative to trace fossils and sample-surface irregularities (e.g., microfractures) together limit the accuracy of the measurements.

The Modified Thompson Tau technique was used to remove statistical outliers within each grid-point dataset, and the remaining values were averaged to produce point-permeability values (P_p) for each grid point. After removal of outliers, P_p values were used to determine permeability variations within the sample and calculate bulk permeability. Bulk permeability is calculated using the arithmetic, geometric, and harmonic mean of all P_p values per sample. Following Gingras et al. (1999), the mean that best represents bulk permeability is dependent on both the degree of burrow connectivity (low, moderate, high) and the presence or absence of preferential fluid flow. In cases with low burrow connectivity, bulk permeability is best represented by the geometric mean, whereas the harmonic mean represents samples with moderate, local burrow connectivity, and the arithmetic mean in examples with high burrow connectivity and preferential fluid flow (i.e., flow along or across burrows; Gingras et al. 1999; La Croix et al. 2013). Bulk permeability is reported as the range of all three mean values. The average ratio of maximum to minimum (K_{max}:K_{min}) permeability values was calculated and used as an indirect indicator of the influence of cm-scale heterogeneities on petrophysical properties (Budd 2002).

Sample 1.—This sample is a moderately well- to well-sorted, very fine–medium-grained, ooid-skeletal-composite grain grainstone with vague preservation of parallel laminae (Fig. 13A). Characteristic of LFF, the sample displays poor preservation of parallel laminae, with moderately well- to well-sorted, very fine sand cemented by isopachous bladed calcite, as well as clear blocky calcite concentrated at grain boundaries, producing meniscus cement fabrics. The laminae alternate with mottled intervals of moderately sorted, fine–medium sand that typically display partial–complete dissolution of isopachous and meniscus calcite cement. The mottled intervals

are coarser grained and less well sorted, with poorly preserved internal stratification, resulting in the cryptobioturbated fabric (ii5; Ichnofabric VI; Fig. 13B–D). The sample also exhibits abundant rhizoliths and few discrete trace fossils, such as *Macaronichnus*, *Planolites*, and *Palaeophycus*. Where preserved, very fine-grained laminae are cemented by isopachous bladed calcite and mosaics of clear blocky calcite concentrated at grain boundaries, producing meniscus cement fabrics, and resulting in the preservation of rounded interparticle pores.

Axial scans and rendered 3D volumes of CT data reveal high burrow connectivity among discrete tube-like features, resulting in a relatively homogenous fabric. Preserved macroporosity is primary interparticle and secondary moldic porosity averaging 21%, but total porosity is likely much higher due to abundant intraparticle microporosity associated with incipient–moderate dissolution of grains. Permeability ranges from 10.7–26.4 D, with a K_{max}:K_{min} value of 2, standard deviation of 5.55 D, and calculated bulk permeability between 14.9 and 16.4 D. Rhizoliths preserved as open macropores preferentially occur within the medium-grained intervals (Fig. 13A, B), corresponding to lower intensity colors in CT data (Fig. 13C, D).

Sample 2.—This sample is a moderately well-sorted, medium-grained ooid-composite grain-skeletal grainstone with well-preserved TCS (Fig. 13E–F). Characteristic of a south-margin LFB deposit, the sample is representative of Ichnofabric V with ii3. Primary interparticle and secondary moldic porosity are occluded by isopachous to meniscus granular calcite cement, and preserved macroporosity is 28%.

Axial scans and rendered 3D volumes of the CT data shows density heterogeneities that correspond to cross laminae of the primary depositional fabric (Fig. 13G–H). Permeability ranges from 1.2–16.3 D, with a K_{max}:K_{min} value of 14, standard deviation of 6.16 D, and

calculated bulk permeability between 3.8 and 8.0 D. Density heterogeneities reflecting the pore distribution and permeability appear to correspond depositional fabric, rather than bioturbation.

Sample 3.—This sample is a moderately sorted, very fine peloid-skeletal grainstone, with vague cross-stratification (LFB). Characteristic of a north-margin LFB in Pleistocene FA1 deposits, the sample is representative of Ichnofabric II with ii5 (Fig. 13I, J). The branched and interconnected burrows are commonly surrounded by a "halo" of clear, equant calcite cement forming low-porosity zones up to 5-mm wide. These cement halos are less porous than either the burrow fill or matrix. Primary interparticle and secondary moldic porosity are occluded by meniscate clear calcite mosaic cement, as well as isopachous fibrous and dogtooth cement, resulting in preserved macroporosity of 23%. In contrast, burrow-fill sediment is typically less well sorted, with looser grain packing and considerably less cement than the host rock. Burrow fill includes slightly coarser, fine-grained sand with looser grain packing and less abundant cement than the matrix, resulting in greater preserved porosity within burrows (up to 24%, double the average matrix porosity).

Axial scans and rendered 3D volumes of the CT data shows interconnected areas of lower density (darker color represents higher porosity) surrounded by higher density (brighter color, lower porosity; Fig. 13K, L). Permeability ranges from 0.25–1.6 D, with a K_{max}:K_{min} value of 6, standard deviation of 0.56 D, and calculated bulk permeability between 0.57 and 0.89 D.

Table A:

Sample	Bioturbation Intensity	Lithofacies	FA	EOD	Porosity (%)	Minimum k (D)	Maximum k (D)	Range (D)	Kmax:Kmin	Standard Deviation	Geometric Mean (D)	Arithmetic Mean (D)	Harmonic Mean (D)
KP2-10	ii4	LFE	FA2	FS	17	0.13	3.18	3.1	25	0.97	0.65	1.0	0.40
KP2-110	ii3	LFE	FA2	FS	N/A	9.76	38.1	28.3	4	9.02	17.9	19.4	16.7
KP2-240	ii3	LFE	FA2	FS	19	1.17	13.4	12.2	11	4.00	5.7	7.0	4.1
KP2-300	ii4	LFF	FA2	BSB	21	5.73	10.6	4.9	2	20.0	8.8	9.0	8.6
KP2-350	ii3	LFF	FA2	BSB	21	2.25	5.74	3.5	3	1.08	3.7	3.8	3.6
KP3-100	ii3	LFB	FA2	USF	20	4.64	44.3	39.7	10	11.6	11.3	14.0	9.6
KP3-190	ii4	LFB	FA2	USF	22	0.35	5.66	5.3	16	1.96	2.2	3.0	1.3
LCH9-138	ii5	LFF	HFA	BSB	21	10.7	26.4	15.7	2	5.55	15.6	16.4	14.9
LP1-MAR3	ii6	LFA	FA2	Reef	19	0.93	15.9	15.0	17	5.83	4.9	7.6	2.9
LP2-1	ii4	LFA	FA2	Reef	15	0.02	3.91	3.9	194	1.58	0.3	1.3	0.06
SAT1-171	ii3	LFE	FA2	FS	21	2.11	26.3	24.2	12	8.07	8.0	11.1	5.5
SAT2-408	ii6	LFF	FA2	BSB	17	0.07	6.47	6.4	97	2.36	0.3	1.0	0.21
SAT4-180	ii6	LFA	FA2	Reef	20	0.49	2.39	1.9	5	0.69	1.3	1.5	1.1
SLR1-240	ii5	LFB	FA1	USF	11	0.04	0.15	0.11	3	0.05	0.09	0.10	0.08
SLR8-365	ii4	LFA	FA1	USF	16	0.02	0.26	0.24	11	0.07	0.07	0.09	0.06
SLR9-180	ii5	LFB	FA1	USF	23	0.25	1.60	1.4	6	0.56	0.73	0.89	0.57
SLR9-290	ii6	LFB	FA1	USF	15	0.10	0.61	0.51	6	3.91	0.27	0.33	0.21
WP1-395	ii3	LFE	FA2	FS	28	2.50	21.5	19.0	9	6.99	8.0	10.1	6.2
WP2-120	ii3	LFB	FA2	USF	28	1.20	16.3	15.1	14	6.16	5.7	8.0	3.8
WP2-420	ii5	LFE	FA2	FS	15	3.00	42.7	39.7	14	14.3	14.7	19.4	10.3
WPB-210	ii6	LFF	FA2	BSB	26	9.43	35.6	26.2	4	8.03	18.3	19.8	16.9